NITRIC OXIDE-RELEASING POLYURETHANE MEMBRANES FOR IMPLANTABLE ELECTROCHEMICAL GLUCOSE SENSORS

Ahyeon Koh

A dissertation submitted to the faculty of the University of North Carolina at Chapel Hill in the partial fulfillment of the requirements for the degree of Doctor of Philosophy in the Department of Chemistry (Analytical Chemistry).

Chapel Hill
2013

Approved by:

Mark H. Schoenfisch

R. Mark Wightman

Steven A. Soper

Joseph L. Templeton

Timothy C. Nichols

ABSTRACT

AHYEON KOH: Nitric Oxide-Releasing Polyurethane Membranes For Implantable Electrochemical Glucose Sensors
(Under the direction of Professor Mark H. Schoenfisch)

The development of novel biocompatible membranes is key to mitigating the host foreign body response (FBR) that limits the utility of implantable electrochemical biosensors for continuous glucose monitoring. Nitric oxide (NO)—an endogenously produced physiological mediator involved in wound healing, angiogenesis, and the inflammatory response—has been shown to reduce the FBR and may enhance sensor utility when released from sensor membranes.

Nitric oxide-releasing glucose sensor membranes with tunable release kinetics and total payloads were fabricated utilizing polyurethane (PU) films doped with NO donor-modified silica nanoparticles. A wide range of NO-release fluxes (5−460 pmol cm^{-2} s^{-1}) and durations (16 h to 14 d) were achieved by altering the type of dopant, as well as the PU sensor membrane composition and concentration. Sensor performance was affected by water uptake and membrane thickness regardless of the type of NO-release vehicle.

To combine the potential benefits of both NO-release and porous scaffolds in one engineered material, NO-releasing fibrous PU membranes were fabricated via

electrospinning. Electrospun PU fibers doped with NO-releasing silica particles exhibited a wide range of NO-release totals and durations (7.5−120 nmol mg^{-1} and 7 h to 14 d, respectively). These materials exhibited ~83% porosity with flexible plastic or elastomeric behavior, and a wide range of fiber diameters (119−614 nm) and mechanical strength (moduli of 1.7−34.5 MPa).

Nitric oxide-releasing electrospun fibers were applied to needle-type glucose sensors as the outermost membrane. The NO-releasing dendrimer-doped PU fiber mats maintained their porosity in serum without dendrimer leaching. Sensor performance was not significantly impacted by the additional porous membrane (≤50 μm thickness). The glucose sensitivity was 2.4 ± 1.6 nA/mM with a dynamic range 1–24 mM, indicating clinically acceptable performance.

In vivo analytical sensor performance was assessed using NO-releasing membrane-modified glucose biosensors in a porcine model. The NO-releasing sensors were shown to continuously monitor glucose for one week with 91.8% of determinations indicated as clinically accurate and acceptable. This research illustrated the ability to create functional NO-releasing glucose sensors so future studies can focus on thoroughly evaluating the benefits of NO release and porosity on in vivo analytical performance.

ACKNOWLEDGEMENTS

My dissertation work would not be possible without support. Foremost, I do appreciate my advisor, Dr. Mark H. Schoenfisch, for all of his mentoring, patience, and support. He has fostered me as an independent scientist and has driven me to achieve the highest quality of research by providing a collaborative scientific environment.

I am grateful for all the support of past and present members in the Schoenfisch lab and other collaborators. The work presented herein could not have been completed without the assistance of Dr. Daniel Riccio, Dr. Bin Sun, Dr. Alexis Carpenter, and Dr. Yuan Lu who provided NO-releasing materials and shared their knowledge. I greatly thank Dr. Scott Nichols, Danielle Slomberg, Rebecca Hunter, Dr. Peter Coneski, Nga Brown, and Dr. Bruce Klitzman for helping me to conduct experiments and providing great insights on my projects. I also thank Wesley Storm, Katey Reighard, Chris Backlund, Justin Johnson, Brittany Worley, Angela Broadnax, and Robert Soto for providing great discussions, motivation, and friendships. During my time at UNC, I was fortunate to work with the most creative and intelligent scientists as well as to call all of them my friends.

Last but not the least, I would like to thank my parents and sisters for all supporting and encouraging with love. Being away from my family was tough but they are always with me.

TABLE OF CONTENTS

LIST OF TABLES

LIST OF FIGURES

LIST OF ABBREVIATIONS AND SYMBOLS

~	Approximately
^{o}C	Degree(s) Celsius
±	Statistical margin of error
>	Greater than
<	Less than
≥	Greater than or equal to
≤	Less than or equal to
$	US dollar
%	Percent
[...]	Concentration
×*g*	Times the force of gravity
α	Confidence interval
Δ	Change
σ	Standard deviation
µC	Microcoulomb(s)
µL	Microliter(s)
µm	Micrometer(s)
µM	Micromolar
µmol	Micromole(s)
µS	Microsiemens

ρ	Density of the electrospun fiber mats
ρ_0	Density of the bulk polymer
AA	Ascorbic acid
AEAP3	*N*-(2-Aminoethyl)-3-aminopropyltrimethoxysilane
Ag	Silver
Ag/AgCl	Silver/silver chloride reference electrode
AHAP	*N*-(6-Aminohexyl)aminopropyl trimethoxysilane
AHAP3	*N*-(6-Aminohexyl)aminopropyltrimethoxysilane
AL-25-80A	Hydrothane polyurethane
AP	Acetaminophen
Ar	Argon gas
ATCC	American Type Culture Collection
atm	Atmosphere(s)
BG	Blood glucose concentration
c	Concentration
CAM	Chick chorioallantoic membrane
CGM	Continuous glucose monitoring
cm	Centimeter
cm^2	Square centimeter(s)
d	Day(s)
DBHD/NO	(Z)-1-[*N*-Methyl-*N*-[6-(*N*-butylammoniohexyl)amino]]-diazen-1-ium-1,2-diolate

DETA/NO	1-[*N*-(Aminoethyl)-*N*-(2-ammonioethyl)amino] diazen-1-ium-1,2-diolate
DI	Deionized
dL	Deciliter
DLS	Dynamic light scattering
DMEM	Dulbecco's modified Eagle's medium
DMF	*N,N*-Dimethylformamide
DNA	Deoxyribonucleic acid
DX	Dexamethasone
e.g.	For example
ECM	Extra cellular membrane
ED	1,2-Epoxy-9-decene
EDRF	Endothelial-derived relaxation factor
eNOS	Endothelial NOS
ESEM	Environmental scanning electron microscope
et al.	And others
etc.	And so forth
EtOH	Ethanol
FBGC	Foreign body giant cell
FBR	Foreign body response
FBS	Fetal bovine serum
FDA	Food and Drug Administration
$FeCl_3$	Ferric chloride

g	Gram(s)
G4	Fourth generation
G(t)	Glucose concentration
GDH	Glucose dehydrogenase
Glu	Glucose
GOx	Glucose oxidase
GSNO	*S*-Nitrosoglutathione
h	Hour(s)
H&E	Hematoxylin and eosin
H_2O	Water
H_2O_2	Hydrogen peroxide
HP-93A-100	Tecophilic polyurethane
HPU	Hydrothane AL 25-80A
i.e.	That is
I(t)	Current reading
I_0	Background current
ICP-OES	Inductively coupled plasma-optical emission spectroscopy
IF	Interstitial fluid
IgG	Immunoglobulin G
iNOS	Inducible NOS
Ir	Iridium
ISO	International Standard Organization

KCl	Potassium chloride
kDa	Kilodalton(s)
kPa	Kilopascal
kV	Kilovolt(s)
LFD	Large-field detector
LMW	Low molecular weight
LPS	Lipopolysaccharide
m	Meter(s)
M	Molar
MΩ	Magaohm(s)
MAD	Mean absolute difference
MAP3	3-Methylaminopropyltrimethoxysilane
MARD	Mean absolute relative difference
max	Maximum
MCP-1	Monocyte chemoattractant protein-1
MedAD	Median absolute difference
MedARD	Median absolute relative difference
mg	Milligram(s)
min	Minute(s)
mL	Milliliter(s)
mM	Millimolar
mm	Millimeter(s)

mmHg	Millimeter of mercury
mol	Mole(s)
MPa	Megapascal
MPTMS	3-Mercaptopropyltrimethoxysilane
MTMOS	Methyltrimethoxysilane
MTS	3-(4,5-Dimethylthiazol-2-yl)-5-(3-carboxymethoxyphenyl)-2-(4-sulfophenyl)-2H-tetrazolium inner salt
N_2	Nitrogen gas
N/A	Not applicable
nm	Nanometer
nM	Nanomolar
nNOS	Neuronal NOS
NO	Nitric oxide
$[NO]_{max}$	Maximum NO flux
NO_2^-	Nitrite
NOA	Chemiluminescence Nitric Oxide Analyzer
NOS	Nitric oxide synthase
O_2	Oxygen
O_2^-	Superoxide
$ONOO^-$	Peroxynitrite
P_i^e	Permeability
PAES	Polyarylethersulfone

PAMAM	Poly(amidoamine)
PBS	Phosphate buffered saline, pH 7.4
PCL	Poly(ε-caprolactone)
pH	-Log of proton concentration
PLGA	Poly(lactic-co-glycolic acid)
PLLA	Poly(L-lactic acid)
pmol	Picomole(s)
PMS	Phenazine methosulfate
ppb	Parts per billion
ppm	Parts per million
PROLI/NO	1-[(2-Carboxylato)pyrrolidin-1-yl]]diazen-1-ium-1,2-diolate
PRP	Platelet rich plasma
PS	Penicillin streptomycin
Pt	Platinum
PTFE	Polyterafluoroethylene
PU	Polyurethane
RITC	Rhodamine isothiocyanate
rpm	Revolution per minute
RSNO	*S*-Nitrosothiol
s	Second(s)
S	Sensitivity
SG-80A	Tecoflex polyurethane

SNAC	*S*-Nitroso-*N*-acetylcysteine
t	Time
$t_{1/2}$	Half-life
$t_{95\%}$	Response time
t_d	Duration
t_{max}	Time to max nitric oxide flux
TEOS	Tetraethoxysilane
THF	Tetrahydrofuran
TMOS	Tetramethoxysilane
TP-470	Tecoplast polyurethane
TPU	Tecoflex SG-80A
U	Unit(s)
UA	Uric acid
U.S.	The United States of America
UV	Ultraviolet
V	Volt(s)
v/v	Volume/volume
VEGF	Vascular endothelial growth factor
vs.	Versus
w/v	Weight/volume
w/w	Weight/weight
wt%	Percent by weight

CHAPTER 1: BIOCOMPATIBLE MEMBRANES FOR IMPLANTABLE ELECTROCHEMICAL GLUCOSE SENSORS

Text, tables, and figures are adapted and reprinted with permission from the corresponding journal. Original articles are two papers: (1) a review article co-authored with Scott P. Nichols and Mark H. Schoenfisch published in *Journal of Diabetes and Science Technology* in 2011, titled "Glucose sensor membranes for mitigating the foreign body response", vol. 5 (5), pp 1052-1059; and (2) a review article co-authored with Scott P. Nichols, Wesley L. Storm, Jae Ho Shin, and Mark H. Schoenfisch published in *Chemical Reviews* in 2013, titled "Biocompatible materials for continuous glucose monitoring devices", vol. 113 (4), pp 2528-2549.

1.1 Electrochemical continuous glucose monitoring biosensors

1.1.1 Overview of implantable electrochemical glucose sensors

Diabetes mellitus is a worldwide epidemic characterized by chronic hyperglycemia that results from either a deficiency in or tolerance to insulin.[1] In the United States, 8.3% of the population currently suffers from diabetes, with that number projected to increase to 1 in 3 adults by 2050 if current trends continue.[2] Consequently, diabetes is the seventh leading cause of death in the United States with an annual cost burden of $174 billion.[2]

Blood glucose levels in diabetics fluctuate significantly throughout the day, which can result in serious complications, including heart attacks, strokes, high blood pressure, kidney failure, blindness, and limb amputation.[1,2] Therefore, diabetes patients should use potable glucose sensors to monitor blood glucose levels and manage insulin levels to reduce the morbidity and mortality of diabetes mellitus. As such, glucose sensors

represent more than 85% of global market for biosensors in medical diagnostics.[3,4] The traditional glucose monitoring techniques are primarily based on the use of electrochemical amperometric glucose sensors. The most successful technologies for measuring glucose concentrations are based on enzyme-modified electrodes and electrochemical amperometric detection with a number of useful designs. In 1967, Updike and Hicks first developed a sensor that detects glucose by monitoring the consumption of oxygen using two oxygen electrodes (one covered with the enzyme and one for reference), comparing the differential current between these electrodes to correct for background variations in oxygen.[5] Alternatively, hydrogen peroxide produced enzymatically by glucose oxidase can be quantified amperometrically to indirectly determine glucose concentration, as first demonstrated by Guilbault and Lubrano in 1973.[6] Amperometric enzyme-based glucose sensors vary greatly in electrode design, electrode material, enzyme immobilization method, and polymeric membrane compositions. To date, the U.S. Food and Drug Administration (FDA) has approved more than 25 glucose monitors, with the majority employing test strips consisting of either glucose dehydrogenase (GDH) or glucose oxidase (GOx) immobilized on a screen printed electrode.[4] The analysis is based on obtaining a small blood sample (<1 μL) through a finger prick that is subsequently introduced into the test strip via capillary action.[4,7]

While such measurements have augmented the health outcomes for people with diabetes by improving blood glucose management, in vitro glucose monitoring only provides instantaneous blood glucose concentrations that are unable to warn of emerging

hyper- or hypoglycemic conditions. Additionally, the sample collection (i.e., finger prick) method is inconvenient and can be painful for adolescents, resulting in poor patient compliance. Analytical methods that enable continuous monitoring of blood glucose have thus been sought.[8] Continuous glucose monitoring (CGM) provides real-time information on trends (i.e., whether the glucose levels are increasing or decreasing), magnitude, duration, and frequency of blood glucose fluctuations during the day.[8,9] Ideally, analytically functional CGM devices could be linked to an insulin delivery pump, creating an artificial pancreas.[8,9]

The development of continuous glucose monitoring technologies is predominantly focused on subcutaneously implanted amperometric electrochemical glucose sensors.[10] Due to the high selectivity and sensitivity afforded by the specific biocatalytic reactions of an immobilized enzyme and the prospect of miniaturization, electrochemical biosensors are among the most widely studied and commercially available devices.[4] Implantable electrochemical sensors measure the rate of glucose oxidation as a change in oxygen or hydrogen peroxide concentration upon reaction of glucose with a glucose-specific enzyme (e.g., GOx or GDH), similar to in vitro glucose sensors. First generation enzyme-based electrochemical biosensors were fabricated by immobilizing the enzyme on the surface of the electrode. The enzyme is reduced upon converting glucose to gluconolactone with ambient oxygen facilitating the conversion of the reduced enzyme back to its oxidized form with concomitant production of hydrogen peroxide.[4,11]

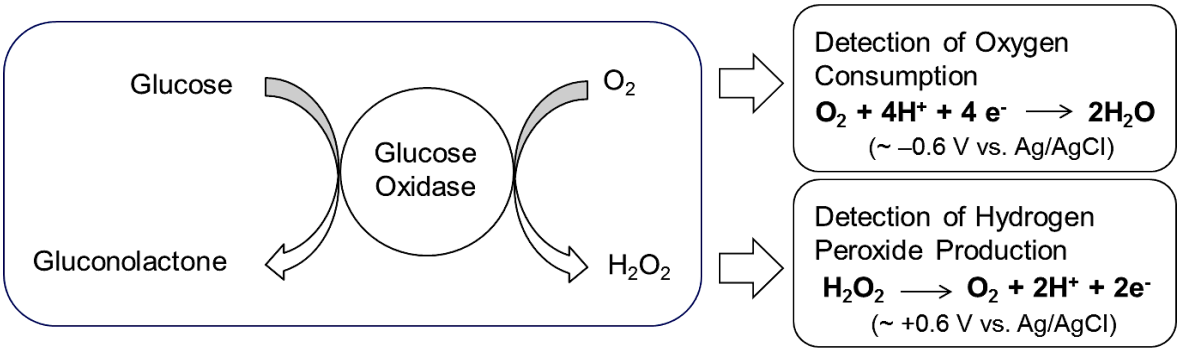

Figure 1.1. The enzymatic oxidation of glucose to gluconolactone by glucose oxidase with subsequent electrochemical detection of oxygen depletion and/or hydrogen peroxide formation.

The glucose concentration correlates with the amperometric signal obtained from either the electrochemical oxidation of produced hydrogen peroxide or the reduction of consumed oxygen (Figure 1.1). Although enzyme-based electrochemical glucose biosensors are characterized with high selectivity and sensitivity due their enzymatic nature, the dynamic range of such sensors is limited by the co-substrate (i.e., oxygen) availability. An outer diffusion limiting membrane is often employed and eliminates oxygen deficiency problems, albeit with slightly delayed sensor response. Additionally, the working electrode potential required to monitor hydrogen peroxide (i.e., ~ +0.6 V vs. Ag/AgCl) will also oxidize electroactive endogenous species (e.g., ascorbic acid and acetaminophen) and create high current densities.[11] To address these shortcomings, other electrochemical glucose biosensors designs have employed electron mediators (e.g., $[Os(4,4'\text{-dimethoxy-}2,2'\text{-bipyridine})_2Cl]^{+/2+}$) "wired" to the enzyme on a hydrophilic polymer matrix (e.g., poly(vinylpyridine) or poly(vinylimidazole)). Such mediators are capable of shuttling electrons from the redox center of the enzyme to the surface of the electrode, allowing for a lower applied electrode potential.[12,13] In turn, the sensor response becomes independent of the co-substrate and interferences. Unfortunately, most mediators are toxic and competition between the mediator and oxygen still exists.[9,11] The concept however has evolved to where the enzyme cofactor is covalently linked to the electrode, enabling direct electron transfer through the wiring nano-material (e.g., carbon nanotube). Toxicity still remains a concern for in vivo use.

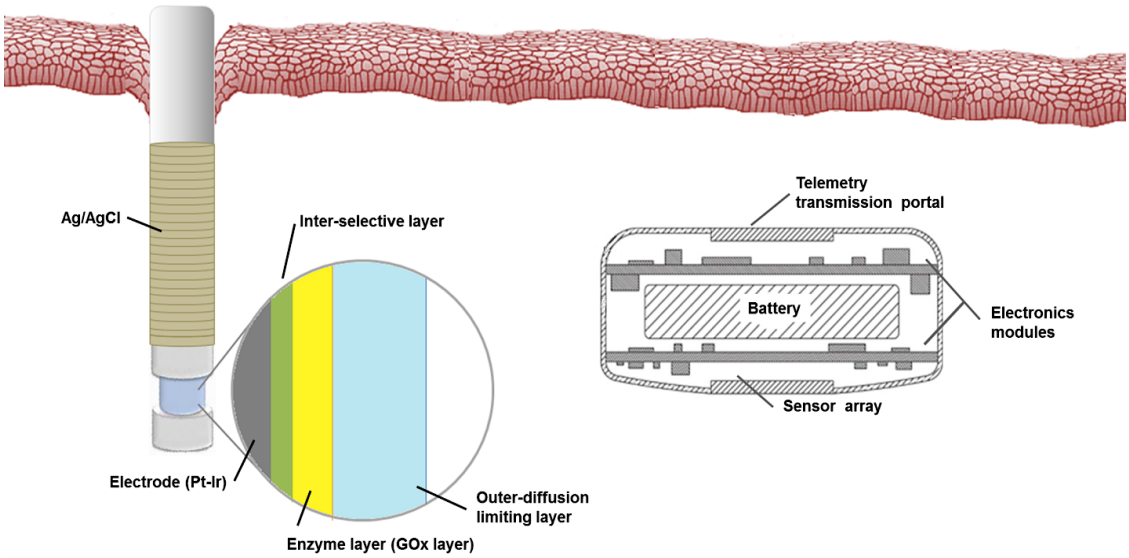

Figure 1.2. Sensor design percutaneous (left) and fully implantable subcutaneous (right) electrochemical glucose biosensors.

Enzyme-immobilized amperometric biosensors have been implanted fully subcutaneously for month to years or percutaneously for <1 month, and most often only 3–5 days. Subcutaneous glucose sensors generally consist of a disk-type sensor with a titanium housing and measure oxygen consumption (Figure 1.2 right). Gough et al. reported on a subcutaneous sensor design based on differential electrochemical detection of oxygen via a two-step chemical reaction catalyzed by glucose oxidase and catalase.[14] Accurate glucose measurements were carried out for >1 year by taking into account the difference in oxygen reduction at a working electrode producing a glucose-modulated current and a reference electrode producing an oxygen-dependent current.[14] Sensor (oxygen) response changes due to collagen encapsulation, variations in local microvascular perfusion, and limitations in oxygen availability were thus relative, reducing the demand of device calibrations. The subcutaneous nature of the sensors likely minimizes any micromotion effects that also elevate the foreign body response (FBR).[15] Unfortunately, implantation and subsequent replacement of the sensors required surgery, with each instance followed by a long (~2–3 week) stabilization period. Faulty devices for whatever reason would be costly to remove and/or replace. The size of the sensor is also significantly larger than percutaneous CGM systems (~3 cm vs. 350 μm) due to power (i.e., battery) requirements to support long-term use.

Percutaneous needle-type microsensors monitor hydrogen peroxide production amperometrically as a measure of the glucose concentration (Figure 1.2, left).[9,16,17] The sensing cavity generally consists of a Pt-Ir wire working electrode coated with three functional layers: an inner-selective layer, an enzyme layer, and the outer diffusion

limiting membrane. Though such sensors are characterized as having a shorter stabilization period (e.g., 2–4 h) compared to subcutaneous glucose sensors, the device penetrates through an opening in the dermis with concomitant infection and dislodging risks. Additionally, frequent calibration (e.g., >2 times per day) using intermittent glucose monitoring (via finger pricks) is required due to erratic analytical performance. The percutaneous nature of the device creates additional forces on the sensor that can lead to even greater inflammation.[15] In this regard, compliance regarding the use of such devices remains poor. Nevertheless, only percutaneous implantable electrochemical glucose sensors are currently FDA approved and commercially available among the various continuous glucose monitoring technologies.[18]

1.1.2 Implantable glucose sensor design and challenges for bioanalytical performance

Reliable in vivo glucose sensing can be achieved based on understanding physiology and biological response. A number of interferents (e.g., acetaminophen, ascorbic acid, and uric acid) can affect sensor response, as they are also electroactive at the electrode potential used to oxidize hydrogen peroxide. Permselective sensor membranes via size exclusion and/or electrostatic repulsion are often used to improve the selectivity of implantable glucose sensors.[4] The range of polymeric materials that have been evaluated as effective permselective films include cellulose acetate, Nafion, electropolymerized films (e.g., polyphenol), and multilayer hybrids of these polymers.[4,19] Polyphenol permselective membranes are able to electropolymerize within an enzyme layer and the film thickness is self-limiting (10–100 nm) in a controllable manner, making this approach attractive for reducing interferences.[20,21] In some cases, such

membranes also exclude surface-active macromolecules (i.e., proteins and platelets), protecting the electrode from biofouling.[4]

Since the electrochemical detection of hydrogen peroxide requires oxygen, a cofactor in the GOx enzymatic reaction, oxygen concentration and fluctuation in vivo should be accounted for sensor design. Oxygen concentration in interstitial fluid is approximately ten times lower than the concentration of glucose resulting in an "oxygen deficit" state. Low concentrations of oxygen lead to problems with the biosensor response to glucose (particularly sensor sensitivity and linearity) due to stoichiometric imbalance between the two cofactors.[11,22] Moreover, subcutaneous oxygen tension for humans ranges from 40 (~5 kPa) to 130 mm Hg (~17kPa) with partial pressures affected by anesthetics and hypoxia at the implantation site.[23] Sensor performance issues due to changing oxygen levels are exacerbated by the foreign body response (FBR) that results in local consumption of oxygen and glucose by inflammatory cells at the vicinity of the sensor. Additionally, oxygen diffusion to the sensor decays exponentially after sensor implantation due to changes in tissue permeability.[14] To overcome oxygen deficiency, polymeric membranes such as polyurethane, Nafion, silicone elastomer, polycarbonate, and layer-by-layer assembled polyelectrolytes are utilized to reduce glucose diffusion.[24-28] Polyurethane in particular is widely used as an outermost membrane of implantable glucose sensor to overcome this complication by controlling the oxygen/glucose ratio with sufficient dynamic range.[29] Implantable glucose sensors exhibiting dynamic ranges up to >12 mM have been shown to exhibit no oxygen dependency in vivo.[29]

In addition to the issue of electroacitve interference and oxygen deficit for sensor fabrication, patient variability and physiological fluctuation are equally important factors for CGM device utility. Since percutaneous sensors are implanted through the epidermis, dermis, and subcutaneous layers, the effects of tissue heterogeneity are relevant to the analytical performance of the sensor. Temporal and spatial glucose dynamics are both influenced by tissue composition, distribution, and thickness.[30-32] Temperature fluctuations in subcutaneous tissue will also impact sensor performance by altering glucose oxidase activity.[33] Additionally, external pressure (e.g., posture change) on the CGM sensor has also caused erratic analytical performance.[34] Such behavior is attributed in part to blood occlusion due to pressures applied to the tissue adjacent to the sensor.[15,35] Moreover, these performance limitations may be more pronounced in diabetic patients due to differences in physiology.[36] Therefore, these fluctuations and their possible impact on interstitial fluid physiology demand careful attention when characterizing in vivo sensor performance.

1.2 Biocompatibility concerns for subcutaneously implanted glucose sensors

While the design, fabrication, and use criteria are of importance to CGM device use, none of these impacts the bioanalytical and clinical utility as much as the foreign body response (FBR). The FBR is the inflammatory response initiated by macrophages and foreign body giant cells, which leads to a modified wound-healing process following implantation of almost any medical device.[37] Therefore, the development of biocompatible coatings is necessary to reduce this innate immune response and thus

improve the performance of medical devices in vivo. In general, the term "biocompatible" can be defined as material properties that avoid any negative local and systemic effects, and elicit the most appropriate local tissue response adjacent to an the implant allowing for improved performance.[38] Along with this idea, most long-term medical implants to date are considered biocompatible or inert once the FBR resolves and the device is encapsulated by a collagen layer.[39] Although CGM devices have similar circumstances, the combination of the FBR, oxygen and glucose availability, and need for immediate and frequent calibration have significantly impeded their utility and implementation as effective devices for diabetes management.

1.2.1 The effect of the foreign body response on in vivo glucose sensor performance

Once a continuous glucose monitoring system is implanted, the host recognizes the sensor as foreign material and attempts to isolate the sensors as shown in Figure 1.3.[37,40] All implantable medical devices perturb the host medium, damage capillaries, and produce to an immune response that includes: (1) the formation of a provisional matrix (minutes–hours); (2) acute inflammation (days); (3) chronic inflammation (weeks); (4) granulation tissue formation (weeks); and, (5) fibrous capsule formation (weeks–months).[37,40] Specifically for glucose biosensors, the surface changes based on each stage of this immune response, cumulatively or independently affecting on sensor performance in vivo.

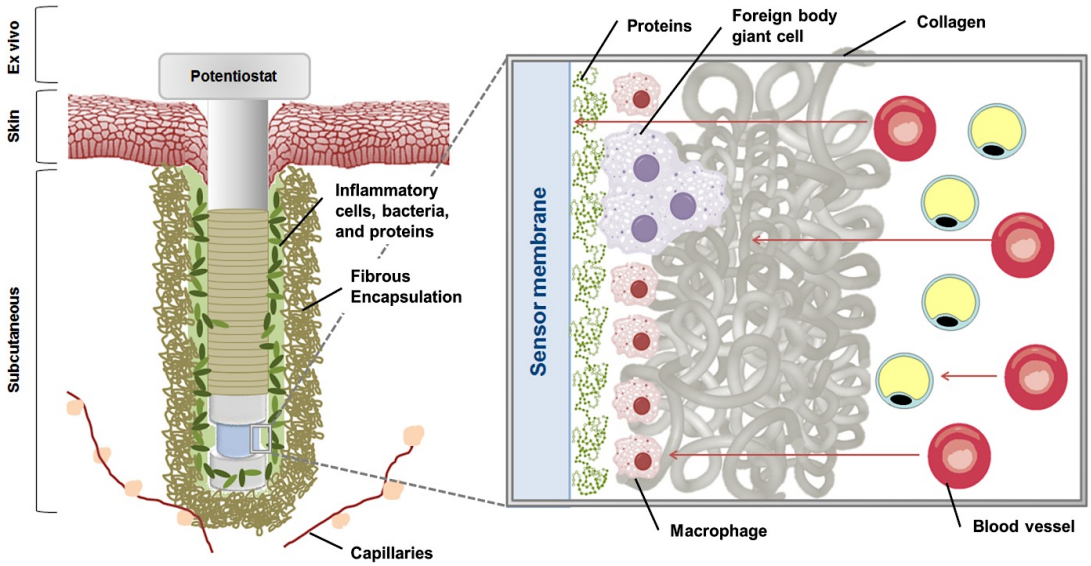

Figure 1.3. The foreign body response to a percutaneous glucose sensor upon tissue implantation. Arrows in the magnified area show diffusion of glucose form blood vessels toward the sensor through native tissue (e.g., adipocytes), the collagen capsule, localized inflammatory cells, and biofouling layer near the sensor surface. As illustrated, glucose may be consumed by native tissue or inflammatory cells prior to reaching the sensor.

In the very early process of implantation, a provisional matrix instantaneously forms on and around foreign objects along with blood/material interactions and protein adhesion.[19,37] The initial protein adsorption and fibrin-predominant provisional matrix is closely linked to the overall FBR by providing structural, biochemical, and cellular components for the inflammatory response.[37] The chemoattractance, cytokines, growth factors, and other bioactive agents from the provisional matrix modulate the phenotype of macrophages as well as proliferation and activation of other cells.[37] With this regard, the provisional matrix may be considered as a naturally derived membrane releasing bioactive agents to control subsequent phases of inflammatory response.[37] In this stage, the adhesion of biomolecules to the sensor membrane typically results in a >50% decrease in the sensor response to glucose, with the greatest reduction in response caused by biomolecules <15 kDa.[40-43] Proteomic analysis using mass spectroscopy of biomolecules adhered on implanted sensors in a rodent model showed both inflammatory cells and fragments of larger proteins infiltrated the sensor membranes and caused diminished glucose diffusivity.[43] This protein adsorption is a time dependent process and mostly consists of biomolecules related to inflammatory response, including serum albumin, IgG, immunoglobulin, and fibrinogen.[43] While this loss of sensitivity is reversible, the extent of signal reduction is unpredictable and requires frequent in vivo sensor calibration.[10,41]

As a sequential extension of provisional matrix formation, acute inflammation occurs through the infiltration of leukocytes, mast cell degranulation with histamine release, and fibrinogen adsorption.[40] The biological role of the acute inflammatory

response is to phagocytose the foreign material. The process of macrophages digesting the implant may further impact in vivo sensor performance due to the local pH drop as low as 3.6, which may negatively affect GOx activity.[44] In the acute inflammatory stage, the released concentrations and types of chemokines and cytokines control the extent and/or degree of acute inflammatory response and the subsequent development of the FBR based on cell recruitment and ultimate phagocytosis.[45] Additionally, the activation state (i.e., M1 or M2) of the macrophage is an important factor that influences the overall FBR.[46] While limited studies have demonstrated distinct surface-induced phenotypes of macrophages on the wound healing process, the phenotype of activated macrophages is considered an indicator of tissue response variable inflammatory mediators.[46,47]

Following acute inflammation, chronic inflammation occurs in a sequential fashion and may be identified by the presence of macrophages, monocytes, and lymphocytes, as well as the proliferation of blood vessels and connective tissue. This process initiates frustrated phagocytosis leading to the fusion of macrophages into foreign body giant cells (FBGCs) that attempt to further consume/degrade the implant.[44,48-50] This effect further reduces analyte diffusion and the relative concentration of analyte in the localized tissue. Additionally, the consumption of oxygen and glucose by macrophages produces superoxide and peroxide, which for certain electrochemical sensors negatively impacts response (and thus accuracy).[9,51] The extent of the chronic inflammatory response is dependent on both the physical and chemical properties of the implant, and the mechanical stress (i.e., due to movement) at the implant site.[40] Following the resolution of the chronic inflammatory response, granulation tissue is formed as a

precursor to fibrous capsule formation due to the persistence of macrophages and infiltration of fibroblasts to the wound site.[40]

During the final step in the immune sequence, a fibrous capsule is formed with collagen surrounding the implant to isolate it completely from the local tissue environment.[37] The collagen encapsulation (typical thickness 50–200 μm) with absence of the microvasculature consequently prevents implant interaction with surrounding native tissue.[52] As such, diffusion of glucose is inhibited and the sensor fails to measure/report the actual blood glucose level of host. Ultimately, thick fibrous encapsulation significantly increases the sensor lag time, while lower subcutaneous vessel density and diminished capsule porosity lead to attenuation of analyte (i.e., glucose and oxygen) diffusion and response.[53-55]

Overall, the complex immune reaction and all stages of the FBR should be considered when designing outer tissue contacting membranes for implantable sensors. The developments of biosensor membranes that may enhance tissue integration and mitigate the FBR are obviously important for reducing the deleterious effects of the FBR on glucose sensor performance.

1.3 Current strategies to improve biocompatibility of sensor membranes

Since the FBR is a complex series of events connected with various biological pathways, both modulating the FBR and determining its actual effect on sensor performance are difficult. Additionally, the chemical, physical, and morphological properties of an implanted materials surface can play independent and/or cumulative

roles on the FBR.[37,38] Thus, the biocompatibility of the sensor membrane is the most important factor in mitigating the highly complex FBR and integrating a device into the surrounding tissue. This facilitates measurement of glucose with clinically relevant accuracy and short lag time over the lifetime of the in vivo biosensor.[38] Current strategies for improving glucose sensor biocompatibility are grouped into two areas: active release and passive coatings. Active release relies on the release of pharmaceutical molecules that may modify the FBR and direct the wound healing process to favor tissue integration of the sensor. Alternatively, passive coatings rely on the modification of chemical or physical characteristics at the tissue-sensor interface.

1.3.1 Active release

In a recent initiative, implant coatings have been synthesized to release biologically active molecules or pharmaceutical agents to improve biocompatibility. Upon release from the coating to the surrounding tissue the molecules are intended to influence the immune response, reduce collagen encapsulation, and/or increase angiogenesis. Several parameters should be considered in the design of an active-releasing surface, including the desired active molecule, toxicity, release kinetics and duration, relative amount, and delivery with each parameter being dependent on the molecule's properties.

Researchers have focused primarily on the local delivery of endogenous molecules and anti-inflammatory drugs. Since the wound-healing response is signaled in part by the generation of cytokines and chemokines from macrophages on the surface of the implant,[37] release of those signaling molecules may help direct the FBR at the sensor-

tissue interface and improve tissue integration. While many cytokines exist, vascular endothelial growth factor (VEGF) has been widely studied as a release reagent relevant to tissue-based glucose biosensors.[56-62] Vascular endothelial growth factor is a cytokine released by macrophages and keratinocytes during wound reconstruction to promote angiogenesis.[63-65] The expression of VEGF is induced in response to other growth factors and/or tissue hypoxia, with VEGF ultimately binding to tyrosine kinase receptors to stimulate angiogenesis.[63,66] Additionally, VEGF has also been referred to as vascular permeability factor due to its ability to induce vascular leakage.[67] However, a concern regarding VEGF use is an increase in local inflammation due to cell migration and proliferation correlated with angiogenesis.[68,69] Nevertheless, the potential for greater capillary densities via VEGF release have led researchers to evaluate the utility of this strategy for improving in vivo glucose sensor performance.[60] Upregulation of VEGF showed enhanced glucose sensor response compared to controls in a chick chorioallantoic membrane (CAM) model, exemplifying the usefulness of VEGF for in vivo biosensors.[60] Additionally, surfaces that release VEGF (e.g., VEGF embedded poly(lactic-co-glycolic acid) (PLGA) microsphere-doped hydrogel) have shown to improve the vascularity of the surrounding tissue.[56-62,70] Unfortunately, Ward et al. reported that surfaces releasing VEGF affected only a relatively small area of influence in subcutaneous tissue.[61,62] Direct and continuous delivery of this cytokine was necessary to promote improved wound healing. The functional lifetime of sensors near VEGF-releasing pumps was greater than control sensors near saline pumps.[61] Additionally, the sensor lag time decreased and the mean absolute relative difference (MARD) for glucose

analysis increased, indicating sensor accuracy was improved.[61] While the histological analysis revealed increased vascularization in tissue up to 13 mm away from the pumps, Clarke Error Grid analysis indicated that only sensors 1 mm from the VEGF-eluting pumps showed sensor accuracy improvements versus controls.[61,62] This study highlighted the importance of the spatial release profile of angiogenic drug to improve sensor performance in vivo. Although recent studies indicate the potential of VEGF to influence the vasculature adjacent to implanted materials, the corresponding increase in inflammation is particularly troublesome and would likely diminish glucose sensor performance.

Rather than increasing vascularity, anti-inflammatory drugs may reduce the FBR and represent potential active release agents from glucose sensor coatings. Dexamethasone (DX), an anti-inflammatory glucocorticoid steroid, is widely prescribed due to its ability to inhibit pro-inflammatory cytokine expression, leukocyte infiltration and collagen deposition.[71-73] Furthermore, glucocorticoids alter inflammatory cell trafficking, death, and cellular responses, possibly indicating a phenotypic change in the cells.[74] Although the exact mechanism of glucocorticoid action is not completely understood, the active release of DX from implants has been demonstrated to reduce inflammation at the implantation site.[57,59,75-77] Patil et al. reported that the localized zero-order DX release (from an implant surface) significantly diminished the acute and chronic inflammatory response over a 1 month period.[77] The influence of DX release duration on FBR was also studied by Bharwaj et al. in a rodent model; they concluded that DX release simply delayed the immune response.[78] This study clearly indicated that

DX must be delivered continuously (i.e., for the duration of an implant) in order to maintain any anti-inflammatory benefits. However, systemic use of DX can cause serious side effects by depressing the innate immune response, thus increasing the likelihood of infection.[79,80]

To fully circumvent the FBR, hydrogels that release both VEGF and DX from a membrane were studied to reduce the inflammatory response to the implant while increasing angiogenesis.[57,59] Unfortunately, the DX release significantly diminished the angiogenic benefits of VEGF.[57] Other reports have also shown that glucocorticoid steroids, and in particular DX, inhibit VEGF activity in vivo.[81-83] While concurrent release would be a promising approach to address the FBR as a whole, two active release agents that affect the FBR in a synergistic or non-antagonistic manner have yet to be identified.

1.3.2 Nitric oxide-releasing membranes

In lieu of distinct anti-inflammatory and angiogenic agents, it may be possible to achieve more ideal tissue integration with nitric oxide (NO). Since NO was reported as the endothelial-derived relaxation factor (EDRF) in 1986,[84] the role of nitric oxide in a variety of physiological pathways has been studied.[85] Nitric oxide (NO), an endogenously produced diatomic molecule, plays a wide range of roles in biological process, including angiogenesis, wound healing, neurotransmission, smooth muscle relaxation, and immunoinflammation.[86] These biological responses to NO are highly dependent on location, source, and concentration.[86,87] Nitric oxide is synthesized in vivo by NO synthase (NOS), which catalyzes the oxidation of a guanidine nitrogen in L-arginine.[86,87]

Nitric oxide synthases exist as three isoforms: neuronal NOS (nNOS), endothelial NOS (eNOS), and inducible NOS (iNOS).[88,89] The nNOS isoform is localized in neurons and skeletal muscles, and regulates synaptic signaling, muscle contractility and local blood flow.[90] The eNOS isoform is exclusively present in the endothelium, and regulated blood pressure, platelet aggregation, leukocyte adherence, and vascular smooth muscle cell mitogenesis.[91] Nitric oxide produced from the nNOS and eNOS isoforms is relatively low in concentration (i.e., nM). The iNOS isoform is expressed in a wide array of cells and tissues (e.g., macrophages and neutrophils), and becomes activated upon exposure to endogenous pro-inflammatory mediators and endotoxins such as lipopolysaccharide (LPS).[92] Relatively high concentration (i.e., μM) of NO derived by iNOS involves wound repair and host defense in related to inflammation, infection, and diabetes.[92]

While the mechanisms of exactly how NO influences the FBR have not been completely elucidated, immense evidence suggests NO may increase in vivo glucose sensor performance by mitigating the FBR.[93-95] Nitric oxide has been known as an angiogenic signaling molecule, up-regulating VEGF production and increasing blood vessel growth.[96,97] This angiogenic behavior of NO may avoid the avascular collagen encapsulation by increasing vessel formation around implanted sensors. The improved blood vessel density at the site of the sensor surface may allow enhanced diffusion of glucose and oxygen, and thus improve glucose sensor accuracy. Additionally, the recruitment and activation of inflammatory cells in the early stages of the FBR relies on NO down-regulated pro-inflammatory cytokine expression (e.g., macrophage chemoattractant protein-1).[95,98] Carreau et al. reported reduced leukocyte adhesion at

elevated NO concentrations, suggesting NO could reduce the localized inflammatory response at the device-tissue interface as well as mitigate the subsequent FBR.[99] As such, NO may be able to accomplish the hypothesized actions of a dual DX/VEGF release while avoiding the antagonistic behavior between the drugs. Additionally, NO has a short half-life (<1 s in the presence of oxygen and hemoglobin) in biological milieu, arising from its high reactivity with transition metals, heme-containing proteins, and thiols.[85,86] Thus, NO's sphere of influence is limited to a few μm, thus eliminating undesirable cytotoxicity concerns.[100,101] In the presence of superoxide ($O_2^{\bullet -}$), NO will react to form peroxynitrite ($ONOO^-$), an even greater oxidant involved in the inflammatory response.[102] The demonstrated antibacterial activity of NO against both gram-positive and gram-negative bacteria may also allow for a reduced risk of infection due to percutaneous implantation.[103,104]

Given the role of NO in the immune response and as a bactericidal agent, NO-releasing substrates have been developed to achieve favorable tissue reactions regarding therapeutic applications.[94] Due to the reactive nature of gaseous NO, chemical strategies for NO storage and release have been designed to capture NO's pharmacological potential. To achieve in vivo NO release, NO donors have been employed as a method to store NO until breakdown of the donor upon some trigger.[105,106] The most common NO donors include *N*-diazeniumdiolates and *S*-nitrosothiols (Figure 1.4).

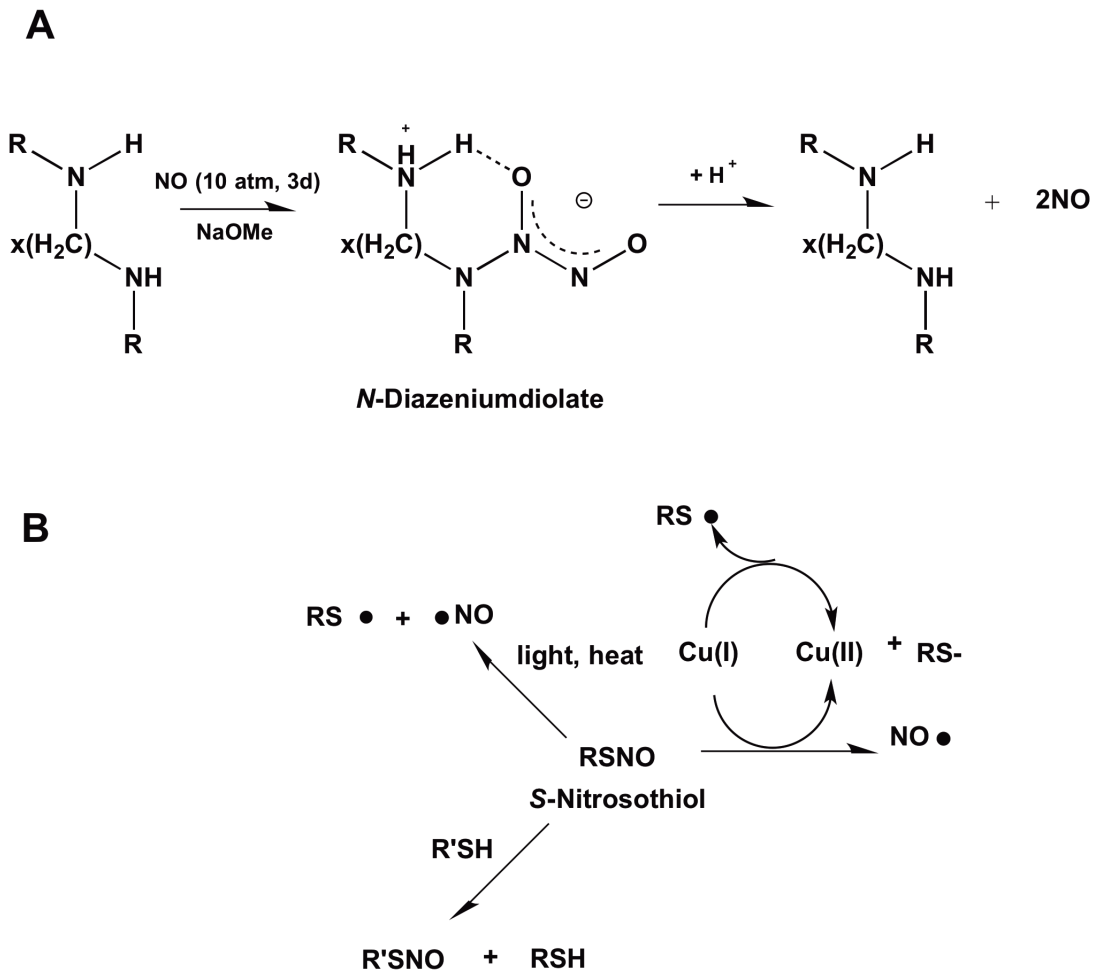

Figure 1.4. (A) *N*-diazeniumdiolate and (B) *S*-nitrosothiol nitric oxide (NO) donors with decomposition pathways. Decomposition kinetics is dependent on the chemical structure of the NO donor, pH, temperature, and/or presence of other biological milieu.

N-diazeniumdiolates are formed on secondary amines upon exposure to NO gas in basic solution.[107] In the presence of a proton source (e.g., water), the *N*-diazeniumdiolate breaks down to release two molecules of NO and the amine precursor.[107] The rate of NO release from this class of donor is highly dependent on the amine precursor structure, the surrounding chemical environment (e.g., hydrophobicity), and the solution condition (e.g., pH, ionic strength).[107,108] *S*-nitrosothiols are formed on thiols upon reaction with nitrosating agents (e.g., acidified nitrite). They decompose through various mechanisms when exposed to light, copper (I) ion, or heat.[109] The NO-release kinetics of *S*-nitrosothiols are dependent on the structure of the NO donor (e.g., steric hindrance) and release one equivalent of NO per thiol.[110] Organic molecules or macromolecules can be modified with both classes of NO donors to achieve targeted NO delivery. The concept of using NO-releasing materials for improving biocompatibility was initially investigated by utilizing low molecular weight (LMW) NO donors,[93,111,112], including 1-[(2-carboxylato)pyrrolidin-1-yl]]diazen-1-ium-1,2-diolate (PROLI/NO), 1-[*N*-(aminoethyl)-*N*-(2-ammonioethyl)amino] diazen-1-ium-1,2-diolate (DETA/NO), *S*-nitrosoglutathione (GSNO), and *S*-nitroso-*N*-acetylcysteine (SNAC). Unfortunately, materials utilizing LMW NO donors have limited NO release durations and payloads, as well as toxicity concerns. Significant effort has thus focused on the synthesis of macromolecular NO donors to improve NO payloads, durations, and cytotoxicity.[113] A number of macromolecular scaffolds capable of NO storage and delivery have been reported including xerogels,[114-116] silica nanoparticles,[117,118] dendrimers,[119-123] micelles,[124] NO donor-doped polymer matrices,[111,125-127] and synthetic polymer.[128-132]

Nitric oxide release from macromolecular scaffolds has been shown to reduce the FBR in vivo. Hetrick et al. reported a reduced inflammatory response, thinner capsule formation, and greater blood vessel formation for NO-releasing subcutaneous implants in rodent model at extended periods (>3 weeks) despite only 72 h of measureable NO released.[114] In this study, NO was released from xerogel membranes coated on medical grade silicone rubber. The secondary amine of *N*-(6-aminohexyl)aminopropyl trimethoxysilane (AHAP) on xerogel membrane was converted to *N*-diazeniumdiolates for NO storage resulting in NO payloads of 1.3 μmol cm^{-2} over 3 days.[114] This level of NO release reduced collagen encapsulation by ~20–25% at 3 and 6 weeks compare to controls. Reduced inflammatory cell adhesion near the implant was also noted with enhanced vascular density at 1 and 3 weeks.[114] Although the NO-releasing xerogel films clearly showed the effect of NO on reducing the FBR, the effect of NO flux and payload on mitigating the FBR was not evaluated in this study. Nichols et al. reported the effect of NO flux on subcutaneous implants in a porcine model.[133] The NO-releasing silica particle-doped polyurethane membranes exhibiting various NO release kinetics and payload (total NO released from 2.7 to 9.3 μmol/cm^2 and release duration from 6 h to 2 weeks) were coated on mock sensors and subcutaneously implanted. Although the initial bolus release of NO had a negative effect on the FBR (resulting in increased collagen density), the sustained release of NO with greater total NO release significantly reduced collagen capsule thickness and density.[133] The results indicated a possible benefit of NO-releasing membranes for improving in vivo glucose sensor performance.

Based on the potential of NO-releasing membranes for reducing the FBR, NO-releasing glucose sensor membranes have been developed by the Schoenfisch lab.[125,134,135] Since the harsh procedure required to modify membrane with *N*-diazeniumdiolate caused inadequate permeability of analyte, the NO-releasing glucose sensor membranes were fabricated by doping NO-releasing sol-gel particles in the polyurethane film[125] or a hydrophilic polymer (i.e., poly(vinylpyrrolidone)) in NO-releasing xerogel film,[135] as well as by micro-patterning NO-releasing xerogel membrane.[134] Of note, these NO-releasing membranes exhibited adequate analyte diffusion, demonstrating compatibility of NO release with enzyme-based glucose sensing. Additionally, the fabricated NO-releasing glucose sensors demonstrated not only sufficient sensor performance but also reduced bacterial adhesion holding potential to prevent the risk of infection during percutaneous implantation.

In vivo microdialysis studies were conducted by Nichols et al. in the subcutaneous space of rats to investigate the effects of NO on glucose recovery (i.e., resistance to mass transfer).[136] Polyarylethersulfone (PAES) microdialysis probes were perfused with saturated NO solutions for 8 h per day over 2 weeks to enable consistently high, though intermittent, NO release (162 pmol cm^{-2} s^{-1} of NO flux).[136] Using this methodology, zero-order NO-release kinetics were achieved with a daily total NO released of 4.6 μmol cm^{-2}. After 7 d, the NO-releasing probes recovered greater glucose concentrations compared to controls, indicating lower resistance to mass transfer in the surrounding tissue. Histological analysis of the tissue surrounding the implant after 14 d revealed reduced capsule thickness and inflammatory cell density. The authors concluded

that the mitigated FBR by NO release was thus at least partially responsible for the superior glucose recovery.[136]

Only one in vivo report evaluating the effect of NO release on subcutaneously implanted electrochemical glucose sensor performance has been published. Gifford et al. doped (Z)-1-[*N*-methyl-*N*-[6-(*N*-butylammoniohexyl)amino]]-diazen-1-ium-1,2-diolate (DBHD/NO) (i.e., LMW NO donor) into a polyurethane/polydimethylsiloxane glucose sensor membrane.[100] These membranes released NO with average NO flux of 7.52 $pmol \cdot cm^{-2} \cdot s^{-1}$. All of the NO was released after only 18 h.[100] Despite the quick depletion of NO, the analytical performance (i.e., sensor accuracy) of percutaneous NO-releasing sensors in rodent model was improved by 2.4 and 2.1% relative to controls on days 1 and 3, respectively. Histological analysis of the tissue adjacent to the sensors showed decreased inflammation at 24 but not 48 h.[100] Additionally, the NO-releasing glucose sensor exhibited a ~30 min run-in time (i.e., time required to stabilize sensor response after implantation), whereas a 4–10 h run-in time was observed for control sensors.[100] This work suggests that NO release may represent an important strategy for improving in vivo glucose sensor performance.

1.3.3 Passive coatings

Passive strategies have also been sought to improve the tissue-integration ability of glucose biosensors.[137] Since the surface chemistry at the tissue-sensor interface has a large influence on the activation of the immune response, research in this area has focused on modifying the chemical/physical properties of the outermost sensor surface.[138,139] Coating the sensor with biomolecules is one passive strategy used to

circumvent the FBR, since certain materials may allow the implant to appear less foreign to the host. A wide range of biomolecules have been used to interact with the surrounding tissue and mitigate the FBR including collagen,[140,141] chitosan,[142] cellulose,[143,144] heparin,[145] and dextran.[146,147] Although these materials are still capable of eliciting an immunogenic response and are often undesirably biodegradable,[144,148] biomolecules may prove beneficial for in vivo use. For example, phospholipids—a major component of cell membranes—has utilized as an outer layer to disguise the implant as more native than foreign.[149] These phospholipid membranes have a high resistance to biofouling, possibly arising from the high water uptake of the materials.[150] However, the phospholipid membranes have exhibited poor stability when grafted onto medical devices.[151] To improve stability, the phospholipids have been incorporated within polymers. The resulting phospholipid-containing polymers have shown favorable inflammatory response.[152,153] Kim et al. reported that macrophage adhesion to the phospholipid-containing polymer was reduced at 3 d relative to controls; however, it was not significantly affected at 7, 14 and 21 d, indicating only short-term advantages in terms of reducing an inflammatory response.[151] The general consensus is that despite the short-term benefits, phospholipid membranes are not capable of circumventing the FBR that plagues sensors.

Rather than relying on biomolecules to improve biocompatibility, polymers can be designed to reduce biofouling and mitigate the FBR. Synthetic polymers have been used due to their ability to resist biofouling caused by protein adsorption.[149] Nafion, a perfluorosulfonic acid-based polymer, has gathered attention as a biocompatible sensor

membrane.[154] The utility of Nafion is further enhanced by its negative charge and hydrophobicity, preventing interfering species from passing through the membrane. Additionally, Nafion is simple to apply and is durable for short-term (<1 week) implantations.[155,156] As an alternative to Nafion, hydrogels have also been proposed as outer glucose sensor membranes to enhance sensor lifetimes due to mechanical properties that mimic those of the surrounding subcutaneous tissue and lead to better tissue integration and reduced biofouling.[157-160] In multiple in vivo studies, the use of hydrogel coatings of various compositions resulted in less fibrous encapsulation compared to non-coated materials.[159-161] Of note, Zhang et al. recently reported zwitterionic hydrogels implanted on subcutaneous tissue in a rodent model demonstrated almost no capsule formation for 3 months.[162] In general when hydrogels were coupled to glucose sensors, the functional lifetime of the sensors was significantly increased, which was attributed to the improved biocompatibility at the sensor-tissue interface.[159,161] Due to the tunablity of water uptake, hydrogels are attractive as glucose sensing platforms.[157] The use of hydrogels has improved the linear range and reduced the oxygen dependence of glucose sensors due to their ability to store oxygen.[27,163] While hydrogels represent a promising strategy to enhance long-term sensor performance, concerns pertaining to their stability (e.g., adherence to underlying substrates, low mechanical strength, and leaching and subsequent cytotoxicity of the polymer precursors) make their use problematic. In contrast, polyurethane (PU) has been used extensively as an outer membrane that serves as a biocompatible interface with the surrounding host tissue. Early studies by Zhang and Wilson evaluated the in vitro and in vivo performance of PU as an outer membrane,

exhibiting its potential as a material for glucose sensor fabrication and use.[29] A number of studies have shown decreased collagen capsule formation and reduced FBGC adhesion by blending copolymers with PU (e.g., polyether PU, polycarbonate PU, and silicon modified PU).[164-167] Biocompatibility aside, PU allows for sufficient oxygen transport while limiting glucose diffusion to the sensor.[29] For these reasons, the outermost membranes of commercially available implantable glucose sensors mostly consist of PU.[168]

In addition to chemical composition, the physical characteristics of an implant surface play an important role in mitigating the FBR. In vitro tests have shown that surface structure affects protein[169,170] and leukocyte adhesion and activation.[139,171-174] Open pore structured surfaces generally lead to a more favorable FBR in vivo.[171,172] When varied on chemically identical materials, pore size greatly influences how the host tissue heals around the implant. The synthesis of porous materials as biocompatible coatings has been achieved by sphere-templating,[175] gas-foaming,[176] phase-separation techniques,[177] and electrospinning.[178-180] The ideal pore size required to improve wound healing ranges from 5–500 μm, depending on the desired application and polymer composition.[181] When implanted in vivo, porous materials in this size range have been demonstrated to promote angiogenesis and diminish fibrous encapsulation.[182,183] For example, Marshall and coworkers reported that a hydrogel with 35 μm pore size, synthesized through sphere-templating, promoted angiogenesis and reduce collagen thickness and density in rodent subcutaneous tissue.[183] The process by which different pore sizes mitigate the FBR has been attributed to the disruption of fibrous tissue

deposition while fostering vascularized cellular and tissue growth.[184] Additionally, pore sizes of 30–40 μm may force macrophages into a reconstructive phenotype, but will not cause macrophages to spread or phagocytose the material.[183,185]

The mechanical properties of a material also impact the resulting host response when implanted. External forces exerted on an implanted device can elicit an additional inflammatory response in the surrounding tissue.[15,186] Additionally, the modulus at the skin-device interface must be considered. The mismatches in the elastic modulus between an implant and the skin that surrounds the device (e.g., sensor) can result in sheer forces that induce a more severe FBR.[187] For example, the modulus of small fiber materials (<6 μm) has proved critical, with lower modulus fibers (e.g., polyurethane) showing reduced capsule formation compared to higher modulus materials (e.g., polyethylene and polyester).[188] This phenomenon poses a challenge in the design of percutaneous implanted glucose sensors because the modulii of the dermis and subcutaneous tissue fall in different ranges (56–260 and 0.12–23 kPa, respectively).[15,189-191]

1.3.4 Electrospinning porous membrane

Considering the aforementioned passive approaches for mitigating the FBR, electrospun fiber mats hold great potential as biocompatible sensor membranes among the available porous materials. Electrospun fibers are formed by the elongation and stretching of a polymer-containing liquid droplet under an electric field (typically between a high voltage needle and a grounded collector) when the applied electrostatic potential overcomes the surface tension of Taylor cone.[178-180] During the flight of fibers to the collector, solvent evaporates and electronic charges quickly accumulate at

favorably oriented ends of fiber surface, repelling until the dry fiber network arrives on the collector.[178] Electrospun fiber mats have monodisperse fiber diameters and a open porous structure, which can be controlled by fabrication parameters, polymer solution properties, and manner of collection.[180] The diameter, distribution, and shape of fibers are mostly affected by the viscosity and conductivity of the polymer solution. Additionally, solvent composition, electric field, distance between needle and collector, feed rate, and needle size can all affect the fiber properties.[178,180,192,193] The various fiber assemblies (e.g., such as random or aligned fibers, patterned fibers, and even three-dimensional fibrous architectures) can be achieved by using dynamic collection devices (e.g., rotating drum and parallel gap electrodes).[192] The resulting fiber mats exhibit high surface area to volume ratios, thus enabling cell infiltration and tissue incorporation due to the porous structure mimicking an extra cellular membrane (ECM).[171,194] Additionally, electrospun fiber mats have superior mechanical properties and flexibilities in surface functionalization compared to their non-porous analogs.[180,195] Moreover, therapeutic molecules such as antibiotics, DNA, growth factors, and anti-inflammatory drugs can be encapsulated and released in a controlled fashion.[195] Indeed, the electrospun fibers have been widely studied for biomedical applications, including wound dressings, tissue engineering scaffolds, and drug carriers.[194-197]

Along with the advantages of electrospun fibers, the effect of fiber properties on the FBR in vitro and in vivo has been reported.[198,199] The fiber diameter clearly influences the host response; small fibers (~600 nm of diameter) reduce the FBR more effectively than larger (>6 μm) fibers.[171,200] Saino et al. reported that poly(L-lactic acid)

(PLLA) nano-fibers had lower in vitro macrophage activation in the early inflammation stage (first 24 h) than micro-fibers, indicating the importance of fiber diameter (rater than fiber alignment) in determining the inflammatory response.[201] In contrast, Cao et al. reported that both alignment and orientation of the electrospun fibers greatly modulates the FBR in vivo; collagen capsule thickness for poly(ε-caprolactone) (PCL) fibers was decreased when their orientation was either aligned (~5 fold reduction) or random (~9 fold reduction) compared to solid films made from the same polymer.[171] The aligned fibers also demonstrated better cellular infiltration both in vivo and in vitro, while randomly oriented fibers exhibited distinct surface boundaries between the material and the fibrous capsule.[171]

Although electrospun fibers indicate great promise for use as biomaterials, only one report has been published for implantable glucose sensor applications. Wang et al. recently reported the randomly oriented polyurethane electrospun fibers coated on needle-type glucose sensors, utilizing the porous membrane as an outermost diffusion controlled membrane to mitigate the FBR.[202] Due to the solvent-free process of electrospun fiber formation, porous electrospun fibers can be coated directly onto enzyme-based electrochemical biosensors without compromising glucose oxidase activity.[202] However, the development of porous glucose sensor membranes incorporating an active release agent has not been reported to date.

Although drug-releasing sensor membranes have not been reported, many studies have demonstrated the controlled release of drugs from electrospun fibers.[195,198] For example, Vacanti et al. reported the development of DX-releasing electrospun fibers,[203]

where dexamethasone was incorporated into PLLA and PCL electrospun fibers exhibited distinct release durations (~1 month and 90 min, respectively) due to intermolecular interactions.[203] Of note, only DX-releasing PLLA fibers (i.e., longer release duration) significantly reduced inflammatory capsule formation compared to control PLLA and PCL scaffolds and DX-releasing PCL fibers.[203] This research highlighted that prolonged release of DX from porous materials may greatly benefit biomedical applications.

Coneski et al. reported on NO-releasing electrospun fibers.[126] The LMW molecule (i.e., disodium 1-[2-(carboxylate)pyrrolidin-1-yl]diazen-1-ium-1,2-diolate (PROLI/NO)) was doped into polyurethane and poly(vinyl chloride) solutions, and electrospun onto grounded disk-type collector to achieve microsized polymer fibers. The NO-release kinetics were controlled by the hydrophobicity of polymer with a certain concentration of dopant. As expected, NO release was limited due to use of the LMW NO donor. Nevertheless, this work set the stage for future studies aimed at longer NO-releasing fibers and fabrication of biosensors with fibrous sensor membranes.

1.4 Summary of dissertation research

My dissertation research has focused on the development of NO-releasing polyurethane membranes for implantable glucose biosensors. I have developed polyurethane films and porous membranes doped with NO-releasing scaffolds and evaluated the ability to fabricate needle-type glucose biosensors coated with these membranes. My specific aims have included:

1) developing controllable NO-releasing silica particle-doped polyurethane film membranes (i.e., release kinetics and total payload) by using polymers with varied water uptake and tuning the concentration of NO donor;
2) developing NO-releasing silica particle-doped porous materials via electrospinning and characterizing the NO release, fiber diameter, and mechanical properties;
3) fabricating needle-type implantable glucose biosensors coated with NO-releasing dendrimer-doped porous electrospun polyurethane membranes to combine the most promising active and passive anti-FBR strategies;
4) evaluating in vivo performance of the NO-releasing silica particle-doped polyurethane film-coated glucose biosensors in a healthy porcine model to study the effect of NO.

The goal of this introductory chapter was to provide the current status and ongoing challenges of continuous glucose monitoring systems, with a focus on percutaneously implanted electrochemical enzyme-based glucose sensors and the effect of the FBR on in vivo sensor performance. Additionally, this chapter covered the two approaches to developing biocompatible sensor membranes—active release of pharmaceutical agents and modification of chemical and physical membrane properties—to mitigate the FBR. In Chapter 2, fabrication and characterization of NO-releasing polyurethane sensor membranes using NO donor-modified silica nanoparticles is described in terms of the ability to achieve controlled NO release and adequate sensor performance. In Chapter 3, the development of NO-releasing silica nanoparticle-doped

polyurethane electrospun fibers is described in terms of NO release, fiber diameter, and mechanical properties. Chapter 4 describes the fabrication of implantable needle-type glucose sensors coated with a NO-releasing porous polyurethane membrane via electrospinning. Characterization of the NO-releasing porous membrane coated glucose sensors is detailed in terms of membrane stability and sensor performance. Chapter 5 details preliminary in vivo experiments using the NO-releasing silica particle-doped polyurethane membrane-coated glucose biosensors. The analytical performance of implanted NO-releasing glucose sensors is described with regard to the effect of NO in a freely moving healthy porcine model. Finally, Chapter 6 summarizes this research and provides future directions for expanding on this work.

1.5 References

(1) WHO "World Health Statistics 2012," World Health Organization, **2012**.

(2) "National diabetes fact sheet: national estimates and general information on diabetes and prediabetes," U.S. Department of Health and Human Services, Centers for Disease Control and Prevention, Atlanta, GA, **2011**.

(3) "Biosensors–A global market overview," IndustryExperts, Hyderabad, India, **2012**. BA326444671EN.

(4) Wang, J. "Electrochemical glucose biosensors" *Chemical Reviews* **2008**, *108*, 814-825.

(5) Updike, S. J.; Hicks, G. P. "The enzyme electrode" *Nature* **1967**, *214*, 986-988.

(6) Guilbault, G. G.; Lubrano, G. J. "An enzyme electrode for the amperometric determination of glucose" *Analytica Chimica Acta* **1973**, *64*, 439-455.

(7) Newman, J. D.; Turner, A. P. F. "Home blood glucose biosensors: a commercial perspective" *Biosensors and Bioelectronics* **2005**, *20*, 2435-2453.

(8) Heller, A. "Implanted electrochemical glucose sensors for the management of diabetes" *Annual Review of Biomedical Engineering* **1999**, *1*, 153-175.

(9) Wilson, G. S.; Hu, Y. B. "Enzyme based biosensors for in vivo measurements" *Chemical Reviews* **2000**, *100*, 2693-2704.

(10) Wilson, G. S.; Zhang, Y. "Introduction to the glucose sensing problem" In *In Vivo Glucose Sensing*; Cunningham, D. D., Stenken, J. A., Eds.; Wiley, 2010.

(11) Vaddiraju, S.; Burgess, D. J.; Tomazos, I.; Jain, F. C.; Papadimitrakopoulos, F. "Technologies for continuous glucose monitoring: Current problems and future promises" *Journal of Diabetes Science and Technology* **2010**, *4*, 1540-1562.

(12) Degani, Y.; Heller, A. "Direct electrical communication between chemically modified enzymes and metal electrodes. I. Electron transfer from glucose oxidase to metal electrodes via electron relays, bound covalently to the enzyme" *The Journal of Physical Chemistry* **1987**, *91*, 1285-1289.

(13) Pishko, M. V.; Katakis, I.; Lindquist, S.-E.; Ye, L.; Gregg, B. A.; Heller, A. "Direct electrical communication between graphite electrodes and surface adsorbed glucose oxidase/redox polymer complexes" *Angewandte Chemie International Edition in English* **1990**, *29*, 82-84.

(14) Gough, D. A.; Kumosa, L. S.; Routh, T. L.; Lin, J. T.; Lucisano, J. Y. "Function of an implanted tissue glucose sensor for more than 1 year in animals" *Science Translational Medicine* **2010**, *2*, 42ra53.

(15) Helton, K. L.; Ratner, B. D.; Wisniewski, N. A. "Biomechanics of the sensor–tissue interface—Effects of motion, pressure, and design on sensor performance and the foreign body response—Part I: Theoretical framework" *Journal of Diabetes Science and Technology* **2011**, *5*, 632-646.

(16) Shichiri, M.; Asakawa, N.; Yamasaki, Y.; Kawamori, R.; Abe, H. "Telemetry glucose monitoring device with needle-type glucose sensor: A useful tool for blood glucose monitoring in diabetic individuals" *Diabetes Care* **1986**, *9*, 298-301.

(17) Bindra, D. S.; Zhang, Y.; Wilson, G. S.; Sternberg, R.; Thevenot, D. R.; Moatti, D.; Reach, G. "Design and in vitro studies of a needle-type glucose sensor for subcutaneous monitoring" *Analytical Chemistry* **1991**, *63*, 1692-1696.

(18) Henning, T. "Commercially available continuous glucose monitoring systems" In *In Vivo Glucose Sensing*; Cunningham, D. D., Stenken, J. A., Eds.; John Wiley & Sons, Inc., 2010.

(19) Wilson, G. S.; Gifford, R. "Biosensors for real-time *in vivo* measurements" *Biosensors and Bioelectronics* **2005**, *20*, 2388-2403.

(20) Barlett, P. N.; Cooper, J. M. "A review of the immobilization of enzymes in electropolymerized films" *Journal of Electroanalytical Chemistry* **1993**, *362*, 1-12.

(21) Chen, X.; Matsumoto, N.; Hu, Y.; Wilson, G. S. "Electrochemically mediated electrodeposition/electropolymerization to yield a glucose microbiosensor with improved characteristics" *Analytical Chemistry* **2002**, *74*, 368-372.

(22) Wilson, G. S.; Johnson, M. A. "In-vivo electrochemistry: What can we learn about living systems?" *Chemical Reviews* **2008**, *108*, 2462-2481.

(23) Koschwanez, H. E.; Reichert, W. M. "In vitro, in vivo and post explantation testing of glucose-detecting biosensors: Current methods and recommendations" *Biomaterials* **2007**, *28*, 3687-3703.

(24) Cambiaso, A.; Delfino, L.; Grattarola, M.; Verreschi, G.; Ashworth, D.; Maines, A.; Vadgama, P. "Modelling and simulation of a diffusion limited glucose biosensor" *Sensors and Actuators B: Chemical* **1996**, *33*, 203-207.

(25) Galeska, I.; Chattopadhyay, D.; Moussy, F.; Papadimitrakopoulos, F. "Calcification-resistant nafion/Fe^{3+} assemblies for implantable biosensors" *Biomacromolecules* **2000**, *1*, 202-207.

(26) Ishihara, K.; Tanaka, S.; Furukawa, N.; Nakabayashi, N.; Kurita, K. "Improved blood compatibility of segmented polyurethanes by polymeric additives having phospholipid polar groups. I. Molecular design of polymeric additives and their functions" *Journal of Biomedical Materials Research* **1996**, *32*, 391-399.

(27) Tipnis, R.; Vaddiraju, S.; Jain, F.; Burgess, D. J.; Papadimitrakopoulos, F. "Layer by layer assembled semipermeable membrane for amperometric glucose sensors" *Journal of Diabetes Science and Technology* **2007**, *1*, 193-200.

(28) Moussy, F.; Harrison, D. J.; O'Brien, D. W.; Rajotte, R. V. "Performance of subcutaneously implanted needle-type glucose sensors employing a novel trilayer coating" *Analytical Chemistry* **1993**, *65*, 2072-2077.

(29) Zhang, Y.; Wilson, G. S. "In vitro and in vivo evaluation of oxygen effects on a glucose oxidase based implantable glucose sensor" *Analytica Chimica Acta* **1993**, *281*, 513-520.

(30) Groenendaal, W.; Basum, G. v.; Schmidt, K. A.; Hilbers, P. A. J.; vanRiel, N. A. W. "Quantifying the composition of human skin for glucose sensor development " *Journal of Diabetes Science and Technology* **2010**, *4*, 1032-1040.

(31) Alexeeva, N. V.; Arnold, M. A. "Impact of tissue heterogeneity on noninvasive near-infrared glucose measurements in interstitial fluid of rat skin" *Journal of Diabetes Science and Technology* **2010**, *4*, 1041–1054.

(32) Gibney, M. A.; Arce, C. H.; Byron, K. J.; Hirsch, L. J. "Skin and subcutaneous adipose layer thickness in adults with diabetes at sites used for insulin injections:

implications for needle length recommendations" *Current Medical Research and Opinion* **2010**, *26*, 1519-1530.

(33) Myrer, J. W.; Gary Measom, R.; Durrant, E.; Fellingham, G. W. "Cold- and hot-pack contrast therapy: Subcutaneous and intramuscular temperature change" *Journal of Athletic Training* **1997**, *32*, 238-241.

(34) Gilligan, B. C.; Shults, M.; Rhodes, R. K.; Jacobs, P. G.; Brauker, J. H.; Pintar, T. J.; Updike, S. J. "Feasibility of continuous long-term glucose monitoring from a subcutaneous glucose sensor in humans" *Diabetes Technology and Therapeutics* **2004**, *6*, 378-386.

(35) Castle, J. R.; Ward, W. K. "Amperometric glucose sensors: Sources of error and potential benefit of redundancy" *Journal of Diabetes Science and Technology* **2010**, *4*, 221-225.

(36) Petrofsky, J. S. "The effect of type-2 diabetes-related vascular endothelial dysfunction on skin physiology and activities of daily living " *Journal of Diabetes Science and Technology* **2011**, *5*, 657-667.

(37) Anderson, J. M.; Rodriguez, A.; Chang, D. T. "Foreign body reaction to biomaterials" *Seminars in Immunology* **2008**, *20*, 86-100.

(38) Williams, D. F. "On the mechanisms of biocompatibility" *Biomaterials* **2008**, *29*, 2941-2953.

(39) Isenhath, S. N.; Fukano, Y.; Usui, M. L.; Underwood, R. A.; Irvin, C. A.; Marshall, A. J.; Hauch, K. D.; Ratner, B. D.; Fleckman, P.; Olerud, J. E. "A mouse model to evaluate the interface between skin and a percutaneous device" *Journal of Biomedical Materials Research Part A* **2007**, *83*, 915-22.

(40) Anderson, J. M. "Biological responses to materials" *Annual Review of Materials Research* **2001**, *31*, 81-110.

(41) ThomeDuret, V.; Gangnerau, M. N.; Zhang, Y.; Wilson, G. S.; Reach, G. "Modification of the sensitivity of glucose sensor implanted into subcutaneous tissue" *Diabetes & Metabolism* **1996**, *22*, 174-178.

(42) Gerritsen, M.; Jansen, J. A.; Kros, A.; Vriezema, D. M.; Sommerdijk, N. A. J. M.; Nolte, R. J. M.; Lutterman, J. A.; Van Hövell, S. W. F. M.; Van der Gaag, A.

"Influence of inflammatory cells and serum on the performance of implantable glucose sensors" *Journal of Biomedical Materials Research* **2001**, *54*, 69-75.

(43) Gifford, R.; Kehoe, J. J.; Barnes, S. L.; Kornilayev, B. A.; Alterman, M. A.; Wilson, G. S. "Protein interactions with subcutaneously implanted biosensors" *Biomaterials* **2006**, *27*, 2587-2598.

(44) Zhao, Q. H.; McNally, A. K.; Rubin, K. R.; Renier, M.; Wu, Y.; Rose-Caprara, V.; Anderson, J. M.; Hiltner, A.; Urbanski, P.; Stokes, K. "Human plasma α2-macroglobulin promotes in vitro oxidative stress cracking of pellethane 2363-80A: In vivo and in vitro correlations" *Journal of Biomedical Materials Research* **1993**, *27*, 379-388.

(45) Luttikhuizen, D. T.; Harmsen, M. C.; VanLuyn., M. J. A. "Cellular and molecular dynamics in the foreign body reaction" *Tissue Engineering* **2006**, *12*, 1955-1970.

(46) Anderson, J. M.; Jones, J. A. "Phenotypic dichotomies in the foreign body reaction" *Biomaterials* **2007**, *28*, 5114-5120.

(47) Jones, J. A.; Chang, D. T.; Meyerson, H.; Colton, E.; Kwon, I. K.; Matsuda, T.; Anderson, J. M. "Proteomic analysis and quantification of cytokines and chemokines from biomaterial surface-adherent macrophages and foreign body giant cells" *Journal of Biomedical Materials Research Part A* **2007**, *83A*, 585-596.

(48) Zhao, Q.; Topham, N.; Anderson, J. M.; Hiltner, A.; Lodoen, G.; Payet, C. R. "Foreign-body giant cells and polyurethane biostability: In vivo correlation of cell adhesion and surface cracking" *Journal of Biomedical Materials Research* **1991**, *25*, 177-183.

(49) Anderson, J. M.; Defife, K.; McNally, A.; Collier, T.; Jenney, C. "Monocyte, macrophage and foreign body giant cell interactions with molecularly engineered surfaces" *Journal of Materials Science: Materials in Medicine* **1999**, *10*, 579-88.

(50) Kao, W. J.; Zhao, Q. H.; Hiltner, A.; Anderson, J. M. "Theoretical analysis of in vivo macrophage adhesion and foreign body gaint cell formation on polydimethylsiloxane, low density polyethylene, and polyetherurethanes" *Journal of Biomedical Materials Research* **1994**, *28*, 73-79.

(51) Forster, J.; Morris, A. S.; Shearer, J. D.; Mastrofrancesco, B.; Inman, K. C.; Lawler, R. G.; Bowen, W.; Caldwell, M. D. "Glucose uptake and flux through

phosphofructokinase in wounded rat skeletal muscle." *American Journal of Physiology* **1989**, *256*, E788-E797.

(52) Sieminski, A. L.; Gooch, K. J. "Biomaterial-microvasculature interactions" *Biomaterials* **2000**, *21*, 2233-2241.

(53) Novak, M.; Yuan, F.; Reichert, W. "Modeling the relative impact of capsular tissue effects on implanted glucose sensor time lag and signal attenuation" *Analytical and Bioanalytical Chemistry* **2010**, *398*, 1695-1705.

(54) Sharkawy, A. A.; Klitzman, B.; Truskey, G. A.; Reichert, W. M. "Engineering the tissue which encapsulates subcutaneous implants. I. Diffusion properties" *Journal of Biomedical Materials Research Part A* **1997**, *37*, 401-412.

(55) Jablecki, M.; Gough, D. A. "Simulations of the frequency response of implantable glucose sensors" *Analytical Chemistry* **2000**, *72*, 1853-1859.

(56) Sung, J.; Barone, P. W.; Kong, H.; Strano, M. S. "Sequential delivery of dexamethasone and VEGF to control local tissue response for carbon nanotube fluorescence based micro-capillary implantable sensors" *Biomaterials* **2009**, *30*, 622-631.

(57) Norton, L. W.; Koschwanez, H. E.; Wisniewski, N. A.; Klitzman, B.; Reichert, W. M. "Vascular endothelial growth factor and dexamethasone release from nonfouling sensor coatings affect the foreign body response" *Journal of Biomedical Materials Research Part A* **2007**, *81*, 858-869.

(58) Norton, L. W.; Tegnell, E.; Toporek, S. S.; Reichert, W. M. "In vitro characterization of vascular endothelial growth factor and dexamethasone releasing hydrogels for implantable probe coatings" *Biomaterials* **2005**, *26*, 3285-3297.

(59) Patil, S. D.; Papadmitrakopoulos, F.; Burgess, D. J. "Concurrent delivery of dexamethasone and VEGF for localized inflammation control and angiogenesis" *Journal of Controlled Release* **2007**, *117*, 68-79.

(60) Klueh, U.; Dorsky, D. I.; Kreutzer, D. L. "Enhancement of implantable glucose sensor function in vivo using gene transfer-induced neovascularization" *Biomaterials* **2005**, *26*, 1155-63.

(61) Ward, W. K.; Wood, M. D.; Casey, H. M.; Quinn, M. J.; Federiuk, I. F. "The effect of local subcutaneous delivery of vascular endothelial growth factor on the function of a chronically implanted amperometric glucose sensor" *Diabetes Technology and Therapeutics* **2004**, *6*, 137-145.

(62) Ward, W. K.; Quinn, M. J.; Wood, M. D.; Tiekotter, K. L.; Pidikiti, S.; Gallagher, J. A. "Vascularizing the tissue surrounding a model biosensor: how localized is the effect of a subcutaneous infusion of vascular endothelial growth factor (VEGF)?" *Biosensors and Bioelectronics* **2003**, *19*, 155-63.

(63) Werner, S.; Grose, R. "Regulation of wound healing by growth factors and cytokines" *Physiological Reviews* **2003**, *83*, 835-870.

(64) Brown, L.; Yeo, K.; Berse, B.; Yeo, T.; Senger, D.; Dvorak, H.; van de Water, L. "Expression of vascular permeability factor (vascular endothelial growth factor) by epidermal keratinocytes during wound healing" *The journal of experimental medicine* **1992**, *176*, 1375-1379.

(65) Frank, S.; Hübner, G.; Breier, G.; Longaker, M. T.; Greenhalgh, D. G.; Werner, S. "Regulation of vascular endothelial growth factor expression in cultured keratinocytes.: Implications for normal and impaired wound healing" *Journal of Biological Chemistry* **1995**, *270*, 12607-12613.

(66) Ferrara, N. "Vascular endothelial growth factor: Basic science and clinical progress" *Endocrine Reviews* **2004**, *25*, 581-611.

(67) Nagy, J.; Benjamin, L.; Zeng, H.; Dvorak, A.; Dvorak, H. "Vascular permeability, vascular hyperpermeability and angiogenesis" *Angiogenesis* **2008**, *11*, 109-119.

(68) Zhao, Q.; Egashira, K.; Inoue, S.; Usui, M.; Kitamoto, S.; Ni, W.; Ishibashi, M.; Hiasa, K.-i.; Ichiki, T.; Shibuya, M.; Takeshita, A. "Vascular endothelial growth factor Is necessary in the development of arteriosclerosis by recruiting/activating monocytes in a rat model of long-term inhibition of nitric oxide synthesis" *Circulation* **2002**, *105*, 1110-1115.

(69) Reinders, M. E. J.; Sho, M.; Izawa, A.; Wang, P.; Mukhopadhyay, D.; Koss, K. E.; Geehan, C. S.; Luster, A. D.; Sayegh, M. H.; Briscoe, D. M. "Proinflammatory functions of vascular endothelial growth factor in alloimmunity" *The Journal of Clinical Investigation* **2003**, *112*, 1655-1665.

(70) Klueh, U.; Dorsky, D. I.; Kreutzer, D. L. "Use of vascular endothelial cell growth factor gene transfer to enhance implantable sensor function in vivo" *Journal of Biomedical Materials Research Part A* **2003**, *67*, 1072-86.

(71) El Azab, S. R.; Rosseel, P. M. J.; de Lange, J. J.; Groeneveld, A. B. J.; van Strik, R.; van Wijk, E. M.; Scheffer, G. J. "Dexamethasone decreases the pro-to-anti-inflammatory cytokine ratio during cardiac surgery" *British Journal of Anaesthesia* **2002**, *88*, 496-501.

(72) Strecker, E. P.; Gabelmann, A.; Boos, I.; Lucas, C.; Xu, Z.; Haberstroh, J.; Freudenberg, N.; Stricker, H.; Langer, M.; Betz, E. "Effect on intimal hyperplasia of dexamethasone released from coated metal stents compared with non-coated stents in canine femoral arteries" *CardioVascular and Interventional Radiology* **1998**, *21*, 487-496.

(73) Beer, H. D.; Fässler, R.; Werner, S. "Glucocorticoid-regulated gene expression during cutaneous wound repair" *Vitam Horm* **2000**, *59*, 217-239.

(74) Coutinho, A. E.; Chapman, K. E. "The anti-inflammatory and immunosuppressive effects of glucocorticoids, recent developments and mechanistic insights" *Molecular and Cellular Endocrinology* **2011**, *335*, 2-13.

(75) Hickey, T.; Kreutzer, D.; Burgess, D. J.; Moussy, F. "In vivo evaluation of a dexamethasone/PLGA microsphere system designed to suppress the inflammatory tissue response to implantable medical devices" *Journal of Biomedical Materials Research* **2002**, *61*, 180-187.

(76) Hickey, T.; Kreutzer, D.; Burgess, D. J.; Moussy, F. "Dexamethasone/PLGA microspheres for continuous delivery of an anti-inflammatory drug for implantable medical devices" *Biomaterials* **2002**, *23*, 1649-56.

(77) Patil, S. D.; Papadimitrakopoulos, F.; Burgess, D. J. "Dexamethasone-loaded poly(lactic-co-glycolic) acid microspheres/poly(vinyl alcohol) hydrogel composite coatings for inflammation control" *Diabetes Technology and Therapeutics* **2004**, *6*, 887-897.

(78) Bhardwaj, U.; Sura, R.; Papadimitrakopoulos, F.; Burgess, D. J. "Controlling acute inflammation with fast releasing dexamethasone-PLGA microsphere/PVA hydrogel composites for implantable devices" *Journal of Diabetes Science and Technology* **2007**, *1*, 8-17.

(79) Ziesché, E.; Scheiermann, P.; Bachmann, M.; Sadik, C. D.; Hofstetter, C.; Zwissler, B.; Pfeilschifter, J.; Mühl, H. "Dexamethasone suppresses interleukin-22 associated with bacterial infection in vitro and in vivo" *Clinical & Experimental Immunology* **2009**, *157*, 370-376.

(80) Jamieson, A. M.; Yu, S.; Annicelli, C. H.; Medzhitov, R. "Influenza virus-induced glucocorticoids compromise innate host defense against a secondary bacterial infection" *Cell Host & Microbe* **2010**, *7*, 103-114.

(81) Edelman, J. L.; Lutz, D.; Castro, M. R. "Corticosteroids inhibit VEGF-induced vascular leakage in a rabbit model of blood-retinal and blood-aqueous barrier breakdown" *Experimental Eye Research* **2005**, *80*, 249-258.

(82) Machein; Kullmer; Rönicke; Krieg; Damert; Breier; Risau; Plate "Differential downregulation of vascular endothelial growth factor by dexamethasone in normoxic and hypoxic rat glioma cells" *Neuropathology and Applied Neurobiology* **1999**, *25*, 104-112.

(83) Wu, W. S.; Wang, F. S.; Yang, K. D.; Huang, C. C.; Kuo, Y. R. "Dexamethasone induction of keloid regression through effective suppression of VEGF expression and keloid fibroblast proliferation" *Journal of Investigative Dermatology* **2006**, *126*, 1264-71.

(84) Ignarro, L. J.; Buga, G. M.; Wood, K. S.; Byrns, R. E.; Chaudhuri, G. "Endothelium-derived relaxing factor produced and released from artery and vein is nitric oxide" *Proceedings of the National Academy of Sciences* **1987**, *84*, 9265-9269.

(85) Ignarro, L. J. "Nitric oxide: A unique endogenous signaling molecule in vascular biology (Nobel lecture)" *Angewandte Chemie International Edition* **1999**, *38*, 1882-1892.

(86) Ignarro, L. J. *Nitric oxide : biology and pathobiology*; Academic Press: San Diego, Calif.; London, 2000.

(87) Williams, D. L. H. "A chemist's view of the nitric oxide story" *Organic and Biomolecular Chemistry* **2003**, *1*, 441-449.

(88) Walford, G.; Loscalzo, J. "Nitric oxide in vascular biology" *Journal of Thrombosis and Haemostasis* **2003**, *1*, 2112-2118.

(89) Griffith, O. W.; Stuehr, D. J. "Nitric oxide synthases: Properties and catalytic mechanism" *Annual Review of Physiology* **1995**, *57*, 707-734.

(90) Mungrue, I. N.; Bredt, D. S. "nNOS at a glance: implications for brain and brawn" *Journal of Cell Science* **2004**, *117*, 2627-2629.

(91) Shaul, P. W. "Regulation of endothelial nitric oxide synthase: Location, Location, Location" *Annual Review of Physiology* **2002**, *64*, 749-774.

(92) Lechner, M.; Lirk, P.; Rieder, J. "Inducible nitric oxide synthase (iNOS) in tumor biology: The two sides of the same coin" *Seminars in Cancer Biology* **2005**, *15*, 277-289.

(93) Amadeu, T. P.; Seabra, A. B.; de Oliveira, M. G.; Monte-Alto-Costa, A. "Nitric oxide donor improves healing if applied on inflammatory and proliferative phase" *Journal of Surgical Research* **2008**, *149*, 84-93.

(94) Carpenter, A. W.; Schoenfisch, M. H. "Nitric oxide release: Part II. Therapeutic applications" *Chemical Society Reviews* **2012**, *41*, 3742-3752.

(95) Coleman, J. W. "Nitric oxide in immunity and inflammation" *International Immunopharmacology* **2001**, *1*, 1397-1406.

(96) Cooke, J. P. "NO and angiogenesis" *Atherosclerosis Supplements* **2003**, *4*, 53-60.

(97) Dulak, J.; Józkowicz, A. "Regulation of vascular endothelial growth factor synthesis by nitric oxide: Facts and controversies" *Antioxidants & Redox Signaling* **2003**, *5*, 123-132.

(98) Schwentker, A.; Vodovotz, Y.; Weller, R.; Billiar, T. R. "Nitric oxide and wound repair: role of cytokines?" *Nitric Oxide* **2002**, *7*, 1-10.

(99) Carreau, A.; Kieda, C.; Grillon, C. "Nitric oxide modulates the expression of endothelial cell adhesion molecules involved in angiogenesis and leukocyte recruitment" *Experimental Cell Research* **2011**, *317*, 29-41.

(100) Gifford, R.; Batchelor, M. M.; Lee, Y.; Gokulrangan, G.; Meyerhoff, M. E.; Wilson, G. S. "Mediation of in vivo glucose sensor inflammatory response via nitric oxide release" *Journal of Biomedical Materials Research Part A* **2005**, *75A*, 755-766.

(101) Shin, J. H.; Schoenfisch, M. H. "Improving the biocompatibility of in vivo sensors via nitric oxide release" *Analyst* **2006**, *131*, 609-615.

(102) Nablo, B. J.; Prichard, H. L.; Butler, R. D.; Klitzman, B.; Schoenfisch, M. H. "Inhibition of implant-associated infections via nitric oxide" *Biomaterials* **2005**, *26*, 6984-6990.

(103) Hetrick, E. M.; Schoenfisch, M. H. "Reducing implant-related infections: active release strategies" *Chemical Society Reviews* **2006**, *35*, 780-789.

(104) Hetrick, E. M.; Schoenfisch, M. H. "Antibacterial nitric oxide-releasing xerogels: Cell viability and parallel plate flow cell adhesion studies" *Biomaterials* **2007**, *28*, 1948-1956.

(105) Wang, P. G.; Xian, M.; Tang, X.; Wu, X.; Wen, Z.; Cai, T.; Janczuk, A. J. "Nitric oxide donors: chemical activities and biological applications" *Chemical Reviews* **2002**, *102*, 1091-1134.

(106) Barman, I.; Kong, C.-R.; Singh, G. P.; Dasari, R. R.; Feld, M. S. "Accurate spectroscopic calibration for noninvasive glucose monitoring by modeling the physiological glucose dynamics" *Analytical Chemistry* **2010**, *82*, 6104-6114.

(107) Hrabie, J. A.; Keefer, L. K. "Chemistry of the nitric oxide-releasing diazeniumdiolate ("nitrosohydroxylamine") functional group and its oxygen-substituted derivatives" *Chemical Reviews* **2002**, *102*, 1135-1154.

(108) Davies, K. M.; Wink, D. A.; Saavedra, J. E.; Keefer, L. K. "Chemistry of the diazeniumdiolates. 2. Kinetics and mechanism of dissociation to nitric oxide in aqueous solution" *Journal of the American Chemical Society* **2001**, *123*, 5473-5481.

(109) Williams, D. L. H. "The chemistry of *S*-Nitrosothiols" *Accounts of Chemical Research* **1999**, *32*, 869-876.

(110) Riccio, D. A.; Coneski, P. N.; Nichols, S. P.; Broadnax, A. D.; Schoenfisch, M. H. "Photoinitiated nitric oxide-releasing tertiary *S*-nitrosothiol-modified xerogels" *ACS Applied Materials & Interfaces* **2012**, *4*, 796-804.

(111) Frost, M. C.; Reynolds, M. M.; Meyerhoff, M. E. "Polymers incorporating nitric oxide releasing/generating substances for improved biocompatibility of blood-contacting medical devices" *Biomaterials* **2005**, *26*, 1685-1693.

(112) Seabra, A. B.; Duran, N. "Nitric oxide-releasing vehicles for biomedical applications" *Journal of Materials Chemistry* **2010**, *20*, 1624-1637.

(113) Riccio, D. A.; Schoenfisch, M. H. "Nitric oxide release: Part I. Macromolecular scaffolds" *Chemical Society Reviews* **2012**, *41*, 3731-3741.

(114) Hetrick, E. M.; Prichard, H. L.; Klitzman, B.; Schoenfisch, M. H. "Reduced foreign body response at nitric oxide-releasing subcutaneous implants" *Biomaterials* **2007**, *28*, 4571-4580.

(115) Nablo, B. J.; Rothrock, A. R.; Schoenfisch, M. H. "Nitric oxide-releasing sol-gels as antibacterial coatings for orthopedic implants" *Biomaterials* **2005**, *26*, 917-924.

(116) Riccio, D. A.; Dobmeier, K. P.; Hetrick, E. M.; Privett, B. J.; Paul, H. S.; Schoenfisch, M. H. "Nitric oxide-releasing *S*-nitrosothiol-modified xerogels" *Biomaterials* **2009**, *30*, 4494-4502.

(117) Shin, J. H.; Metzger, S. K.; Schoenfisch, M. H. "Synthesis of nitric oxide-releasing silica nanoparticles" *Journal of the American Chemical Society* **2007**, *129*, 4612-4619.

(118) Riccio, D. A.; Nugent, J. L.; Schoenfisch, M. H. "Stöber synthesis of nitric oxide-releasing *S*-nitrosothiol-modified silica particles" *Chemistry of Materials* **2011**, *23*, 1727-1735.

(119) Lu, Y.; Sun, B.; Li, C.; Schoenfisch, M. H. "Structurally diverse nitric oxide-releasing poly(propylene imine) dendrimers" *Chemistry of Materials* **2011**, *23*, 4227-4233.

(120) Stasko, N. A.; Fischer, T. H.; Schoenfisch, M. H. "*S*-nitrosothiol-modified dendrimers as nitric oxide delivery vehicles" *Biomacromolecules* **2008**, *9*, 834-841.

(121) Stasko, N. A.; Johnson, C. B.; Schoenfisch, M. H.; Johnson, T. A.; Holmuhamedov, E. L. "Cytotoxicity of polypropylenimine dendrimer conjugates on cultured endothelial cells" *Biomacromolecules* **2007**, *8*, 3853-3859.

(122) Stasko, N. A.; Schoenfisch, M. H. "Dendrimers as a scaffold for nitric oxide release" *Journal of the American Chemical Society* **2006**, *128*, 8265-8271.

(123) Sun, B.; Slomberg, D. L.; Chudasama, S. L.; Lu, Y.; Schoenfisch, M. H. "Nitric oxide-releasing dendrimers as antibacterial agents" *Biomacromolecules* **2012**, *13*, 3343-3354.

(124) Jo, Y. S.; van der Vlies, A. J.; Gantz, J.; Thacher, T. N.; Antonijevic, S.; Cavadini, S.; Demurtas, D.; Stergiopulos, N.; Hubbell, J. A. "Micelles for delivery of nitric oxide" *Journal of the American Chemical Society* **2009**, *131*, 14413-14418.

(125) Shin, J. H.; Marxer, S. M.; Schoenfisch, M. H. "Nitric oxide-releasing sol-gel particle/polyurethane glucose biosensors" *Analytical Chemistry* **2004**, *76*, 4543-4549.

(126) Coneski, P. N.; Nash, J. A.; Schoenfisch, M. H. "Nitric oxide-releasing electrospun polymer microfibers" *ACS Applied Materials & Interfaces* **2011**, *3*, 426-432.

(127) Koh, A.; Riccio, D. A.; Sun, B.; Carpenter, A. W.; Nichols, S. P.; Schoenfisch, M. H. "Fabrication of nitric oxide-releasing polyurethane glucose sensor membranes" *Biosensors and Bioelectronics* **2011**, *28*, 17-24.

(128) Mowery, K. A.; Schoenfisch, M. H.; Saavedra, J. E.; Keefer, L. K.; Meyerhoff, M. E. "Preparation and characterization of hydrophobic polymeric films that are thromboresistant via nitric oxide release" *Biomaterials* **2000**, *21*, 9-21.

(129) Parzuchowski, P. G.; Frost, M. C.; Meyerhoff, M. E. "Synthesis and characterization of polymethacrylate-based nitric oxide donors" *Journal of the American Chemical Society* **2002**, *124*, 12182-12191.

(130) Zhou, Z.; Meyerhoff, M. E. "Polymethacrylate-based nitric oxide donors with pendant *N*-diazeniumdiolated alkyldiamine moieties: Synthesis, characterization, and preparation of nitric oxide releasing polymeric coatings" *Biomacromolecules* **2005**, *6*, 780-789.

(131) Coneski, P. N.; Rao, K. S.; Schoenfisch, M. H. "Degradable nitric oxide-releasing biomaterials via post-polymerization functionalization of cross-linked polyesters" *Biomacromolecules* **2010**, *11*, 3208-3215.

(132) Coneski, P. N.; Schoenfisch, M. H. "Synthesis of nitric oxide-releasing polyurethanes with S-nitrosothiol-containing hard and soft segments" *Polymer Chemistry* **2011**, *2*, 906-913.

(133) Nichols, S. P.; Koh, A.; Brown, N. L.; Rose, M. B.; Sun, B.; Slomberg, D. L.; Riccio, D. A.; Klitzman, B.; Schoenfisch, M. H. "The effect of nitric oxide surface flux on the foreign body response to subcutaneous implants" *Biomaterials* **2012**, *33*, 6305-6312.

(134) Oh, B. K.; Robbins, M. E.; Nablo, B. J.; Schoenfisch, M. H. "Miniaturized glucose biosensor modified with a nitric oxide-releasing xerogel microarray" *Biosensors and Bioelectronics* **2005**, *21*, 749-757.

(135) Schoenfisch, M. H.; Rothrock, A. R.; Shin, J. H.; Polizzi, M. A.; Brinkley, M. F.; Dobmeier, K. P. "Poly(vinylpyrrolidone)-doped nitric oxide-releasing xerogels as glucose biosensor membranes" *Biosensors and Bioelectronics* **2006**, *22*, 306-312.

(136) Nichols, S. P.; Le, N. N.; Klitzman, B.; Schoenfisch, M. H. "Increased in vivo glucose recovery via nitric oxide release" *Analytical Chemistry* **2011**, *83*, 1180-1184.

(137) Ward, W. K.; Duman, H. M. "Strategies to overcome biological barriers to biosensing" In *In Vivo Glucose Sensing*; John Wiley & Sons, Inc., 2010.

(138) Brodbeck, W. G.; Voskerician, G.; Ziats, N. P.; Nakayama, Y.; Matsuda, T.; Anderson, J. M. "In vivo leukocyte cytokine mRNA responses to biomaterials are dependent on surface chemistry" *Journal of Biomedical Materials Research Part A* **2003**, *64A*, 320-329.

(139) Dinnes, D. L. M.; Marçal, H.; Mahler, S. M.; Santerre, J. P.; Labow, R. S. "Material surfaces affect the protein expression patterns of human macrophages: A proteomics approach" *Journal of Biomedical Materials Research Part A* **2007**, *80*, 895-908.

(140) Ju, Y. M.; Yu, B.; Koob, T. J.; Moussy, Y.; Moussy, F. "A novel porous collagen scaffold around an implantable biosensor for improving biocompatibility. I. In vitro/in vivo stability of the scaffold and in vitro sensitivity of the glucose sensor with scaffold" *Journal of Biomedical Materials Research Part A* **2008**, *87*, 136-46.

(141) Ju, Y. M.; Yu, B.; West, L.; Moussy, Y.; Moussy, F. "A novel porous collagen scaffold around an implantable biosensor for improving biocompatibility. II. Long-term in vitro/in vivo sensitivity characteristics of sensors with NDGA- or GA-crosslinked collagen scaffolds" *Journal of Biomedical Materials Research Part A* **2010**, *92*, 650-658.

(142) Weng, L.; Romanov, A.; Rooney, J.; Chen, W. "Non-cytotoxic, in situ gelable hydrogels composed of N-carboxyethyl chitosan and oxidized dextran" *Biomaterials* **2008**, *29*, 3905-3913.

(143) Cai, Z.; Kim, J. "Bacterial cellulose/poly(ethylene glycol) composite: characterization and first evaluation of biocompatibility" *Cellulose* **2010**, *17*, 83-91.

(144) Helenius, G.; Bäckdahl, H.; Bodin, A.; Nannmark, U.; Gatenholm, P.; Risberg, B. "In vivo biocompatibility of bacterial cellulose" *Journal of Biomedical Materials Research Part A* **2006**, *76*, 431-438.

(145) Go, D. H.; Joung, Y. K.; Park, S. Y.; Park, Y. D.; Park, K. D. "Heparin-conjugated star-shaped PLA for improved biocompatibility" *Journal of Biomedical Materials Research Part A* **2008**, *86*, 842-848.

(146) Draye, J. P.; Delaey, B.; Van de Voorde, A.; Van Den Bulcke, A.; De Reu, B.; Schacht, E. "In vitro and in vivo biocompatibility of dextran dialdehyde cross-linked gelatin hydrogel films" *Biomaterials* **1998**, *19*, 1677-1687.

(147) Cadée, J. A.; van Luyn, M. J. A.; Brouwer, L. A.; Plantinga, J. A.; van Wachem, P. B.; de Groot, C. J.; den Otter, W.; Hennink, W. E. "In vivo biocompatibility of dextran-based hydrogels" *Journal of Biomedical Materials Research* **2000**, *50*, 397-404.

(148) Wisniewski, N.; Moussy, F.; Reichert, W. M. "Characterization of implantable biosensor membrane biofouling" *Fresenius' Journal of Analytical Chemistry* **2000**, *366*, 611-621.

(149) Wisniewski, N.; Reichert, M. "Methods for reducing biosensor membrane biofouling" *Colloids and Surfaces B: Biointerfaces* **2000**, *18*, 197-219.

(150) Ishihara, K.; Nomura, H.; Mihara, T.; Kurita, K.; Iwasaki, Y.; Nakabayashi, N. "Why do phospholipid polymers reduce protein adsorption?" *Journal of Biomedical Materials Research* **1998**, *39*, 323-30.

(151) Kim, K.; Kim, C.; Byun, Y. "Biostability and biocompatibility of a surface-grafted phospholipid monolayer on a solid substrate" *Biomaterials* **2004**, *25*, 33-41.

(152) Sawada, S.; Sakaki, S.; Iwasaki, Y.; Nakabayashi, N.; Ishihara, K. "Suppression of the inflammatory response from adherent cells on phospholipid polymers" *Journal of Biomedical Materials Research Part A* **2003**, *64*, 411-416.

(153) Naumann, C. A.; Prucker, O.; Lehmann, T.; Rühe, J.; Knoll, W.; Frank, C. W. "The polymer-supported phospholipid bilayer: Tethering as a new approach to substrate−membrane stabilization" *Biomacromolecules* **2001**, *3*, 27-35.

(154) Turner, R. F. B.; Harrison, D. J.; Rojotte, R. V. "Preliminary in vivo biocompatibility studies on perfluorosulphonic acid polymer membranes for biosensor applications" *Biomaterials* **1991**, *12*, 361-368.

(155) Mercado, R. C.; Moussy, F. "In vitro and in vivo mineralization of Nafion membrane used for implantable glucose sensors" *Biosensors and Bioelectronics* **1998**, *13*, 133-145.

(156) Moussy, F.; Harrison, D. J.; Rajotte, R. V. "A miniaturized Nafion-based glucose sensor: in vitro and in vivo evaluation in dogs" *The International Journal of Artificial Organs* **1994**, *17*, 88-94.

(157) Jhon, M. S.; Andrade, J. D. "Water and hydrogels" *Journal of Biomedical Materials Research* **1973**, *7*, 509-522.

(158) Lee, K. Y.; Mooney, D. J. "Hydrogels for tissue engineering" *Chemical Reviews* **2001**, *101*, 1869-80.

(159) Yu, B.; Wang, C.; Ju, Y. M.; West, L.; Harmon, J.; Moussy, Y.; Moussy, F. "Use of hydrogel coating to improve the performance of implanted glucose sensors" *Biosensors and Bioelectronics* **2008**, *23*, 1278-1284.

(160) Quinn, C. A. P.; Connor, R. E.; Heller, A. "Biocompatible, glucose-permeable hydrogel for in situ coating of implantable biosensors" *Biomaterials* **1997**, *18*, 1665-1670.

(161) Wang, C.; Yu, B.; Knudsen, B.; Harmon, J.; Moussy, F.; Moussy, Y. "Synthesis and rerformance of novel hydrogels coatings for implantable glucose sensors" *Biomacromolecules* **2008**, *9*, 561-567.

(162) Zhang, L.; Cao, Z.; Bai, T.; Carr, L.; Ella-Menye, J.-R.; Irvin, C.; Ratner, B. D.; Jiang, S. "Zwitterionic hydrogels implanted in mice resist the foreign-body reaction" *Nature Biotechnology* **2013**, *31*, 553-556.

(163) Vaddiraju, S.; Singh, H.; Burgess, D. J.; Jain, F. C.; Papadimitrakopoulos, F. "Enhanced glucose sensor linearity using poly(vinyl alcohol) hydrogels" *Journal of Diabetes Science and Technology* **2009**, *3*, 863-874.

(164) Yu, B.; Long, N.; Moussy, Y.; Moussy, F. "A long-term flexible minimally-invasive implantable glucose biosensor based on an epoxy-enhanced polyurethane membrane" *Biosensors and Bioelectronics* **2006**, *21*, 2275-2282.

(165) Ward, W. K.; Jansen, L. B.; Anderson, E.; Reach, G.; Klein, J. C.; Wilson, G. S. "A new amperometric glucose microsensor: in vitro and short-term in vivo evaluation" *Biosensors and Bioelectronics* **2002**, *17*, 181-189.

(166) Ward, W. K.; Slobodzian, E. P.; Tiekotter, K. L.; Wood, M. D. "The effect of microgeometry, implant thickness and polyurethane chemistry on the foreign body response to subcutaneous implants" *Biomaterials* **2002**, *23*, 4185-4192.

(167) Jones, J. A.; Dadsetan, M.; Collier, T. O.; Ebert, M.; Stokes, K. S.; Ward, R. S.; Hiltner, P. A.; Anderson, J. M. "Macrophage behavior on surface-modified polyurethanes" *Journal of Biomaterials Science, Polymer Edition* **2004**, *15*, 567-584.

(168) Cummingham, D. D.; Stenken, J. A. *In vivo glucose sensing*; John Wiley & Sons, Inc., 2010.

(169) Deligianni, D. D.; Katsala, N.; Ladas, S.; Sotiropoulou, D.; Amedee, J.; Missirlis, Y. F. "Effect of surface roughness of the titanium alloy Ti-6Al-4V on human bone marrow cell response and on protein adsorption" *Biomaterials* **2001**, *22*, 1241-1251.

(170) Roach, P.; Farrar, D.; Perry, C. C. "Surface tailoring for controlled protein adsorption: effect of topography at the nanometer scale and chemistry" *Journal of the American Chemical Society* **2006**, *128*, 3939-3945.

(171) Cao, H.; McHugh, K.; Chew, S. Y.; Anderson, J. M. "The topographical effect of electrospun nanofibrous scaffolds on the in vivo and in vitro foreign body reaction" *Journal of Biomedical Materials Research Part A* **2010**, *93A*, 1151-1159.

(172) Bota, P. C. S.; Collie, A. M. B.; Puolakkainen, P.; Vernon, R. B.; Sage, E. H.; Ratner, B. D.; Stayton, P. S. "Biomaterial topography alters healing in vivo and

monocyte/macrophage activation in vitro" *Journal of Biomedical Materials Research Part A* **2010**, *95*, 649-657.

(173) Paul, N. E.; Skazik, C.; Harwardt, M.; Bartneck, M.; Denecke, B.; Klee, D.; Salber, J.; Zwadlo-Klarwasser, G. "Topographical control of human macrophages by a regularly microstructured polyvinylidene fluoride surface" *Biomaterials* **2008**, *29*, 4056-4064.

(174) Refai, A. K.; Textor, M.; Brunette, D. M.; Waterfield, J. D. "Effect of titanium surface topography on macrophage activation and secretion of proinflammatory cytokines and chemokines" *Journal of Biomedical Materials Research Part A* **2004**, *70*, 194-205.

(175) Marshall, A. J.; Ratner, B. D. "Quantitative characterization of sphere-templated porous biomaterials" *AIChE Journal* **2005**, *51*, 1221-32.

(176) Harris, L. D.; Kim, B. S.; Mooney, D. J. "Open pore biodegradable matrices formed with gas foaming" *Journal of Biomedical Materials Research* **1998**, *42*, 396-402.

(177) Hua, F. J.; Kim, G. E.; Lee, J. D.; Son, Y. K.; Lee, D. S. "Macroporous poly(L-lactide) scaffold 1. Preparation of a macroporous scaffold by liquid–liquid phase separation of a PLLA–dioxane–water system" *Journal of Biomedical Materials Research* **2002**, *63*, 161-167.

(178) Reneker, D. H.; Yarin, A. L. "Electrospinning jets and polymer nanofibers" *Polymer* **2008**, *49*, 2387-2425.

(179) Leung, V.; Ko, F. "Biomedical applications of nanofibers" *Polymers for Advanced Technologies* **2011**, *22*, 350-365.

(180) Huang, Z.-M.; Zhang, Y.-Z.; Koraki, M.; Ramakrishna, S. "A review on polymer nanofibers by electrospinning and their applications in nanocomposites" *Composites Science and Technology* **2003**, *63*, 2223-2253.

(181) Yang, S.; Leong, K. F.; Du, Z.; Chua, C. K. "The design of scaffolds for use in tissue engineering. Part 1. Traditional factors" *Tissue Engineering* **2001**, *7*, 679-689.

(182) Koschwanez, H. E.; Yap, F. Y.; Klitzman, B.; Reichert, W. M. "In vitro and in vivo characterization of porous poly-L-lactic acid coatings for subcutaneously

implanted glucose sensors" *Journal of Biomedical Materials Research Part A* **2008**, *87A*, 792-807.

(183) Marshall, A. J.; Irvin, C. A.; Barker, T.; Sage, E. H.; Hauch, K. D.; Ratner, B. D. "Biomaterials with tightly controlled pore size that promote vascular in-growth" *ACS Polymer Preprints* **2004**, *45*, 100-101.

(184) Sharkawy, A. A.; Klitzman, B.; Truskey, G. A.; Reichert, W. M. "Engineering the tissue which encapsulates subcutaneous implants. II. Plasma–tissue exchange properties" *Journal of Biomedical Materials Research* **1998**, *40*, 586-597.

(185) Madden, L. R.; Mortisen, D. J.; Sussman, E. M.; Dupras, S. K.; Fugate, J. A.; Cuy, J. L.; Hauch, K. D.; Laflamme, M. A.; Murry, C. E.; Ratner, B. D. "Proangiogenic scaffolds as functional templates for cardiac tissue engineering" *Proceedings of the National Academy of Sciences* **2010**, *107*, 15211-15216.

(186) Helton, K. L.; Ratner, B. D.; Wisniewski, N. A. "Biomechanics of the sensor–tissue interface—Effects of motion, pressure, and design on sensor performance and the foreign body response—Part II: Examples and application" *Journal of Diabetes Science and Technology* **2011**, *5*, 647-656.

(187) Holt, B.; Tripathi, A.; Morgan, J. "Viscoelastic response of human skin to low magnitude physiologically relevant shear" *Journal of Biomechanics* **2008**, *41*, 2689-2695.

(188) Sanders, J. E.; Nicholson, B. S.; Mitchell, S. B.; Ledger, R. E. "Polymer microfiber mechanical properties: A system for assessment and investigation of the link with fibrous capsule formation" *Journal of Biomedical Materials Research Part A* **2003**, *67A*, 1412-1416.

(189) Hendriks, F. M.; Brokken, D.; Van Eemeren, J. T. W. M.; Oomens, C. W. J.; Baaijens, F. P. T.; Horsten, J. B. A. M. "A numerical-experimental method to characterize the non-linear mechanical behaviour of human skin" *Skin Research and Technology* **2003**, *9*, 274-283.

(190) Diridollou, S.; Black, D.; Lagarde, J. M.; Gall, Y.; Berson, M.; Vabre, V.; Patat, F.; Vaillant, L. "Sex- and site-dependent variations in the thickness and mechanical properties of human skin in vivo" *International Journal of Cosmetic Science* **2000**, *22*, 421-435.

(191) Serup, J.; Jemec, G. B. E.; Grove, G. L. *Handbook of Non-Invasive Methods And The Skin*; CRC/Taylor & Francis, 2006.

(192) Teo, W. E.; Ramakrishna, S. "A review on electrospinning design and nanofibre assemblies" *Nanotechnology* **2006**, *17*, R89-R106.

(193) Theron, S. A.; Zussman, E.; Yarin, A. L. "Experimental investigation of the governing parameters in the electrospinning of polymer solutions" *Polymer* **2004**, *45*, 2017-2030.

(194) Jang, J.-H.; Castano, O.; Kim, H.-W. "Electrospun materials as potential platforms for bone tissue engineering" *Advanced Drug Delivery Reviews* **2009**, *61*, 1065-1083.

(195) Wang, B.; Wang, Y.; Yin, T.; Yu, Q. "Applications of electrospinning technique in drug delivery" *Chemical Engineering Communications* **2010**, *197*, 1315-1338.

(196) Zhang, Y.; Lim, C.; Ramakrishna, S.; Huang, Z.-M. "Recent development of polymer nanofibers for biomedical and biotechnological applications" *Journal of Materials Science: Materials in Medicine* **2005**, *16*, 933-946.

(197) Zahedi, P.; Rezaeian, I.; Ranaei-Siadat, S.-O.; Jafari, S.-H.; Supaphol, P. "A review on wound dressings with an emphasis on electrospun nanofibrous polymeric bandages" *Polymers for Advanced Technologies* **2010**, *21*, 77-95.

(198) Agarwal, S.; Wendorff, J. H.; Greiner, A. "Use of electrospinning technique for biomedical applications" *Polymer* **2008**, *49*, 5603-5621.

(199) Li, W.-J.; Laurencin, C. T.; Caterson, E. J.; Tuan, R. S.; Ko, F. K. "Electrospun nanofibrous structure: A novel scaffold for tissue engineering" *Journal of Biomedical Materials Research* **2002**, *60*, 613-621.

(200) Sanders, J. E.; Cassisi, D. V.; Neumann, T.; Golledge, S. L.; Zachariah, S. G.; Ratner, B. D.; Bale, S. D. "Relative influence of polymer fiber diameter and surface charge on fibrous capsule thickness and vessel density for single-fiber implants" *Journal of Biomedical Materials Research Part A* **2003**, *65A*, 462-467.

(201) Saino, E.; Focarete, M. L.; Gualandi, C.; Emanuele, E.; Cornaglia, A. I.; Imbriani, M.; Visai, L. "Effect of electrospun fiber diameter and alignment on macrophage activation and secretion of proinflammatory cytokines and chemokines" *Biomacromolecules* **2011**, *12*, 1900-1911.

(202) Wang, N.; Burugapalli, K.; Song, W.; Halls, J.; Moussy, F.; Ray, A.; Zheng, Y. "Electrospun fibro-porous polyurethane coatings for implantable glucose biosensors" *Biomaterials* **2013**, *34*, 888-901.

(203) Vacanti, N. M.; Cheng, H.; Hill, P. S.; Guerreiro, J. D. T.; Dang, T. T.; Ma, M.; Watson, S.; Hwang, N. S.; Langer, R.; Anderson, D. G. "Localized delivery of dexamethasone from electrospun fibers reduces the foreign body response" *Biomacromolecules* **2012**, *13*, 3031-3038.

CHAPTER 2: FABRICATION OF NITRIC OXIDE-RELEASING POLYURETHANE GLUCOSE SENSOR MEMBRANES

Original article was co-authored with Daniel A. Riccio, Bin Sun, Alexis W. Carpenter, Scott P. Nichols, and Mark H. Schoenfisch. Text, figures, and tables are adapted and reprinted with permission of Elsevier: Ahyeon Koh, Daniel A. Riccio, Bin Sun, Alexis W. Carpenter, Scott P. Nichols, Mark H. Schoenfisch, "Fabrication of nitric oxide-releasing polyurethane glucose sensor membranes", *Biosensors and Bioelectronics*, Volume 28, Issue 1, 15 October 2011, Pages 17-24, ISSN 0956-5663, 10.1016/j.bios.2011.06.005.

2.1 Introduction

Strict monitoring and control of blood glucose levels are essential for effective diabetes management.[1] Since conventional glucose monitoring (e.g., the finger prick method) provides only discrete snapshots of blood glucose levels, analytical methods that enable continuous monitoring of glucose concentration fluctuations via implantable enzyme-based electrochemical sensors have been sought to improve diabetes management.[2-4] Despite US Food and Drug Administration approval for certain devices, most sensors have serious shortcomings including poor accuracy, unpredictable signal stability, lag time in sensor response, frequent calibration requirement, and short lifetimes that limit their clinical utility.[3,5] Undesirable sensor performance has been attributed to the foreign body response (FBR) and biofouling.[6,7] As the outer surface of the sensor influences the FBR directly, recent work has focused on the development of more biocompatible sensor membranes to mitigate the FBR.[8,9] The general consensus is that new strategies to improve long-term in vivo sensor performance should: (1) reduce the

initial inflammatory response; (2) enhance wound healing; and, (3) avoid biosensor degradation.[10]

Due to nitric oxide's (NO) role as an endogenous antibacterial agent,[11] the synthesis of sol-gel-derived coatings (e.g., xerogels) capable of storing and spontaneously releasing NO has studied previously.[12-14] These materials were shown to reduce bacterial adhesion,[15,16] kill bacteria that did manage to adhere,[17-19] and reduce in vivo infection rates.[20] Furthermore, the NO release was shown to reduce collagen capsule thickness around a subcutaneous implant by >50 and ~20–25% relative to blanks and controls, respectively, in a rodent model.[21] Concomitantly, the NO-releasing implant lessened the chronic inflammatory response at the tissue/implant interface by >30% and enhanced blood vessel formation by >77% versus controls.[21] Nitric oxide-releasing sensors have exhibited improved biocompatibility and sensor performance.[22,23] For example, Gifford et al. reported reduced inflammatory response for subcutaneously implanted NO-releasing glucose sensors over 3 d.[22] In blood, Yan et al. described improved hemocompatibilty and in vivo sensor performance for an intravenous NO-releasing glucose/lactate sensor.[23] Additionally, the NO-releasing microdialysis probes were recently reported enhanced in vivo glucose recovery from during long-term (i.e., 2 weeks) implantation.[24] Collectively, these studies indicate that NO release is a highly promising strategy that may solve the lingering biocompatibility problems encountered when glucose biosensors are implanted in vivo.

Based on the reduced FBR as a function of NO release, combining chemistries of NO release with enzymatic glucose sensing to fabricate continuous glucose monitoring

devices has sought to improve biocompatibility and extend analytical performance. Although promising with respect to reduced capsule formation and implant-associated infection, the xerogel films resulted in unusually low glucose response when used to fabricate glucose biosensors.[25] The glucose impermeability of the xerogel film was attributed to enhanced hydrolysis and condensation rates catalyzed by the aminosilanes and exposure to high pressures of NO (necessary to form the *N*-diazeniumdiolate-based NO donors). To address the inadequate glucose permeability, we fabricated functional NO-releasing glucose biosensors by patterning xerogel microarrays on top of[26] or physically entrapping ground xerogel particles within[25] standard polyurethane sensor membranes. These polymer configurations allowed for enhanced glucose sensitivity relative to sensors completely coated with xerogel films because significant potions of the underlying electrode surface remained unmodified by the xerogel.

To date, a key challenge for the development of NO-releasing glucose biosensors has been limited NO release. While our previously published hybrid NO-releasing xerogel particle/polyurethane biosensor exhibited excellent analytical response characteristics (e.g., sensitivity, linear response, and lifetime), the NO flux and release duration were limited to a maximum of ~90 pmol·cm^{-2}·s^{-1} for 2 d.[25] The sensors described more recently by Gifford et al. and Yan et al. released NO with average maximum fluxes of 7.52 pmol·cm^{-2}·s^{-1} and 40 pmol·cm^{-2}·s^{-1} for 18 h and 7 d, respectively.[22,23] As such, a void exists regarding the optimal level and duration of NO release required to mitigate the FBR and influence sensor performance. In this Chapter, the fabrication of NO-releasing glucose sensor membranes with a wide range of NO

fluxes (5 pmol·cm^{-2}·s^{-1} to 2.5 nmol·cm^{-2}·s^{-1}) and release durations (16 h to 14 d) using NO donor-modified silica nanoparticles are described. The NO-releasing polymers are then used to fabricate functional glucose biosensors to further evaluate sensor response and stability as a function of NO release.

2.2 Material and methods

2.2.1 Reagents and Materials

Glucose oxidase (type VII from *Aspergillus niger*), hydrogen peroxide (30 % v/v), L-proline, and *β*-D-glucose anhydrous were purchased from Sigma (St. Louis, MO). Ethanol (EtOH), tetrahydrofuran (THF), and aqueous ammonium hydroxide solution (14.8 M) were purchased from Fisher Scientific (Pittsburgh, PA). Methyltrimethoxysilane (MTMOS) was purchased from Fluka (Buchs, Switzerland). *N*-(6-aminohexyl)aminopropyltrimethoxysilane (AHAP3), *N*-(2-aminoethyl)-3-aminopropyltrimethoxysilane (AEAP3), 3-methylaminopropyltrimethoxysilane (MAP3), 3-mercaptopropyltrimethoxysilane (MPTMS), tetramethoxysilane (TMOS), and tetraethoxysilane (TEOS) were purchased from Gelest (Tullytown, PA). Tecoplast TP-470, Tecophilic HP-93A-100, and Tecoflex SG-80A (TPU) were gifts from Thermedics (Woburn, MA). Hydrothane AL 25-80A (HPU) was a gift from AdvanSource Biomaterials Corporation (Wilmington, MA). A Griess reagent kit was purchased from Promega (Madison, WI). Water was purified (18.2 MΩ/cm; total organic contents <6 ppb) with a Milli-Q UV Gradient A10 system (Millipore Corp., Bedford, MA). Nitric oxide, nitric oxide calibration gas (26.4 ppm; balance N_2), nitrogen and argon (Ar) gases were

purchased from National Welders Supply (Durham, NC). All other reagents and solvents were analytical-reagent grade and used as received.

2.2.2 Preparation of NO-releasing dopant

1-[2-(carboxylato)pyrrolidin-1-yl]diazen-1-ium-1,2-diolate (PROLI/NO) was prepared by converting L-proline to NO donor form following a procedure reported by Saavedra et al.[27] Nitric oxide-releasing silica particles were synthesized based on the sol-gel process via the co-condensation of an aminosilane (i.e., MAP3, AEAP3, or AHAP3) or mercaptosilane (i.e., MPTMS) in a range of concentrations (65–75 mol%) with tetraethyoxysilane (TEOS) or tetramethoxysilane (TMOS) similarly to those reported in previous studies.[28-30] Subsequent diazeniumdiolation of the amine-containing particles was performed under high pressure of NO for 3 d in the presence of sodium methoxide at room temperature. Nitrosation of the thiol-containing nanoparticles was carried out by reaction with acidified nitrite in the dark at 0°C. The details of the NO-releasing characteristics and particle sizes for each particle system are shown in Table 2.1.

2.2.3 Hybrid sol-gel/polyurethane glucose sensor fabrication

A platinum macroelectrode (0.3 cm radius and 0.031 cm^2 platinum surface area) was used to fabricate hybrid sol-gel/polyurethane glucose biosensors that consisted of two distinct layers: glucose oxidase and NO-releasing polyurethane. Fabrication of the glucose sensor was adapted from a procedure described by Shin et al.[25]

Table 2.1. Characterization of NO-releasing silica particles.

Type of NO modification	NO donor	mol%[a]	Particle size (nm)	$[NO]_{max}$ ($ppm \cdot mg^{-1}$)	t_{max} (min)	Total [NO] ($\mu mol \cdot mg^{-1}$)	$t_{1/2}$ (min)	t_d (h)
N-diazeniumdiolate	PROLI/NO	N/A	N/A	>406[b]	0.6±0.2	3.45±0.29	1.1±0.1	0.12±0.01
	MAP3/TMOS	70	247.1±4.5[c]	14.0±6.3	1.1±0.2	2.88±0.37	147±18	27.3±4.7
	AEAP3/TMOS	70	191.9±1.7	1.60±0.2	1.2±0.6	2.20±0.17	188±21	21.1±1.5
	AHAP3/TEOS	65	131.2±14.1	25.7±2.9	1.0±0.1	4.00±0.17	137±12	29.8±16.3
S-nitrosothiol	MPTMS/TEOS	75	718.0±51.7	1.3±0.4	2.8±0.4	3.15 ± 0.60[d]	233±14	> 48[e]

[a] Balance TEOS or TMOS backbone silane.

[b] The value was above the maximum limit of detection of NOA chemiluminescence.

[c] Standard deviation represents at least n=3 sensors.

[d] Determined via irradiation with 200 W light for 5 h.

[e] Undetectable NO release due to limit of detection of NOA chemiluminescence after 48 h.

Briefly, glucose oxidase (GOx) was immobilized within a sol-gel matrix on a polished platinum electrode by casting 3 μL of a GOx sol. The enzyme-containing sol was prepared by dissolving 9 mg of GOx into 75 μL of water and adding 50 μL of this solution into 25 μL MTMOS and 100 μL EtOH followed by mixing for 10 min. The NO-releasing layer was prepared by dispersing silica particles in a polyurethane (PU) polymer solution consisting of 20 $mg \cdot mL^{-1}$ 50% w/w TPU and HPU dissolved in 50% v/v THF/EtOH solution. The NO-releasing layer was formed by casting 5 μL of the resulting 9–144 $mg \cdot mL^{-1}$ NO-releasing particles in a PU polymer solution (0.2–2.4 $mg \cdot cm^{-2}$). Particle concentration rather than casting volume was increased when increasing particle concentration per surface area. For instances where an additional polyurethane layer was cast on top of the NO-releasing layer, 20 μL of 20–60 $mg \cdot mL^{-1}$ polyurethane polymer solution dissolved in THF was used and each layer was dried under ambient conditions for 30 min before casting the subsequent layer.

2.2.4 Film fabrication and methods of film study

Glass substrates were prepared via sonication in EtOH and subsequent UV-ozone cleaning for 20 min in a BioForce Tip Cleaner (Ames, IA). The NO-releasing particle-dispersed polyurethane solution described previously was spread-cast (36.2 μL) onto a glass substrate (2.08 cm^2). For films with an additional PU layer on the NO-releasing layer, PU polymer solution was cast (141 μL) in the same manner as the electrode casting procedure. Each layer was dried under ambient conditions for 30 min and stored in the dark at -20 °C under vacuum until used. This storage method was adopted to assure NO donor stability. Although the diazeniumdiolated particle-doped films could be stored at

ambient conditions (humidity 40% at room temperature) without loss of NO for 2 d, NO storage was sacrificed (~10%) under more humid conditions (i.e., 90% humidity, 23.7–25.0 °C). Nitric oxide release from NO-releasing silica particle-doped polyurethane was characterized using a Sievers model 280i chemiluminescence NO analyzer (Boulder, CO). Films were immersed in 0.01 M PBS (pH 7.4) buffer solution at 37 °C sparged with 80 $mL \cdot min^{-1}$ nitrogen with additional nitrogen supported to the flask to match the instrument collection rate of 200 $mL \cdot min^{-1}$. The instrument was calibrated using 26.4 ppm NO gas (balanced N_2) and air passed through a Sievers NO zero filter. When measuring NO from nitrosothiol-based materials, the sample flask was shielded from light to prevent light-initiated NO release. Total NO release was determined spectrophotometrically by measuring the conversion of NO to nitrite (NO_2^-) using the Griess assay.[31] After soaking NO-releasing films in PBS buffer solution at 37 °C for a period exceeding their NO release, 50 μL of solution was mixed with 100 μL of Griess reagent (1% w/v sulfanilamide in 5% v/v phosphoric acid and 0.1% w/v *N*-(1-naphthyl)ethylenediaminedihydrochloride) and incubated at room temperature for 10 min. Absorbance of these solutions was measured at 540 nm using a Labsystem MultiskanRC microplate spectrophotometer (Helsinki, Finland). Total nitrite concentration was determined using a calibration curve constructed with a standard nitrite solution. The water uptake of polyurethane films was determined by measuring the mass of glass substrates cast with 141 μL of 40 $mg \cdot mL^{-1}$ polyurethane before/after soaking in PBS for 3 h. The degree of silica particle leaching from the sensor membranes was assessed via dynamic light scattering (DLS). The NO-releasing polyurethane-coated glass substrates

were immersed in 2 mL PBS and incubated at 37 ^{o}C for 7 d. The concentration of silica particles that leached into the soak solution was determined by measuring the derived count rate that varied linearly with particle concentration.[32,33] The derived count rate was then fit to a calibration curve of known particle concentrations. Film thickness was measured with a Tencor Alpha-Step 200 Profilometer (San Jose, CA). Half of the NO-releasing silica particle-doped polyurethane coating was removed from the glass substrate and the resulting interface was probed to determine film thickness.

2.2.5 Sensor performance of hybrid sol-gel/polyurethane glucose sensor

The analytical performance (i.e., sensitivity, dynamic range, and response time ($t_{95\%}$)) of the biosensors was evaluated via chronoamperometry using a CH Instruments 1030A potentiostat (Austin, TX). All electrochemical measurements were performed in 0.01 M PBS (pH 7.4) at room temperature using a three-electrode configuration with an Ag/AgCl (3.0 M KCl) reference electrode, a platinum wire counter electrode, and glucose biosensor as the working electrode. Glucose sensors were first hydrated in PBS for 1 h and polarized for 20 min to stabilize glucose response. Indeed, sensor response effects due to NO release and changes in membrane permeability (water uptake) were shown to significantly decrease during this preconditioning period (data not shown). Response and calibration curves were obtained by injecting 1 M glucose aliquots into 30 mL PBS at room temperature under constant stirring and an applied potential of +0.6 V vs. Ag/AgCl. [25,34] Permeability (P_i^e) was defined electrochemically as the ratio of peak current at the hybrid sol-gel/polyurethane glucose sensor (ΔI_x) and bare platinum electrode (ΔI_b) response at either 0.79 mM H_2O_2 ($P_{H_2O_2}^e$) or air saturated solution ($P_{O_2}^e$).[34,35]

Amperometric selectivity coefficients were calculated using equation (1),[35] where ΔI_{Glu} and ΔI_j are the measured current values for glucose (Glu) and interfering species (j = ascorbic acid, uric acid, and nitrite), respectively.

$$logK_{Glu,j}^{amp} = log\left(\frac{\Delta I_j/C_j}{\Delta I_{Glu}/C_{Glu}}\right) \quad (1)$$

The concentration of each interfering substance (c_j) was 100 μM. The glucose concentration (c_{Glu}) employed for selectivity coefficient determination was 5.6 mM.

2.3 Results and Discussion

2.3.1 NO-releasing glucose sensor

Nitric oxide-releasing glucose sensor membranes were prepared using polyurethanes doped with NO-releasing silica particles. These membranes were then used as the outermost coating for enzyme-based glucose sensors. Since NO release has previously been reported to increase the background current of amperometric glucose sensors because of the overlapping oxidation potentials of H_2O_2 and NO (+0.7 and +0.9 V vs. Ag/AgCl on platinum electrode, respectively),[22] an applied electrode potential of +0.6 V vs. Ag/AgCl was selected to monitor glucose concentration in the presence of NO release to avoid masking the H_2O_2 oxidation response at large NO fluxes (Figure 2.1). This potential provided the optimal combination of adequate glucose sensitivity and minimal current interference from NO oxidation. Glucose sensitivity was maintained independent of NO release from the membrane.

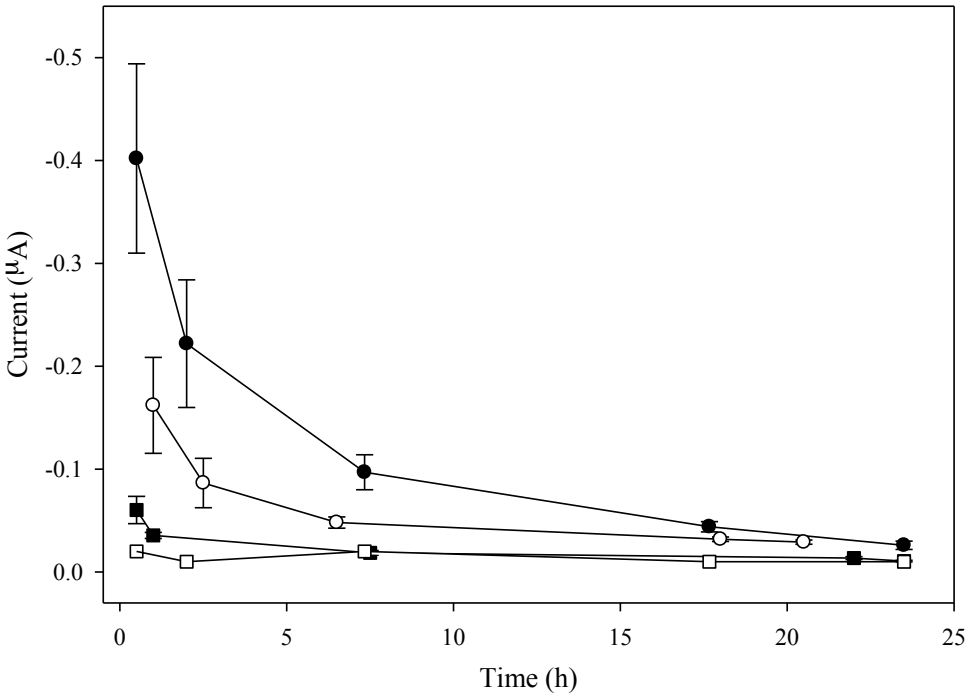

Figure 2.1. Background current of particle-doped glucose sensor with RSNO-modified particles (0.6 mg·cm^{-2}) using applied potentials of (●) +0.80, (○) +0.65, and (■) +0.60 V vs. Ag/AgCl and with control (i.e., non-particle-doped) PU coated sensors (□) at +0.80 V vs. Ag/AgCl.

For example, the normalized sensitivity of RSNO-MPTMS/TEOS particle-doped (0.6 $mg \cdot cm^{-2}$) polyurethane-coated glucose sensors over 3 d was not altered even though the NO flux from the membrane was changing appreciably. Of note, a preconditioning period of 18 h was required with the addition of a polyurethane barrier layer to extend the linear response (Figure 2.2). This change may be attributed to decreased water uptake rate by the thicker membrane, as previously observed for other polyurethane coated glucose sensors. [23,36]

The fabricated NO-releasing particle-doped membranes were characterized as having adequate selectivity over known interferents.[4,9] For example, glucose sensors prepared using RSNO-MPTMS/TEOS particle-doped (0.6 $mg \cdot cm^{-2}$) polyurethane membranes exhibited amperometric selectivity coefficients of 0.55 ± 0.18, 0.88 ± 0.14, and -0.17 ± 0.13 for ascorbic acid, uric acid, and nitrite over glucose, respectively.

2.3.2. Variation of type of NO donors

The NO-donor systems embedded in the 50% w/w TPU/HPU polyurethane membranes enabled the comparison of NO release kinetics and payloads on sensor response. Two NO donor classes were investigated: *N*-diazeniumdiolates and *S*-nitrosothiols. Briefly, *N*-diazeniumdiolates are formed on secondary amines and produce NO upon decomposition by protonation in aqueous solutions.[29,37] Alternatively, *S*-nitrosothiols (RSNO), endogenous transporters of NO, are formed on thiol precursors and degraded by heat, light and/or copper ions to liberate NO.[38]

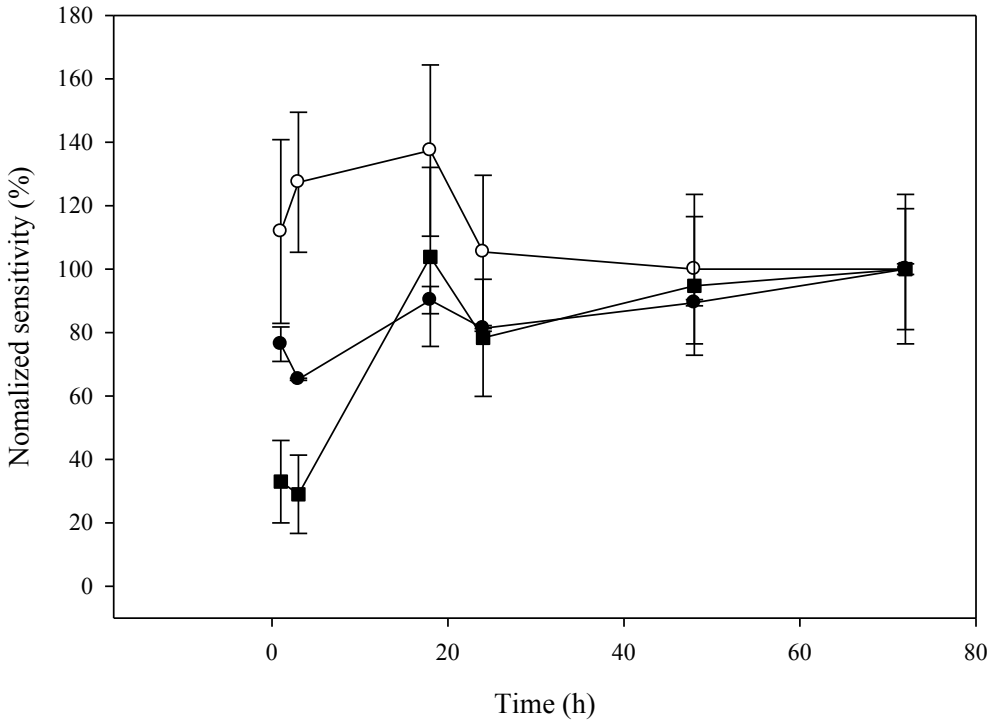

Figure 2.2. Normalized glucose sensor sensitivity by sensitivity at 3 d for the following sensors: (●) RSNO-MPTMS/TEOS particle-doped (0.6 mg·cm^{-2}) glucose sensor; (○) non-NO-releasing particle-doped glucose sensor as a control; and (■) RSNO-MPTMS/TEOS particle-doped glucose sensor with an additional polyurethane layer (20 mg·mL^{-1} TPU).

While NO donors may be synthesized as low molecular weight compounds or larger macromolecules (e.g., dendrimers, and silica particles),[37] the following NO-releasing scaffolds were chosen for study because of their low toxicity, stable nature, and wide range of achievable NO-release: (1) PROLI/NO, a water soluble, diazeniumdiolated low molecular weight compound derived from the amino acid proline; (2) three types of *N*-diazeniumdiolate-modified silica particles (i.e., MAP3/TMOS, AEAP3/TMOS, and AHAP3/TEOS); and (3) RSNO-modified silica particles (i.e., MPTMS/TEOS). The NO release from *N*-diazeniumdiolate-modified silica particles was tuned via altering the structure of the aminosilane precursors. For example, MAP3 does not contain a stabilizing primary amine, and its decomposition rate in solution is greater than AHAP3 or AEAP3.[28,29] While both AEAP3 and AHAP3 contain a secondary and a primary amine, the spacing between the two amines is increased from two to six carbons resulting in altered diazeniumdiolate stability and ensuing NO release. The RSNO-modified silica particle scaffold enables more sustained NO release compared to the *N*-diazeniumdiolate-modified silica particles as the decomposition is based on different mechanisms (thermal vs. proton).[30]

Nitric oxide release from the particle-doped films was monitored in PBS (pH 7.4) at 37 °C to mimic physiological conditions. Corresponding NO release data for each system studied is provided in Table 2.2. Due to the short half-life of PROLI/NO (~1.2 min), 99% of the stored NO (~3 μmol·cm^{-2}) was released within the first 10 min. The total amount of NO delivered from PROLI/NO-doped polyurethane films was greater than any particle-doped system of equivalent wt% of dopant.

Table 2.2. Characterization of NO release from NO donor-doped polyurethane membranes.[a]

Type of NO modification	NO donor[b]	$[NO]_{max}$ ($pmol \cdot cm^{-2} \cdot s^{-1}$)	t_{max}[c] (min)	Total [NO] ($\mu mol \cdot cm^{-2}$)	t_d[d] (h)
N-diazeniumdiolate	PROLI/NO	> 32183[e]	0.7±0.1	3.11±0.48	0.17±0.03
	MAP3/TMOS	325.0±224.8	1.9±0.7	1.98±0.36	16.8±4.0
	AEAP3/TMOS	116.1±49.0	5.7±4.3	1.70±0.29	20.6±6.0
	AHAP3/TEOS	459.8±107.3	2.3±0.7	1.92±0.29	15.1±1.5
S-nitrosothiol	MPTMS/TEOS	426.2±172.5	1.2±0.2	2.01±0.47	309.8±6.5[f]
N-diazeniumdiolate	AHAP/BTMOS xerogel[g]	~110	34	1.35	72

[a] Standard deviation represents at least n=3 sensors.
[b] Doped at concentration of 0.6 $mg \cdot cm^{-2}$.
[c] Time necessary to reach $[NO]_{max}$.
[d] Duration of NO release, defined by fitting first-order kinetics at time point of 99% NO release (R^2=0.99).
[e] NO flux was above the maximum limit of detection of chemiluminesence NO analyzer.
[f] Experimentally defined at time point of 99% NO released.
[g] Previously published data [21].

The AEAP3/TMOS particle-doped polyurethane composition released a similar maximum NO flux (116.1 pmol·cm^{-2}·s^{-1}) and total NO amount (1.70 μmol·cm^{-2}) as previously reported materials shown to reduce capsule formation and the chronic inflammatory response.[21] However, the NO release duration was limited (i.e., 20 h) and the NO flux was exhausted (i.e., undetectable) after 24 h. Although MAP3/TMOS and AHAP3/TEOS particle-doped polyurethane membranes were also characterized by limited NO release durations (i.e., ~15 h), their maximum NO fluxes were ~4 times larger than the AEAP3/TMOS particle-doped films. The MPTMS/TEOS particle-doped films exhibited significantly longer NO release durations (~2 weeks) representing significantly extended release compared to previously published NO-releasing glucose sensors.[22,25] Of note, the maximum NO flux was 4 times larger (i.e., 426.2 pmol·cm^{-2}·s^{-1}) than the previous NO-releasing materials shown to successfully mitigate the FBR.[21] The NO fluxes and delivery totals indicate that each type of NO-releasing sensor membrane, regardless of NO donor type, may hold potential for improving the biocompatibility of implantable glucose sensors. The multitude of NO-releasing membranes offers a wide range of tunability to allow for diverse NO fluxes, durations, and amounts necessary for future studies aimed at exploring the in vivo response of these sensors as a function of NO release.

The analytical performance of the NO-releasing sensors fabricated with the above membranes was evaluated to assess the effects of the scaffold type and NO release on sensor response.

Table 2.3. Analytical performance criteria of glucose sensors with NO donor-doped polyurethane membranes.[a]

NO donor[b]	Glucose sensitivity ($nA \cdot mM^{-1}$)	Response time[c] ($t_{95\%}$, s)	Permeability[d] of H_2O_2	Permeability[d] of O_2	Silica particles leaching (%)
Without particles	360.9±45.9	28.2±9.3	0.68±0.22	0.99±0.24	N/A
PROLI/NO	175.9±20.6	21.2±12.3	0.66±0.21	0.95±0.41	N/A
MAP3/TMOS	155.1±85.0	28.9±13.7	0.28±0.17	0.98±0.20	< 0.6
AEAP3/TMOS	159.1±79.1	11.4±12.8	0.24±0.08	0.64±0.17	< 0.6
AHAP3/TEOS	114.0±43.2	57.2±34.7	0.16±0.04	0.72±0.18	< 0.6
MPTMS/TEOS	162.4±55.8	36.6±32.1	0.22±0.22	0.61±0.31	< 0.3

[a] Standard deviation represents at least n=3 sensors.

[b] Doped at concentration of 0.6 $mg \cdot cm^{-2}$.

[c] Time necessary to reach 95% of stable signal.

[d] Permeability refers to the response current of glucose sensors relative to bare electrodes.

Similar to previously reported in vivo NO-releasing glucose sensors,[22] the sensitivity and response time ($t_{95\%}$) of the fabricated sensors were found to be applicable for in vivo glucose sensing (e.g., ~150 $nA \cdot mM^{-1}$ and <1 min, respectively). Although the permeability of PROLI/NO-doped polyurethane films to H_2O_2 and O_2 was not significantly different from control membranes, glucose sensitivity was decreased by ~51%. We attribute this loss to the production of high local concentrations of NO affecting GOx activity.[25] When larger NO-releasing scaffolds (i.e., silica particles) were used as dopants, glucose sensitivity decreased by ~57% and ~11% as compared to control (i.e., non-particle-doped) and PROLI/NO-doped membrane, respectively. The permeability of H_2O_2 through the particle-doped films also decreased by ~58% compared to films without particles or those doped with PROLI/NO. Perhaps related, the silica particle-doped polyurethane films were significantly thicker than films without particles or with PROLI/NO (14 vs. 2 μm thick). While larger concentrations of NO may affect glucose oxidase activity,[25] the bulk concentration of NO released from these particle-doped membranes (i.e., <100 μM) was not sufficient to alter the glucose oxidase activity as determined using an enzymatic spectroscopic assay.[39] As such, the decrease in H_2O_2 diffusion and glucose sensitivity most likely results from an increase in membrane thickness. Although RSNO particles were 7 times larger in diameter than *N*-diazeniumdiolated particles (Table 2.1), the sensitivity of the resulting sensors was not significantly altered as a function of silica particle size.

Although silica is generally regarded as nontoxic,[40] the stability of the NO-releasing dopant within the polyurethane layer was investigated to further assess the

potential in vivo utility of these membranes. Silica particle leaching from the polyurethane layer into a solution mimicking physiological conditions was examined by soaking NO-releasing silica particle-doped polyurethane films in PBS (pH 7.4 at 37 ^{o}C). For all membrane compositions, the percent leaching was less than their respective limits of detection using DLS (<0.6% and <0.3% for *N*-diazeniumdiolate and RSNO-modified silica nanoparticle-doped films, respectively) after 7 days, regardless of the NO donor (Table 2.3).

2.3.3 Variation of an additional polyurethane layer to alter NO release kinetics

Although NO release from RSNO-functionalized particle-doped polyurethane films was unaffected by the application of an additional polyurethane layer because temperature and not water influences RSNO decomposition (data not shown), NO release from *N*-diazeniumdiolated particle-doped polyurethane films was tunable via additional polymer layers to control water uptake and the resulting diazeniumdiolate decomposition. As shown in Table 2.4, the hydrophobic character of the polyurethane layer cast onto the NO-releasing layer restricted water access to the NO donor material, thus effectively slowing NO release. This behavior was expected based on work done previously by Frost et al.[41] When employing Tecoplast TP-470 PU (having the lowest water uptake) as the outer membrane, the maximum NO flux decreased from 77.2 to 25.7 pmol·cm^{-2}·s^{-1} and NO release duration increased from 2.5 to 189 h relative to Tecophilic HP-93A-100 PU (having the highest water uptake). The time to reach the maximum NO flux was also significantly extended from 4 min to 5 h.

Table 2.4. Characterization of NO release and glucose sensor performance for NO-releasing AEAP3/TMOS particle-doped (0.6 mg·cm^{-2}) polyurethane sensor membranes as a function of additional top-casted polymer layer composition.[a]

Type of additional polyurethane layer[b]	Water uptake of polymer	NO release			Glucose sensor performance		
		$[NO]_{max}$	t_{max}[c]	Total [NO][d]	Glucose sensitivity	Permeability[e] of H_2O_2	Dynamic range[f]
	(mg H_2O·(mg PU)$^{-1}$)	(pmol·cm^{-2}·s^{-1})	(min)	(μmol·cm^{-2})	(nA·mM^{-1})		(mM)
HP-93A-100	2.6±0.3	77.2±12.9	4.3±3.0	1.82±0.21	55.6±28.8	0.25±0.15	1–10
AL-25-80A (HPU)	0.6±0.3	84.1±9.5	8.8±4.7	1.91±0.19	23.3±9.4	0.06±0.02	1–15
SG-80A (TPU)	0.2±0.2	32.2±13.0	231.4±81.8	1.82±0.26	7.3±3.5	0.01±0.01	1–24
TP-470	0.0±0.1	25.7±6.0	305.9±93.6	1.73±0.39	N/A[g]	N/A[g]	N/A[g]

[a] Standard deviation represents at least n=3 sensors.
[b] Cast with concentration of 40 mg·mL^{-1} PU dissolved in THF.
[c] Time necessary to reach $[NO]_{max}$.
[d] Total [NO] was determined via Griess assay (Chae et al. 2004) after incubating films in PBS at 37 °C for 2 d.
[e] Permeability refers to the response current of glucose sensors relative to bare electrodes.
[f] Linear range (R^2>0.97) of calibration curve.
[g] There was no sensor response.

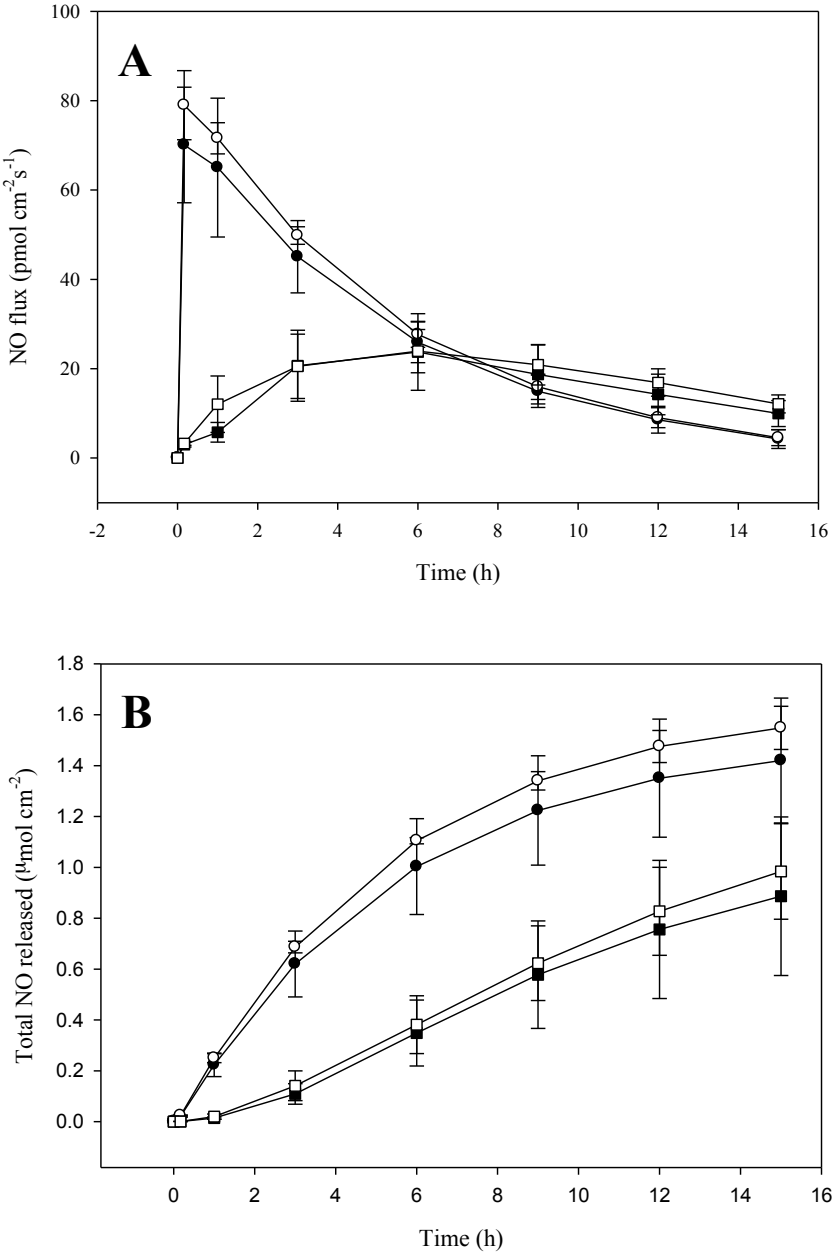

Figure 2.3. (A) Nitric oxide flux and (B) total NO release profile from AEAP3/TMOS particle-doped polyurethane membranes as a function of additional PU layer composition (40 mg·mL^{-1}): (●) Tecophilic HP-93A-100, (○) Hydrothane AL-25-80A, (■) Tecoflex SG-80A, and (□) Tecoplast TP-470.

Although the extent of water uptake differed among the four types of hydrophobic/hydrophilic polyurethanes, NO-release character appeared to be bimodal (Figure 2.3). Both hydrophilic PUs (HP-93A-100 and AL-25-80A) exhibited fast NO release, while the more hydrophobic PUs (SG-80A and TP-470) had more sustained NO release. Of note, these results may be indicative of a minimum threshold of water diffusion (water uptake value between 0.2–0.6 mg $H_2O \cdot (mg\ PU)^{-1}$) necessary to decompose diazeniumdiolates. Seemingly above/below this threshold, there is little effect on NO release kinetics. Both the glucose sensitivity and H_2O_2 permeability decreased as water uptake of the additional PU layer decreased (Table 2.4). However, the dynamic range was extended from 1–6 to 1–25 mM glucose due to reduced O_2 saturation. In the case where the most hydrophobic polyurethane (i.e., TP-470) was used to fabricate sensors, little if any glucose response was achieved due to inadequate analyte permeability (Table 2.4). Thus, there is an inverse relationship between sustained NO release and achieving sufficient glucose permeability.

To further alter NO release from the sensor membranes, the polymer concentration and thus thickness of the additional polyurethane was varied. These studies were carried out using the Tecoflex SG-80A (TPU) polymer to balance sustained NO release with adequate response to glucose. As the concentration of the TPU layer was increased from 20 to 60 $mg \cdot mL^{-1}$ (21–46 μm thick), the NO release duration and time to reach the maximum NO flux both increased. As expected, the maximum NO flux was suppressed as the diffusion of water through the membrane decreased (Figure 2.4). At 60 $mg \cdot mL^{-1}$ TPU, glucose response was no longer achievable (Table 2.5).

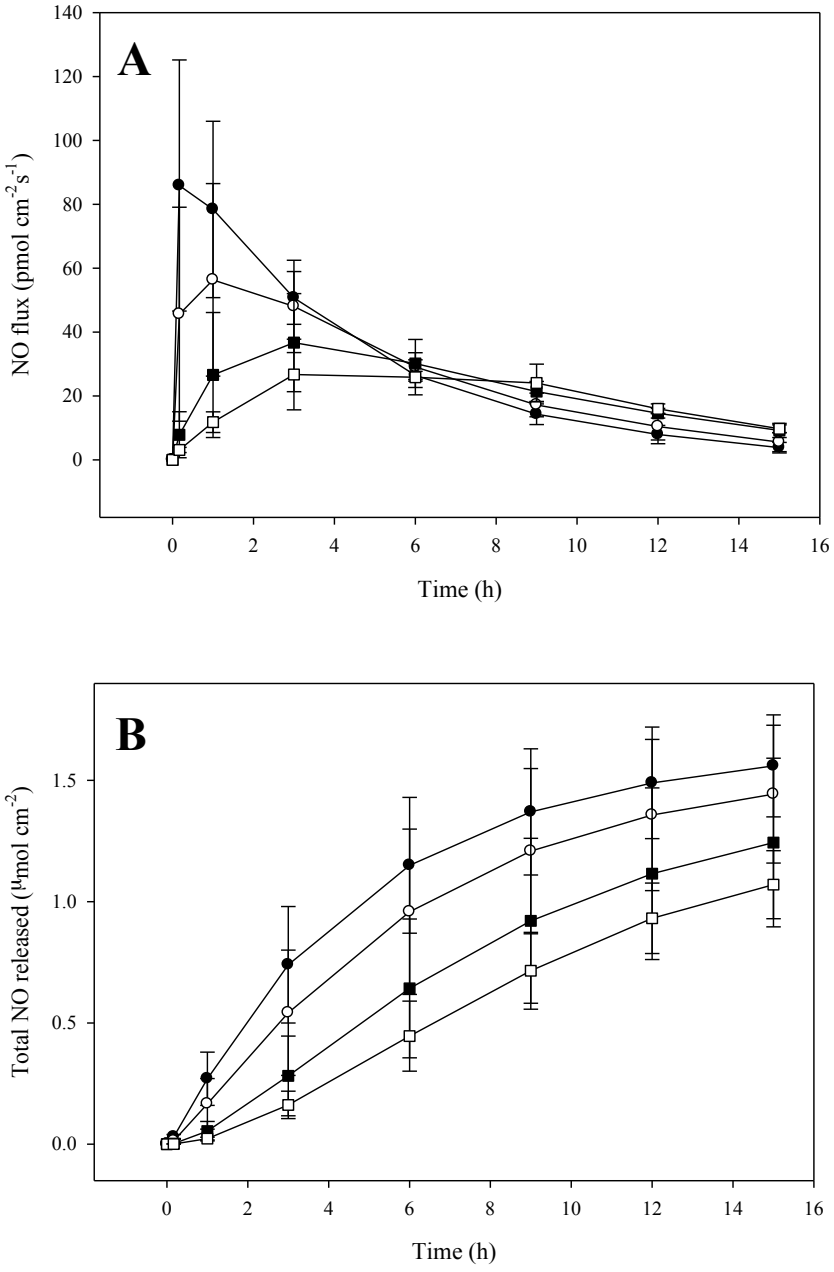

Figure 2.4. (A) Nitric oxide flux, and (B) NO totals from AEAP3/TMOS particle-doped (0.6 mg·cm^{-2}) PU films (●) without and with additional Tecoflex SG-80A (TPU) layer at (○) 20, (■) 40, and (□) 60 mg·mL^{-1} concentration.

Table 2.5. Characterization of NO release and glucose sensor performances for NO-releasing AEAP3/TMOS particle-doped (0.6 mg·cm^{-2}) polyurethane sensor membrane as a function of additional TPU polymer layer concentration.[a]

Concentration of additional Tecoflex SG-80A (TPU) layer	NO release			Glucose sensor performance			
	$[NO]_{max}$ (pmol·cm^{-2}·s^{-1})	t_{max}[b] (min)	t_d[c] (h)	Glucose sensitivity (nA·mM^{-1})	Permeability[d] of H_2O_2	Permeability[d] of O_2	Dynamic range[e] (mM)
without layer	92.9±39.6	10.1±6.3	25.2±6.2	114.0±43.2	0.16±0.04	0.72±0.18	1–6
20 mg·mL^{-1}	64.1±25.5	82.4±104.6	54.4±48.8	14.5±6.1	0.05±0.05	0.63±0.02	1–24
40 mg·mL^{-1}	32.2±13.0	231.4±82.0	64.4±12.2	7.3±3.5	0.01±0.00	0.34±0.19	1–24
60 mg·mL^{-1}	35.6±7.6	286.3±141.2	114.6±24.1	N/A[f]	N/A[f]	N/A[f]	N/A[f]

[a] Standard deviation represents at least n=3 sensors.
[b] Time necessary to reach $[NO]_{max}$.
[c] Duration of NO release, defined by fitting first-order kinetics at time point of 99% NO release (R^2=0.99).
[d] Permeability refers to the response current of glucose sensors relative to bare electrodes.
[e] Linear range (R^2>0.97) of calibration curve.
[f] No glucose response detected.

The preparation of hydrophobic porous membranes via electrospun nanofibers doped with NO donors may prove to be a viable alternative for designing longer NO releasing glucose sensors.[42]

2.3.4. Variation of amount of silica particles doped within polyurethane film

Since the RSNO-modified MPTMS/TEOS particle-doped films enable the longest NO release duration (i.e., 14 d) with minimal silica leaching, this composition was chosen as a model system for studying the effect of particle concentration on NO release characteristics and sensor performance. As expected, the total amount and maximum flux of NO release were enhanced by increasing the concentration of particles doped within the polymer layer from 0.2 to 2.4 $mg \cdot cm^{-2}$, while the casting volume was held constant (corresponding to 5 μL casting volume of 9–144 $mg \cdot mL^{-1}$ particle solution) (Table 2.6). The associated NO release half-life from this film was ~5 h. Moreover, the film continued to release NO above the detection limit (i.e., 0.5 $pmol \cdot cm^{-2} \cdot s^{-1}$) after 14 d (Figure 2.5). The maximum NO flux and total NO release were ~2560 $pmol \cdot cm^{-2} \cdot s^{-1}$ and 9.08 $\mu mol \cdot cm^{-2}$, respectively for membranes prepared using the largest particle concentration (2.4 $mg \cdot cm^{-2}$). Although high levels of NO release may cause apoptosis, NO release from the largest particle concentration doped-membrane was lower than levels reported to be cytotoxic or apoptosis initiating (>100 μM).[43,44] Additionally, Hetrick et al. reported that NO-donor modified particles (70% MAP3/TEOS particles) at 8 $mg \cdot mL^{-1}$ releasing 7.6 μmol NO mg^{-1} inhibited fibroblast proliferation to a lesser extent than clinical concentrations of currently administered antiseptics (e.g., chlorhexidine).[45]

Table 2.6. Characterization of NO release and glucose sensor performance for *S*-nitrosothiol-modified MPTMS/TMOS particle-doped polyurethane sensor membranes as a function of dopant concentration.[a]

	NO release					Glucose sensor performance			
Concentration of dopant ($mg \cdot cm^{-2}$)	$[NO]_{max}$ ($pmol \cdot cm^{-2} \cdot s^{-1}$)	t_{max}[b] (min)	Total [NO] ($\mu mol \cdot cm^{-2}$)	$t_{1/2}$[c] (h)	t_d[d] (d)	Glucose sensitivity ($nA \cdot mM^{-1}$)	Response time[e] ($t_{95\%}$, s)	Permeability[f] of H_2O_2	Film thickness (μm)
0.2	33.8±13.4	3.4±2.0	0.51±0.15	6.1±1.2	13.2±0.4	232.8±53.6	12.2±5.5	0.45±0.37	5.67±3.16
0.6	426.2±172.5	1.2±0.2	2.01±0.47	4.8±0.5	12.9±0.3	162.4±55.8	36.6±32.1	0.22±0.22	14.81±1.97
1.2	1310.0±1439.1	1.3±0.4	4.41±1.50	4.9±0.5	12.3±0.8	103.2±24.9	25.2±31.9	0.19±0.16	17.50±4.51
2.4	2557.0±1833.9	1.3±0.1	9.08±3.74	4.9±0.2	12.2±1.2	67.6±30.2	51.7±56.6	0.07±0.04	51.63±10.21

[a] Standard deviation represents at least n=3 sensors.

[b] Time necessary to reach $[NO]_{max}$.

[c] Half-life of NO release.

[d] Experimentally defined at time point of 99% NO released.

[e] Time necessary to reach 95% of stable signal.

[f] Permeability refers to the response current of glucose sensors relative to bare electrodes.

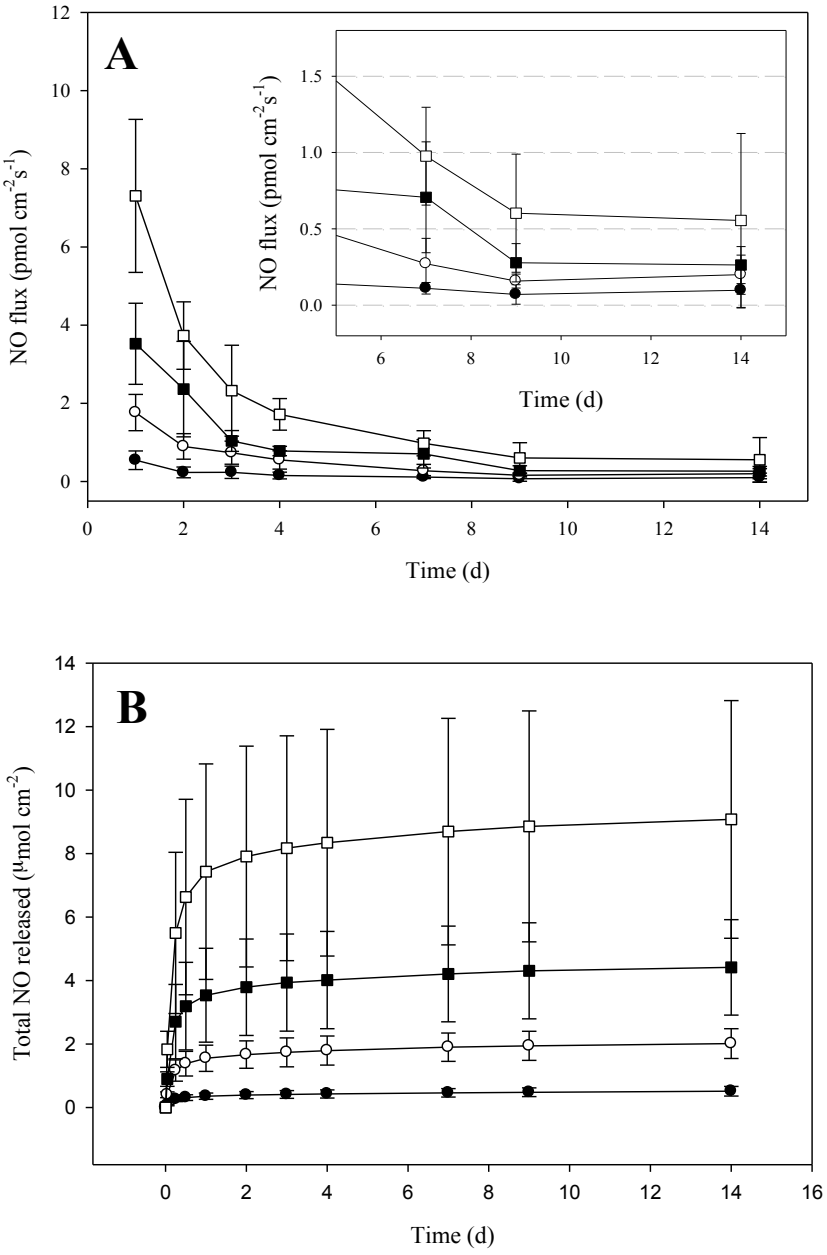

Figure 2.5. (A) Nitric oxide flux and (B) total NO released from RSNO-modified MPTMS/TEOS particle-doped polyurethane films as a function of particle concentration: (●) 0.2, (○) 0.6, (■) 1.2, and (□) 2.4 mg·cm^{-2}. Inset of (A) provides enlarged view of NO flux after 7 d.

Nevertheless, the in vivo utility of these sensor membranes must next be assessed in an appropriate animal model.

As the concentration of the NO-releasing silica scaffold was increased, we observed decreased membrane stability. For example, silica particle leaching and loss of membrane integrity were observed for overloaded polymers, particularly when the particle concentration was ~7 times greater than the polymer concentration in which the particle were dissolved (i.e., 144 $mg \cdot mL^{-1}$ particles in 20 $mg \cdot mL^{-1}$ PU solution). In addition to film instability, larger dopant concentrations hindered our ability to fabricate homogeneous films with consistent NO release. For example, larger standard deviations for maximum NO fluxes were observed for the greatest particle dopant concentrations (Table 2.6). At greater local concentrations of NO, the buildup of NO may facilitate accelerated RSNO decomposition from within the films due to an autocatalytic decomposition mechanism.[46] Film thickness increased from 5.67 to 51.63 μm upon increasing the particle concentration in the films from 0.2 to 2.4 $mg \cdot cm^{-2}$, respectively, despite keeping the casting volume constant. As a result, biosensor sensitivity was decreased and response time increased with larger particle concentrations due to decreased analyte permeability (Table 2.6).

2.4 Conclusion

A total NO release of ~1.35 $\mu mol \cdot cm^{-2}$ from an implant surface was previously shown to reduce the FBR.[21] The total and maximum NO flux of the RSNO-modified MPTMS/TEOS particle-doped (0.6 $mg \cdot cm^{-2}$) films presented here are 6 times greater with a 4-fold longer duration. Thus, the NO-releasing particle-doped sensor membranes

presented here hold promise for improving the biocompatibility of in vivo glucose sensors and potential to improve their analytical utility. Moreover, it is clear that our design allows for tunable NO fluxes and delivery totals by altering: (1) the type of NO-releasing dopant; (2) the type of polymer utilized; (3) the concentration of additional polymer layers; and (4) the amount of dopant in the NO-releasing layer. The glucose sensor performance (i.e., sensitivity, response time, and dynamic range) was affected by these modifications and must be evaluated and optimized for each NO-releasing membrane composition employed in order to fall within the clinically relevant range for in vivo glucose monitoring. While Hetrick et al.[21] demonstrated the feasibility of a particular NO-releasing coating to mitigate the FBR, the materials reported here represent a broader range of NO donor type, polymer matrix, and NO release characteristics.

2.5 References

(1) Wang, J. "Electrochemical glucose biosensors" *Chemical Reviews* **2008**, *108*, 814-825.

(2) Ward, W. K.; Jansen, L. B.; Anderson, E.; Reach, G.; Klein, J. C.; Wilson, G. S. "A new amperometric glucose microsensor: in vitro and short-term in vivo evaluation" *Biosensors & Bioelectronics* **2002**, *17*, 181-189.

(3) Klonoff, D. C. "Continuous glucose monitoring - Roadmap for 21st century diabetes therapy" *Diabetes Care* **2005**, *28*, 1231-1239.

(4) Heller, A.; Feldman, B. "Electrochemical glucose sensors and their applications in diabetes management" *Chemical Reviews* **2008**, *108*, 2482-2505.

(5) Klonoff, D. C. "A review of continuous glucose monitoring" *Diabetes Technology and Therapeutics* **2005**, *7*, 770-775.

(6) Wisniewski, N.; Moussy, F.; Reichert, W. M. "Characterization of implantable biosensor membrane biofouling" *Fresenius' Journal of Analytical Chemistry* **2000**, *366*, 611-621.

(7) Wisniewski, N.; Reichert, M. "Methods for reducing biosensor membrane biofouling" *Colloids and Surfaces B: Biointerfaces* **2000**, *18*, 197-219.

(8) Wilson, G. S.; Hu, Y. B. "Enzyme based biosensors for in vivo measurements" *Chemical Reviews* **2000**, *100*, 2693-2704.

(9) Wilson, G. S.; Gifford, R. "Biosensors for real-time *in vivo* measurements" *Biosensors and Bioelectronics* **2005**, *20*, 2388-2403.

(10) Refai, A. K.; Textor, M.; Brunette, D. M.; Waterfield, J. D. "Effect of titanium surface topography on macrophage activation and secretion of proinflammatory cytokines and chemokines" *Journal of Biomedical Materials Research Part A* **2004**, *70*, 194-205.

(11) Williams, D. L. H. "A chemist's view of the nitric oxide story" *Organic & Biomolecular Chemistry* **2003**, *1*, 441-9.

(12) Nablo, B. J.; Schoenfisch, M. H. "In vitro cytotoxicity of nitric oxide-releasing sol-gel derived materials" *Biomaterials* **2005**, *26*, 4405-4415.

(13) Hetrick, E. M.; Schoenfisch, M. H. "Reducing implant-related infections: active release strategies" *Chemical Society Reviews* **2006**, *35*, 780-9.

(14) Riccio, D. A.; Dobmeier, K. P.; Hetrick, E. M.; Privett, B. J.; Paul, H. S.; Schoenfisch, M. H. "Nitric oxide-releasing *S*-nitrosothiol-modified xerogels" *Biomaterials* **2009**, *30*, 4494-4502.

(15) Nablo, B. J.; Chen, T. Y.; Schoenfisch, M. H. "Sol-gel derived nitric-oxide releasing materials that reduce bacterial adhesion" *Journal of the American Chemical Society* **2001**, *123*, 9712-9713.

(16) Nablo, B. J.; Schoenfisch, M. H. "Antibacterial properties of nitric oxide-releasing sol-gels" *Journal of Biomedical Materials Research Part A* **2003**, *67A*, 1276-1283.

(17) Hetrick, E. M.; Schoenfisch, M. H. "Antibacterial nitric oxide-releasing xerogels: Cell viability and parallel plate flow cell adhesion studies" *Biomaterials* **2007**, *28*, 1948-1956.

(18) Hetrick, E. M.; Shin, J. H.; Stasko, N. A.; Johnson, C. B.; Wespe, D. A.; Holmuhamedov, E.; Schoenfisch, M. H. "Bactericidal efficacy of nitric oxide-releasing silica nanoparticles" *Acs Nano* **2008**, *2*, 235-246.

(19) Privett, B. J.; Nutz, S. T.; Schoenfisch, M. H. "Efficacy of surface-generated nitric oxide against Candida albicans adhesion and biofilm formation" *Biofouling* **2010**, *26*, 973-983.

(20) Nablo, B. J.; Prichard, H. L.; Butler, R. D.; Klitzman, B.; Schoenfisch, M. H. "Inhibition of implant-associated infections via nitric oxide" *Biomaterials* **2005**, *26*, 6984-6990.

(21) Hetrick, E. M.; Prichard, H. L.; Klitzman, B.; Schoenfisch, M. H. "Reduced foreign body response at nitric oxide-releasing subcutaneous implants" *Biomaterials* **2007**, *28*, 4571-4580.

(22) Gifford, R.; Batchelor, M. M.; Lee, Y.; Gokulrangan, G.; Meyerhoff, M. E.; Wilson, G. S. "Mediation of in vivo glucose sensor inflammatory response via nitric oxide release" *Journal of Biomedical Materials Research Part A* **2005**, *75A*, 755-766.

(23) Yan, Q.; Major, T. C.; Bartlett, R. H.; Meyerhoff, M. E. "Intravascular glucose/lactate sensors prepared with nitric oxide releasing poly(lactide-co-glycolide)-based coatings for enhanced biocompatibility" *Biosensors and Bioelectronics* **2011**, *26*, 4276-4282.

(24) Nichols, S. P.; Le, N. N.; Klitzman, B.; Schoenfisch, M. H. "Increased in vivo glucose recovery via nitric oxide release" *Analytical Chemistry* **2011**, *83*, 1180-1184.

(25) Shin, J. H.; Marxer, S. M.; Schoenfisch, M. H. "Nitric oxide-releasing sol-gel particle/polyurethane glucose biosensors" *Analytical Chemistry* **2004**, *76*, 4543-4549.

(26) Oh, B. K.; Robbins, M. E.; Nablo, B. J.; Schoenfisch, M. H. "Miniaturized glucose biosensor modified with a nitric oxide-releasing xerogel microarray" *Biosensors & Bioelectronics* **2005**, *21*, 749-757.

(27) Saavedra, J. E.; Southan, G. J.; Davies, K. M.; Lundell, A.; Markou, C.; Hanson, S. R.; Adrie, C.; Hurford, W. E.; Zapol, W. M.; Keefer, L. K. "Localizing antithrombotic and vasodilatory activity with a novel, ultrafast nitric oxide donor" *Journal of Medicinal Chemistry* **1996**, *39*, 4361-4365.

(28) Shin, J. H.; Schoenfisch, M. H. "Inorganic/organic hybrid silica nanoparticles as a nitric oxide delivery scaffold" *Chemistry of Materials* **2008**, *20*, 239-49.

(29) Shin, J. H.; Metzger, S. K.; Schoenfisch, M. H. "Synthesis of nitric oxide-releasing silica nanoparticles" *Journal of the American Chemical Society* **2007**, *129*, 4612-4619.

(30) Riccio, D. A.; Nugent, J. L.; Schoenfisch, M. H. "Stöber Synthesis of Nitric Oxide-Releasing *S*-Nitrosothiol-Modified Silica Particles" *Chemistry of Materials* **2011**, *23*, 1727-1735.

(31) Chae, S. Y.; Lee, M.; Kim, S. W.; Bae, Y. H. "Protection of insulin secreting cells from nitric oxide induced cellular damage by crosslinked hemoglobin" *Biomaterials* **2004**, *25*, 843-850.

(32) Amstad, E.; Gillich, T.; Bilecka, I.; Textor, M.; Reimhult, E. "Ultrastable iron oxide nanoparticle colloidal suspensions using dispersants with catechol-derived anchor groups" *Nano Letters* **2009**, *9*, 4042-4048.

(33) Lahtinen, M.; P, H. t.; Riekkola, M. L.; Yohannes, G. "Analysis of colloids released from bentonite and crushed rock" *Physics and Chemistry of the Earth, Parts A/B/C* **2010**, *35*, 265-270.

(34) Schoenfisch, M. H.; Rothrock, A. R.; Shin, J. H.; Polizzi, M. A.; Brinkley, M. F.; Dobmeier, K. P. "Poly(vinylpyrrolidone)-doped nitric oxide-releasing xerogels as glucose biosensor membranes" *Biosensors & Bioelectronics* **2006**, *22*, 306-312.

(35) Shin, J. H.; Privett, B. J.; Kita, J. M.; Wightman, R. M.; Schoenfisch, M. H. "Fluorinated xerogel-derived microelectrodes for amperometric nitric oxide sensing" *Analytical Chemistry* **2008**, *80*, 6850-6859.

(36) Bindra, D. S.; Zhang, Y.; Wilson, G. S.; Sternberg, R.; Thevenot, D. R.; Moatti, D.; Reach, G. "Design and in vitro studies of a needle-type glucose sensor for subcutaneous monitoring" *Analytical Chemistry* **1991**, *63*, 1692-1696.

(37) Wang, P. G.; Xian, M.; Tang, X. P.; Wu, X. J.; Wen, Z.; Cai, T. W.; Janczuk, A. J. "Nitric oxide donors: Chemical activities and biological applications" *Chemical Reviews* **2002**, *102*, 1091-1134.

(38) Al-Sa'doni, H. H.; Ferro, A. "*S*-nitrosothiols as nitric oxide-donors: Chemistry, biology and possible future therapeutic applications" *Current Medicinal Chemistry* **2004**, *11*, 2679-2690.

(39) Bergmeyer, H. U.; Gawehn, K.; Grassl, M. *Method of enzymetic analysis*; second ed.; Academic Press Inc.: New York, 1974.

(40) Barbe, C.; Bartlett, J.; Kong, L. G.; Finnie, K.; Lin, H. Q.; Larkin, M.; Calleja, S.; Bush, A.; Calleja, G. "Silica particles: A novel drug-delivery system" *Advanced Materials* **2004**, *16*, 1959-1966.

(41) Frost, M. C.; Reynolds, M. M.; Meyerhoff, M. E. "Polymers incorporating nitric oxide releasing/generating substances for improved biocompatibility of blood-contactincy medical devices" *Biomaterials* **2005**, *26*, 1685-1693.

(42) Coneski, P. N.; Nash, J. A.; Schoenfisch, M. H. "Nitric oxide-releasing electrospun polymer microfibers" *ACS Applied Materials & Interfaces* **2011**, *3*, 426-432.

(43) Cals-Grierson, M. M.; Ormerod, A. D. "Nitric oxide function in the skin" *Nitric Oxide* **2004**, *10*, 179-193.

(44) Lipton, S. A.; Choi, Y.-B.; Pan, Z.-H.; Lei, S. Z.; Chen, H.-S. V.; Sucher, N. J.; Loscalzo, J.; Singel, D. J.; Stamler, J. S. "A redox-based mechanism for the neuroprotective and neurodestructive effects of nitric oxide and related nitroso-compounds" *Nature* **1993**, *364*, 626-632.

(45) Hetrick, E. M.; Shin, J. H.; Paul, H. S.; Schoenfisch, M. H. "Anti-biofilm efficacy of nitric oxide-releasing silica nanoparticles" *Biomaterials* **2009**, *30*, 2782-2789.

(46) Grossi, L.; Montevecchi, P. C. "A kinetic study of *S*-nitrosothiol decomposition" *Chemistry-a European Journal* **2002**, *8*, 380-387.

CHAPTER 3: NITRIC OXIDE-RELEASING SILICA NANOPARTICLE-DOPED POLYURETHANE ELECTROSPUN FIBERS

Original article was co-authored with Alexis W. Carpenter, Danielle L. Slomberg, and Mark H. Schoenfisch. Text, figures, and tables are adopted and reprinted with permission of ACS publications: Ahyeon Koh, Alexis W. Carpenter, Danielle L. Slomberg, and Mark H. Schoenfisch, "Nitric oxide-releasing silica nanoparticle-doped polyurethane electrospun fibers", *ACS Applied Materials and Interfaces*, Volume 5, Issue 16, August 2013, Pages 7956-7964, DOI:10.1021/am402044s.

3.1 Introduction

Nitric oxide (NO) is a key physiological mediator of vasodilation, angiogenesis, wound healing, and phagocytosis, all of which are highly dependent on NO concentration.[1] As many disease states and health ailments are mitigated by NO, exogenous NO donors are widely studied as potential therapeutic agents.[2-5] In particular, macromolecular NO donor scaffolds have been the focus of much research due to their ability to store large amounts of NO and facilitate biological action. Indeed, the NO release achieved using xerogels,[6-9] silica nanoparticles,[10-12] dendrimers,[13-16] biodegradable polyesters,[17-19] and medical-grade polyurethanes[20-22] has demonstrated utility to modulate wound healing,[23,24] kill bacteria and cancer cells,[25-27] and improve the analytical performance of chemical sensors.[28-30] Silica nanoparticles modified with NO donors represent an attractive NO-release vehicle due to straightforward synthesis, ability to achieve significant NO payloads and tunable NO-release kinetics, and their inherent low toxicity.[9,10] In Chapter 2, we employed polymers doped with NO donor-modified silica

particles to prepare NO-releasing glucose sensor membranes.[22] Nitric oxide release from the sensor membranes was tuned by altering the silica particle concentration, NO donor type, water uptake properties of the polyurethane, and the use of an overlaying polymer coating of variable thickness.[22] Unfortunately, the utility of these membranes for sensor applications was limited due to an inverse relationship between NO-release duration and analyte (i.e., glucose) permeability.[22] A more porous NO-releasing coating is thus desirable to maintain adequate analyte permeability.

Electrospinning of polymers is a straightforward method for preparing highly porous materials consisting of fibers.[31,32] The electrospinning process involves propelling an electrically charged viscoelastic jet of polymer solution to a grounded collector via a high voltage electrostatic field.[32] As the jet of polymer solution travels through the air to the grounded collector, polymer nanofibers solidify upon solvent evaporation, resulting in a non-woven web or mat of fibers.[32] Some advantages of polymeric fibers over bulk polymer films include large surface area to volume ratios, flexibility in surface functionality, and superior mechanical properties (e.g., stiffness and tensile strength).[32-34] Additionally, the microporosity of the non-woven fiber mat is believed to be ideal for promoting tissue integration,[35,36] suggesting that these materials may be suitable as outer sensor membranes for subcutaneous glucose sensors.[37] With physical properties that mimic the extracellular matrix, the use of electrospun fibers has been confirmed to promote cell proliferation and differentiation,[35,36,38,39] enhance tissue-scaffold integration, and decrease fibrous encapsulation compared to bulk polymer films.[39,40] Much research is

now focused on developing electrospun fibers as tissue engineering scaffolds, wound dressings, and implant and medical prostheses coatings.[32-34]

The versatility of the electrospinning process has enabled the fabrication of fiber mats capable of releasing silver,[41-43] dexamethasone,[44] and NO.[18,45] With respect to NO release, we previously reported on polyurethane and poly(vinyl chloride) fibers capable of NO release by doping a low molecular weight *N*-diazeniumdiolate NO donor (1-[(2-carboxylato)pyrrolidin-1-yl]diazen-1-ium-1,2-diolate or PROLI/NO) into the polymer solution prior to electrospinning.[45] While the NO-release kinetics of the PROLI/NO-doped fibers proved to be variable depending on the polymer composition and fiber diameter, the NO payloads and release durations were limited.[45] The incorporation of macromolecular NO-release vehicles (i.e., silica particles) may enhance NO-release totals and durations compared to those obtained using PROLI/NO as a dopant. In this chapter, fabrication of macromolecular NO release scaffold-doped fibers as a function of both the NO-releasing particle composition and polymer fiber characteristics (e.g., diameter and water uptake) is described. Due to the size of the particle dopants (50–400 nm), careful attention is focused on the stability and mechanical properties of the ensuing fibers.

3.2 Experimental

3.2.1 Materials

Tecoflex (SG-85A) and Tecophilic (HP-93A-100) polyurethanes were gifts from Thermedics (Woburn, MA). Tecoplast (TP-470) polyurethane was provided by Lubrizol (Cleveland, OH). The following silanes for synthesizing silica particles were purchased from Gelest (Morrisville, PA): *N*-(6-aminohexyl)aminopropyltrimethoxysilane (AHAP3), *N*-(2-aminoethyl)-3-aminopropyltrimethoxysilane (AEAP3), 3-mercaptopropyltrimethoxysilane (MPTMS), tetramethoxysilane (TMOS) and tetraethoxysilane (TEOS). All other salts and solvents were laboratory grade and purchased from Fisher Scientific (St. Louis, MO). Water (18.2 MΩ·cm; total organic content <6 ppb) was purified using a Millipore Milli-Q Gradient A-10 purification system (Bedford, MA). Nitrogen, argon, and nitric oxide gases were purchased from Airgas National Welders Supply (Durham, NC).

3.2.2 Synthesis of NO-releasing silica particles

Nitric oxide-releasing silica particles were synthesized as previously described via the co-condensation of an aminosilane (i.e., AEAP3 or AHAP3) or a mercaptosilane (i.e., MPTMS) at 65–75 mol% with a backbone silane (i.e., TEOS or TMOS).[10,11,46] To form *N*-diazeniumdiolate NO donors, the amine-containing particles were exposed to 10 atm NO gas for 3 d in the presence of sodium methoxide at room temperature with constant stirring in a Parr pressure vessel.[46]

Table 3.1. Characterization of nitric oxide-releasing silica particles.

Type of NO donor	*Particle composition*	*mol%*[a]	*Particle size*[b] (nm)	$[NO]_{max}$[c] (ppm mg^{-1})	t_{max}[d] (min)	*Total [NO]*[e] (μmol mg^{-1})	t_d[f] (h)
N-diazeniumdiolate	AHAP3/TEOS	65	56 ± 7	23.2 ± 19.9	0.9 ± 0.2	1.5 ± 0.3	15.2 ± 2.1
	AHAP3/TEOS	65	93 ± 14	25.7 ± 2.9	0.6 ± 0.1	1.3 ± 0.2	13.0 ± 3.8
	AEAP3/TMOS	70	152 ± 2	1.9 ± 0.4	0.9 ± 0.1	0.4 ± 0.2	9.6 ± 2.2
S-nitrosothiol	MPTMS/TEOS	75	416 ± 23	1.9 ± 0.4	3.3 ± 0.1	3.2 ± 0.6	> 48

[a] Balance TEOS or TMOS backbone silane
[b] Particle size determined by electron microscope representing non-hydrated diameter of particle
[c] Maximum instantaneous concentration of NO released as measured with NOA
[d] Time required to reach $[NO]_{max}$
[e] Total number of moles of NO released per mg of particle as measured by the Griess assay
[f] Duration of NO release.

S-Nitrosothiol NO donor-modified particles were prepared by treating the thiol-containing nanoparticles with acidified nitrite for 2 h in the dark at 0 °C.[11] Full characterization of the NO release from each particle system is provided in Table 3.1. All NO-releasing particle systems were stored in a vacuum-sealed, dark container at -20 °C until further use.

3.2.3 Nitric oxide-releasing silica particle-doped polyurethane fiber formation.

Nitric oxide-releasing silica particle-doped electrospun fibers were fabricated using a custom electrospinning apparatus consisting of a Series 205B High Voltage Power Supply from Bertan Associates, Inc. (Hicksville, NY), a Kent Scientific Genie Plus syringe pump (Torrington, CT), and a circular steel disk (23 cm diameter) collector.[45] Voltage was applied to a standard stainless steel blunt-tip needle (22 gauge and 0.508 mm ID; Jensen Global, Santa Barbara, CA) attached to a solution-filled syringe positioned atop the syringe pump. The grounded collector was covered in aluminum foil (for ease of sample collection) and mounted perpendicular to the direction of the syringe at a distance of 15 cm. Fiber mats were prepared by electrospinning the polymer solution at an applied voltage of 15 kV and a flow rate of 15 μL min^{-1}. Resulting fiber mats were collected from center of disk collector for further evaluations. Polyurethane solutions containing NO-releasing silica particles were prepared by first dissolving the polymer in 1.6 mL of a 3:1 (v/v) tetrahydrofuran (THF): *N,N*-dimethylformamide (DMF) solution, then mixing in a suspension of NO donor-modified silica particles dispersed in methanol (400 μL). The final concentration of polymer in this cocktail ranged from 8–16% (w/v) with particles embedded at 1–10 wt% of the polymer mass. Solution viscosity was

determined using a capillary-viscometer (Schott AVS 360; Hofheim, Germany) at room temperature. The conductivity of the polyurethane solutions was measured using a Malvern Nano Series Zetasizer (Malvern, England) operated in zeta potential mode, and consisted of an average of 5 measurements.

3.2.4 Characterization of NO-releasing silica particle-doped electrospun fibers

Electrospun fibers were imaged using an environmental scanning electron microscope (ESEM) (Quanta 200 field emission gun; FEI company; Hillsboro, OR) with large-field detector (LFD) under low vacuum (i.e., 0.38 Torr). Samples were prepared without an additional metal coating in order to observe particles embedded in the fibers. Reported fiber diameters were measured with ImageJ software (NIH, Bethesda, MD) and reported as averages of at least 75 measurements per sample from three electrospun mats.

The surface area of the fiber mat was measured using a Micromeritics Tristar II 3020 Surface Area and Porosity Analyzer (Norcross, GA). The percent porosity of the fiber mat was calculated according to the following equations (1) and (2).[47-49] The bulk densities of the polyurethanes are 1.13, 1.05, and 1.18 g/cm^3 for Tecophilic, Tecoflex, and Tecoplast, respectively. The film thickness was determined by ESEM and was found to be proportional to the feed volume (e.g., ~50 μm for 1 mL electrospinning solution).

$$apparent\ density\ \left(\frac{g}{cm^3}\right) = \frac{mat\ mass\ (g)}{mat\ thickness\ (cm) \times mat\ area\ (cm^2)} \qquad (1)$$

$$percent\ porosity = \left(1 - \frac{apparent\ density\ \left(\frac{g}{cm^3}\right)}{bulk\ density\ of\ polymer\ \left(\frac{g}{cm^3}\right)}\right) \times 100\% \qquad (2)$$

The tensile strain-strength of the electrospun fiber mats was characterized using an Instron 5566 electromechanical tensile tester (Norwood, MA) at a cross-head speed of 10 mm min^{-1}. Fiber mats were cut into strips (10 mm × 29 mm) for testing and the thickness were determined by ESEM.[50] Modulus was defined as the slope of the tensile stress-strain curve showing elastic deformation. The standard deviation is based on measurements from three different batches. Water uptake was evaluated by weighing a section of the fiber mat before and after soaking in PBS for 3 h.[22] Leaching of silica particles from the fibers was evaluated by quantifying the concentration of silicon (Si) in solutions that the particle-doped electrospun fiber mats had been immersed (15 mL phosphate buffered saline (PBS) and incubated at 37 °C for 7 d). Silicon concentrations in the PBS soak solutions were determined using inductively coupled plasma-optical emission spectroscopy (ICP-OES; Teledyne Leeman labs; Hudson, NH) in an axial configuration at 251.611 nm. Prior to analysis, 0.05–10 ppm silica particle standard solutions (in PBS) were used to construct a calibration curve.

Nitric oxide release was measured using a Sievers chemiluminescence Nitric Oxide Analyzer (NOA, Model 280i; Boulder, CO). To determine NO flux, electrospun samples were placed in a solution of deoxygenated PBS (0.01 M, pH 7.4) at 37 °C. Liberated NO was carried to the NOA by continuously purging the solution and vessel head space with nitrogen gas at a controlled rate as previously described.[11] The NOA was calibrated using a standard 26.80 ppm NO gas (balance nitrogen) and air passed through a Sievers NO zero filter. The sample vessel was shielded from light to prevent light-initiated NO release from *S*-nitrosothiol-based NO donors.[11] Total NO payloads were

determined spectrophotometrically by measuring the conversion of NO to nitrite using the Griess assay.[51] After soaking NO-releasing fibers in PBS at 37 °C for a period exceeding their NO release, 50 μL of the sample solution was mixed with 50 μL of 1% (w/v) sulfanilamide in 5% (v/v) phosphoric acid and 0.1% (w/v) *N*-(1-naphthyl)ethylenediamine dihydrochloride, and incubated at room temperature for 10 min. The absorbance of this solution was then measured at 540 nm using a Labsystem Multiskan RC microplate spectrophotometer (Helsinki, Finland). Total nitrite concentration was determined using a calibration curve constructed with standard nitrite solutions. Of note, the total NO concentration measured by the Griess assay agreed with that obtained from chemiluminescence analysis, confirming that these materials released NO and not nitrite.[51]

3.3 Results and Discussion

3.3.1 Fabrication of NO-releasing silica particle-doped electrospun fiber mats

The therapeutic potential of active NO release from an implant surface has been widely discussed.[3,52] The primary goal of the studies presented here was to fabricate stable NO-releasing silica particle-doped electrospun polyurethane fiber mats with porosities more apt for reducing the foreign body response when implanted subcutaneously,[40] and thus allowing for improved analyte diffusion for sensor applications. Secondly, we aimed to achieve tunable NO-release properties from these fibers, as many of NO's biological activities are concentration dependent.[2] Three polyurethane compositions (i.e., Tecophilic, Tecoflex, and Tecoplast) of varying

hydrophobicity were chosen since water uptake of the polymer has been shown to influence NO release depending on NO-donor class.[22] Silica particles of varied size (50–400 nm), NO-donor class (*N*-diazeniumdiolate and *S*-nitrosothiol), NO payload (0.4–3.2 μmol mg^{-1}), and NO-release duration (9.6 h to >2 d) were employed to tune the NO-release properties from the resulting fiber mats. Two *N*-diazeniumdiolated AHAP3/TEOS silica particle systems of different sizes (i.e., 50 and 100 nm) but similar NO-release properties were used to study the role of particle size on fiber mat incorporation and resulting NO-release. A wide range of NO-release properties was achieved by employing two different types of *N*-diazeniumdiolate-based particle systems, AEAP3/TMOS and AHAP3/TEOS, as well as a *S*-nitrosothiol-based system, MPTMS/TEOS (short, medium and long NO-release kinetics, respectively). Of note, the MPTMS/TEOS system was selected as it allowed for much longer NO release durations, despite having an altered composition and size relative to the AEAP3/TMOS and AHAP3/TEOS systems.[11,46] Indeed, *S*-nitrosothiol-modified silica particles have longer NO release duration relative to the *N*-diazeniumdiolate silica (>48 h vs. ~10 h, respectively).[11] The polymer and silica particle concentration ranges (8–16% (w/v) and 1–10 wt%, respectively) were selected to allow for the greatest amount of particle incorporation within the fibers without inhibiting the electrospinning process.

As shown in Figure 3.1 and 3.2, the particles were successfully embedded inside of the electrospun fibers at the concentration studied with various particle and polyurethane types. Although the nanoparticles were not dispersed homogeneously within individual fibers, they were distributed throughout the entire electrospun fiber mat.

The electrospun polyurethane (PU) fiber mats exhibited random open porous structures with interconnected nano/submicron fibers and a surface area of ~2 $m^2 g^{-1}$. In the absence of silica, the percent porosities of the electrospun fiber mats were 80.3 ± 2.1, 85.8 ± 7.6, and 83.8 ± 3.1% for the 12% (w/v) Tecophilic, Tecoflex, and Tecoplast polyurethanes, respectively. Particle incorporation up to 10 wt% did not significantly influence fiber mat porosity. As expected based on the nature of the bulk polymer, Tecoplast fibers were characterized as having the lowest water uptake (0.8 ± 0.5 mg H_2O/mg of PU fiber mat) followed by the Tecoflex (1.6 ± 0.2 mg H_2O/mg of PU fiber mat), and Tecophilic (4.7 ± 1.0 mg H_2O/mg of PU fiber mat) polymers.[22] The fiber mats exhibited greater water uptake than bulk polymer films of similar thickness after equivalent soaking time, a feature attributed to the open/porous structure of the fiber mats.

As expected, the physical properties of the electrospun fiber mats including fiber diameter, mechanical properties, and stability (i.e., leaching of silica particles) were dependent on the polymer solution concentration, polymer type, and NO donor system (particle type and concentration). Since porosity and fiber diameter represent important factors in mitigating the inflammatory response,[36,39] the effects of a number of electrospinning parameters on fiber diameter, tensile stress-strain, and silica incorporation/stability of the ensuing fiber mat were determined. Varying the applied voltage, needle tip diameter, flow rate, and distance between the collector and needle did not significantly impact the fiber diameter or morphology (data not shown). In contrast, both the viscosity and conductivity of the polymer solution proved important for controlling the geometry of the fiber mat.[45,53]

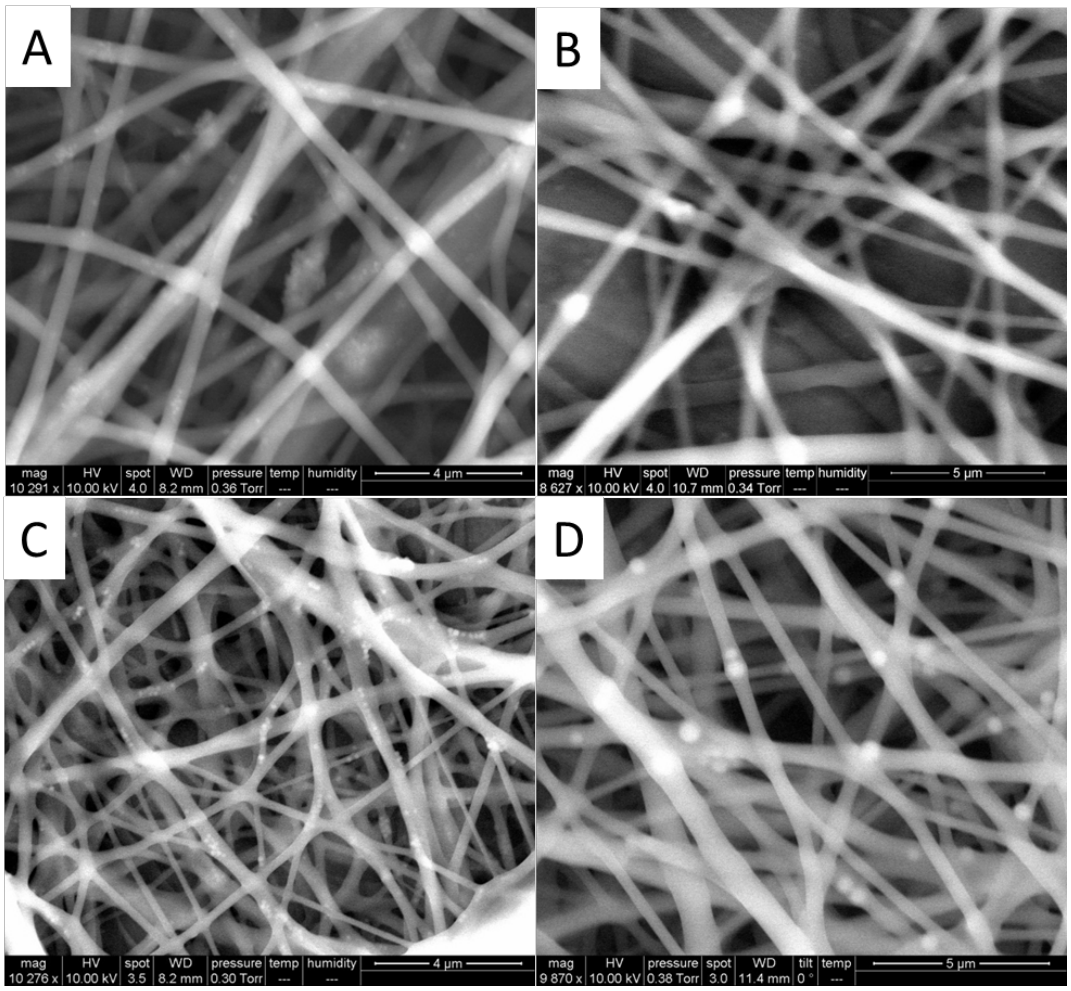

Figure 3.1. Environmental scanning electron microscopy images of 12% (w/v) Tecoflex electrospun fibers doped with 5 wt% of *N*-diazeniumdiolated (A) AHAP3/TEOS (~50 nm), (B) AHAP3/TEOS (~100 nm), and (C) AEAP3/TMOS and (D) *S*-nitrosothiol functionalized MPTMS/TEOS silica nanoparticles.

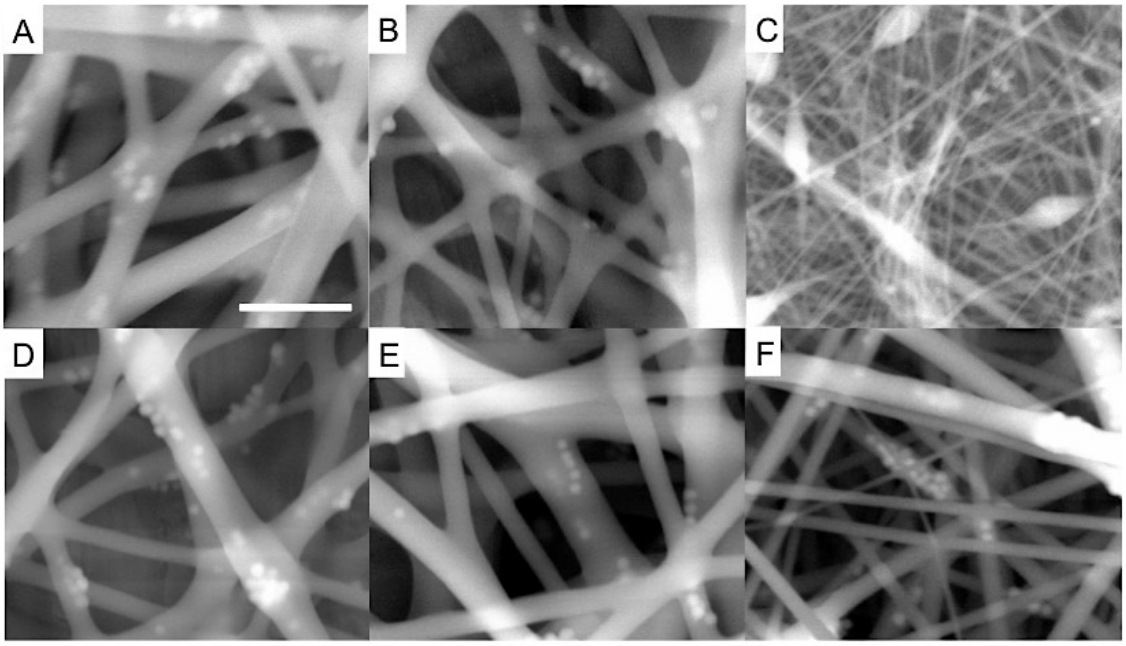

Figure 3.2. Environmental scanning electron microscope images of polyurethane electrospun fibers composed of 5 wt% *N*-diazeniumdiolated-AEAP3/TMOS nanoparticle-doped 8% (w/v) (A) Tecophilic, (B) Tecoflex, and (C) Tecoplast; and 12% (w/v) (D) Tecophilic, (E) Tecoflex, and (F) Tecoplast PU polymer. Scale bar indicates 1 μm.

Bead formation due to insufficient solution cohesion and/or improper Taylor jet elongation[32,45,53,54] was suppressed with increasing the solution viscosity and conductivity. As shown in Figure 3.2C, bead formation was only observed for fibers electrospun using 8% (w/v) Tecoplast polymer solutions, which exhibited a lower kinematic viscosity (45.3 ± 3.3 mm^2 s^{-1}) compared to Tecoflex and Tecophilic PU (67.4 ± 1.0 and 146.6 ± 2.3 and mm^2 s^{-1}, respectively). Increasing the concentration of the Tecoplast polymer from 8 to 12% (w/v) increased the solution's kinematic viscosity from 45.3 ± 3.3 to 94.0 ± 2.2 mm^2 s^{-1}, in turn eliminating bead formation.

As shown in Figure 3.3, the kinematic viscosity of the polymer solution directly affected the diameter of resulting fibers. For example, the average diameter of 5 wt% AEAP3/TMOS particle-doped 12% (w/v) PU electrospun fibers increased from 168 ± 34 to 462 ± 109 and 551 ± 71 nm as the kinematic viscosity increased from 94.0 ± 2.2 to 287.0 ± 1.7 and 405.8 ± 4.5 mm^2 s^{-1} for Tecoplast, Tecoflex, and Tecophilic polyurethanes, respectively. Additionally, the fiber diameter of Tecophilic PU fibers was greater than Tecoflex and Tecoplast fibers regardless of type of dopant (Figure 3.4). Similarly, increasing the polyurethane concentration resulted in larger fiber diameters. For example, changing the concentration of Tecoflex PU in the electrospinning polymer cocktail from 8 to 12 and 16% (w/v) increased the size of the resulting fibers from 257 ± 66 to 462 ± 109 and 625 ± 156 nm, respectively. The largest polymer concentration investigated (i.e., 16% (w/v)) inhibited proper electrospinning of Tecophilic PU due to needle clogging. At this concentration, the viscosity of the polymer solution as 2206.6 ± 82.6 mm^2 s^{-1}.

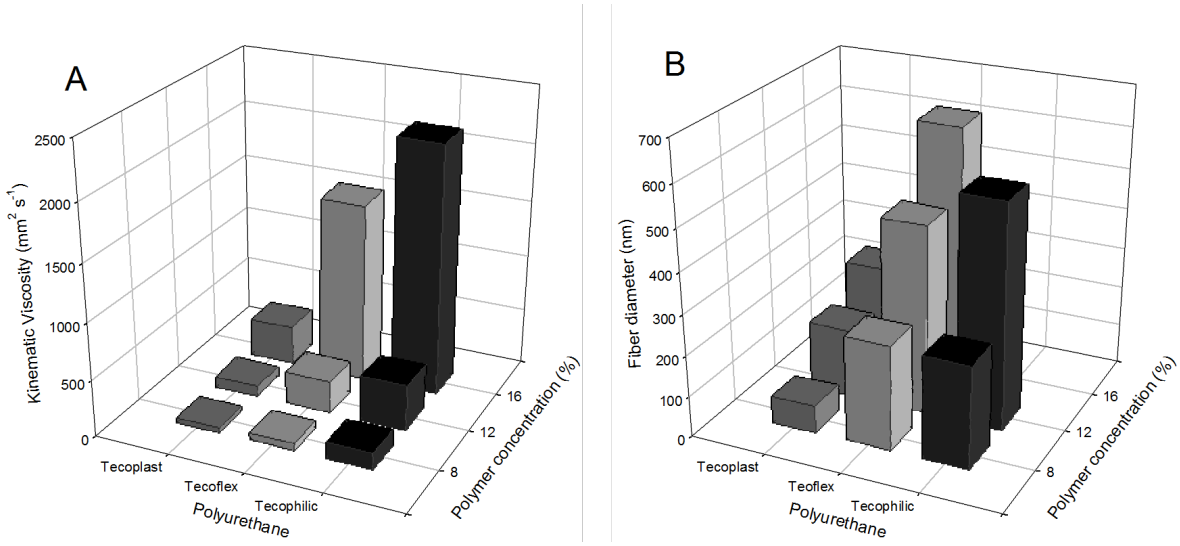

Figure 3.3. (A) Kinematic viscosity of polymer solution and (B) diameters of resulting fibers from polyurethanes doped with 5 wt% *N*-diazeniumdiolated AEAP3/TMOS silica nanoparticles as a function of polymer concentration and type.

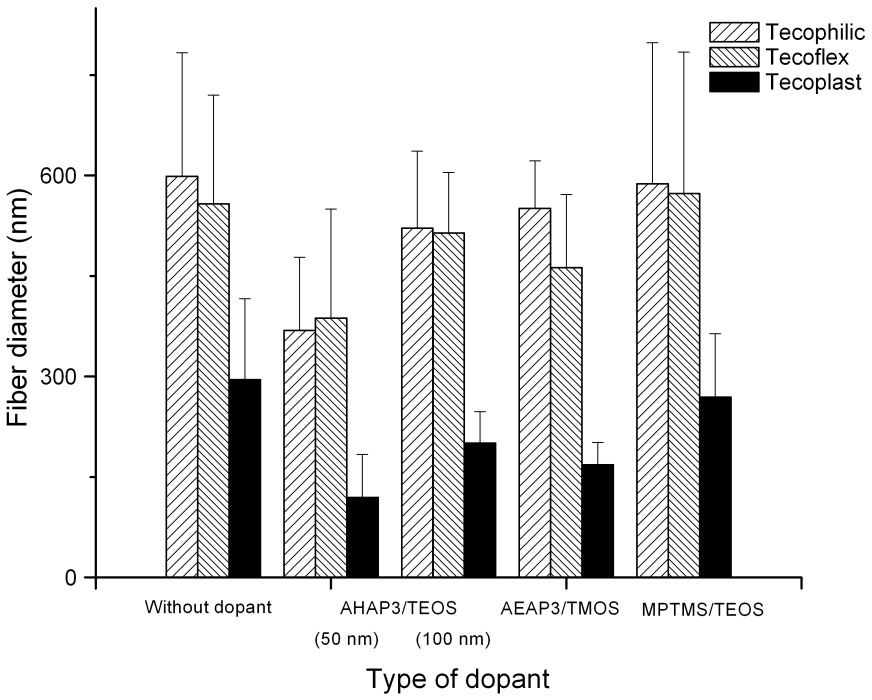

Figure 3.4. Diameters of 5 wt% particle-doped 12% (w/v) polyurethane electrospun fibers as a function of polyurethane type and NO-releasing silica particle dopant. Data is presented as mean ± standard deviation (n=3, >250 measurements).

Such upper limit at 16% (w/v) was not observed for Tecoflex and Tecoplast as the polymer solution viscosities remained moderate (1576.7 ± 24.9 and 342.0 ± 3.0 mm^2 s^{-1}, respectively).

Fiber diameter was also influenced by the conductivity of the polyurethane solution and the type of silica particle dopants employed. The zeta potential (i.e., surface charge) of *S*-nitrosothiol-modified silica particles is low/near zero, and thus the addition of such particles into the polymer solution did not significantly change the solution conductivity. Alternatively, *N*-diazeniumdiolated silica particles carry a large surface charges due to the negatively charged NO donor group. Thus, the addition of *N*-diazeniumdiolated AHAP3/TEOS and AEAP3/TMOS particles resulted in an increase in solution conductivity as shown in Table 3.2, which concomitantly also suppressed bead formation when using Tecoplast PU (Figure 3.5). Overall, the addition of *N*-diazeniumdiolated AEAP3/TMOS particles reduced fiber diameter relative to undoped and control (non-*N*-diazeniumdiolated AEAP3/TMOS particle-doped) fibers because greater solution conductivity elevated both the charge density on the Taylor cone and the elongation force along the elastic jet (Table 3.2).[53] Fiber diameter decreased further with a greater concentration of *N*-diazeniumdiolate particles (up to 10 wt%) for each of the PU systems, albeit slightly. Lastly, the fiber diameter was also influenced by the size of the particle dopants. Fibers prepared with 50 nm *N*-diazeniumdiolated AHAP3/TEOS particles were thinner compared to those doped with 100 nm particles (Figure 3.4). Such behavior is attributed to greater charge density per unit volume for polymer solution containing more *N*-diazeniumdiolated particles.

Table 3.2. Conductivity of initial polymer solution and resulting fiber diameter as a function of dopant type.[a]

Nitric oxide donor	*Type of dopant*	*Particle size (nm)*	*Conductivity ($\mu S\ cm^{-1}$)*	*Fiber diameter (nm)*
None			0.9 ± 0.3	558 ± 162
Control particle	AEAP3/TMOS	152 ± 2	9.4 ± 2.2	491 ± 155
N-diazeniumdiolate	AEAP3/TMOS	152 ± 2	44.3 ± 8.2	462 ±109
	AHAP3/TEOS	56 ± 7	49.0 ± 7.5	387 ± 163
	AHAP3/TEOS	93 ± 14	48.4 ± 3.6	514 ± 190
S-nitrosothiol	MPTMS/TEOS	416 ± 23	1.8 ± 0.9	573 ± 211

[a] 5 wt% particle-doped 12% (w/v) Tecoflex polyurethane electrospun fiber

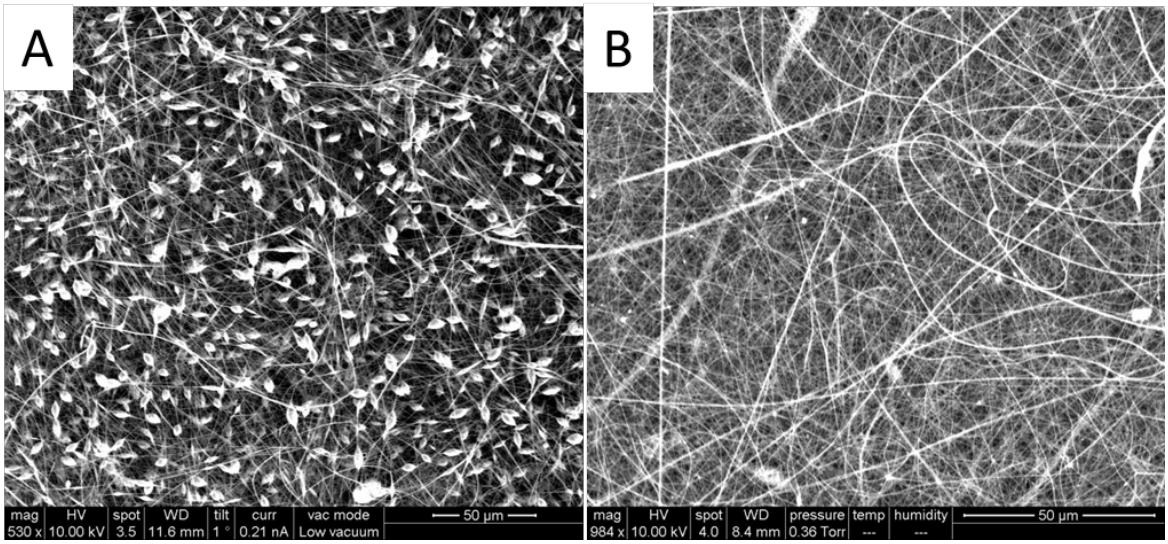

Figure 3.5. Environmental scanning electron microscopy images of 12% (w/v) Tecoplast electrospun fiber mat (A) without and (B) with 5 wt% of *N*-diazeniumdiolated AEAP3/TMOS particles.

To assess the suitability of the PU fiber mats as biomaterials, the mechanical properties of the particle-doped electrospun fibers were characterized in terms of modulus and elongation as a function of PU type and particle concentration. For tissue-based applications (e.g., subcutaneous implants), the mechanical properties of the scaffold should resemble native tissue to minimize shear stress and undesirable collagen deposition.[55] As shown in Figure 3.6A, each type of polyurethane exhibited different mechanical strengths. For example, Tecoplast (12% (w/v)) fiber mats doped with 5 wt% AEAP3/TMOS were characterized by a modulus of 34.5 ± 18.7 MPa and elongation of 92.3 ± 60.7% tensile strain at break, exhibiting flexible plastic-like mechanical behavior. The 5 wt% AEAP3/TMOS Tecophilic and Tecoflex (12% w/v) fiber mats had lower moduli of 1.7 ± 0.5 and 4.9 ± 0.4 MPa, respectively, and greater elongations of 223.0 ± 32.1 and 211.52 ± 29.83 % tensile strain at break, respectively. To determine the effect of mechanical properties on water absorption and potential particle leaching, the tensile strain and stress were determined after incubating the fiber mats in PBS at 37^{o}C for 24 h. The elongations of tensile strain at break were similar regardless of polyurethane. The tensile stress at break decreased ~50 and ~20% with wet fibers for Tecoflex and Tecoplast, respectively. However, the tensile stress at break increased ~100% for wet Tecophilic fiber mats, highlighting hydrophilic polyurethane absorbed more energy up to fracture. Based on these properties, the Tecoplast-based fiber mats would likely be more useful for prosthetic and orthopedic applications, while the Tecophilic and Tecoflex-based fiber mats might be more suitable for pacemaker, wound dressing, and catheter applications.[56,57] Fiber mat modulus and tensile strain were also influenced by the

concentration of particles incorporated into the fibers. As shown in Figure 3.6B, elongation of the electrospun fiber mat decreased proportionally with increasing particle concentration from 1 to 10 wt%. The modulus also increased with increasing particle dopant concentration due to decreased strength in the cross-sectional area of the load-bearing polymer matrix.[58] For example, doping AEAP3/TMOS particles into 12% (w/v) Tecophilic polyurethane fiber mats at a concentration of 1 wt% resulted in a modulus of 0.9 ± 0.1 MPa, which was identical to electrospun fiber mats without additives (0.9 ± 0.2 MPa). However, the moduli of the electrospun fiber mats increased with increasing particle concentration, resulting in moduli of 1.7 ± 0.5 and 2.1 ± 0.3 MPa for 5 and 10 wt% particle concentrations, respectively. These data suggest that Tecoflex and Tecophilic fibers doped with low particle concentrations possess mechanical properties best suited for lessening the FBR at implant-tissue interfaces.

Although silica-based materials are generally regarded as non-toxic, leaching of particles from the fibers was evaluated to assess the stability of the particle-polymer composites. Particle-doped fiber mats were immersed in physiological media (PBS, pH 7.4, 37 ^{o}C), and silicon content in the soak solutions was measured after 7 d to assess the extent of particle leaching. As expected, stability was greatly dependent on the physical and chemical characteristics of the particle dopants as well as the water-uptake of the polymers. Smaller particle dopants showed lower stability as indicated by greater leaching from the fiber mats (Table 3.3).

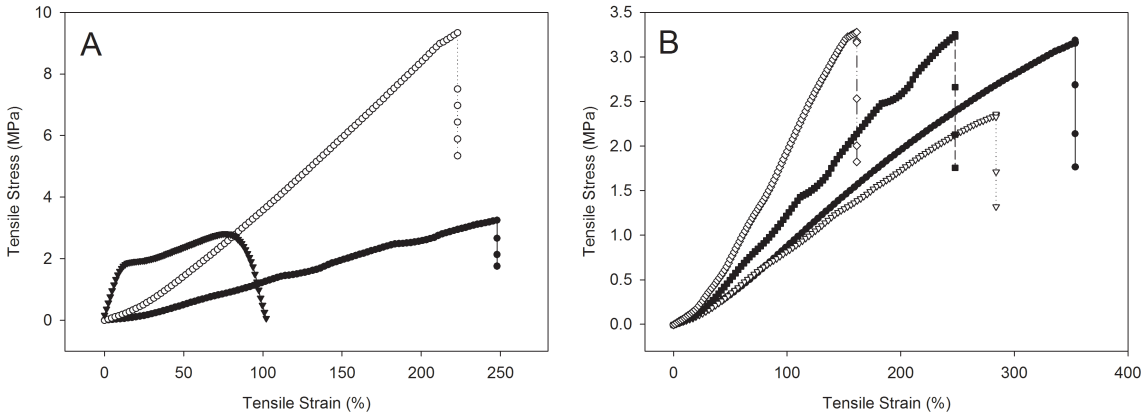

Figure 3.6. Tensile stress-strain curves of (A) 5 wt% AEAP3/TMOS particle-doped 12% (w/v) electrospun fiber mats as a function of polyurethane type: Tecophilic (●), Tecoflex (○), and Tecoplast (▼), and (B) 12% (w/v) Tecophilic electrospun fiber mats as a control (●) and a function of 1 (▽), 5 (■), and 10 wt% (◇) AEAP3/TMOS particle concentrations.

Nearly all of the 50 nm AHAP3/TEOS silica particles but only 70% of the 100 nm particles leached from the polyurethane fibers regardless of polymer composition, indicating smaller particles are more readily liberated upon swelling of the fibers. Fortunately, the particle concentrations doped within the fibers were low, such that even 100% leaching should not result local silica concentrations that are toxic.[46,59-61] Silica particle leaching further decreased for all polymer compositions as the size of the particle dopant increased, with the largest diameter particle (MPTMS/TEOS particles at 416 ± 23 nm) characterized by <2% leaching. Differences in polymer swelling due to water uptake also influenced the overall material stability. Tecoplast fibers, characterized by the lowest water uptake, exhibited the smallest level of particle leaching relative to the Tecophilic and Tecoflex polyurethanes for all dopant types. Overall, the lowest level of silica nanoparticle leaching (i.e., 0.7%) was achieved using the 5 wt% MPTMS/TEOS particles doped into 12% (w/v) Tecoplast electrospun fibers. Taken together, these data suggest that the greatest stability is achieved with lower water-uptake polymers and larger diameter particles.

3.3.2 Nitric oxide release from silica nanoparticle-doped electrospun fiber mat

While our previous report on electrospun fibers demonstrated controlled NO release using a low molecular weight NO donor (i.e., PROLI/NO), neither the NO-release kinetics nor duration of release proved tunable over a wide range.[45] Since optimal mitigation of the FBR via NO release from subcutaneous implants requires at least 48 h of NO release and a large overall NO payload (>1 μmol/cm^2), sustained and controlled NO release is an important aspect in developing NO-releasing biomaterials.[8,62]

Table 3.3. Silica particle leaching from NO-releasing silica particle-doped polyurethane electrospun fiber mats as a function of type of polyurethane and dopant after 7 d soaking in PBS at 37 ^{o}C.

NO-releasing silica nanoparticles (5 wt% of polyurethane mass)	*Polyurethane (12% (w/v) polyurethane)*	*Silica particle leaching (%)*
AHAP3/TEOS (~ 50 nm)	Tecophilic	105.8 ± 12.9
	Tecoflex	105.2 ± 10.3
	Tecoplast	97.2 ±9.7
AHAP3/TEOS (~ 100 nm)	Tecophilic	79.7 ± 5.5
	Tecoflex	84.6 ± 1.1
	Tecoplast	58.9 ± 0.3
AEAP3/TMOS (~ 200 nm)	Tecophilic	66.8 ± 14.3
	Tecoflex	39.3 ± 3.2
	Tecoplast	35.9 ± 9.2
MPTMS/TEOS (~ 400 nm)	Tecophilic	2.1 ± 0.1
	Tecoflex	0.8 ± 0.1
	Tecoplast	0.7 ± 0.1

Four distinct NO-releasing silica particle systems were used to fabricate NO-releasing fibers with diverse NO-release totals (0.4–3.2 μmol mg^{-1}) and durations (up to >48 h). Since the NO-release mechanism of *N*-diazeniumdiolate NO donors is proton-initiated, the NO release is generally controlled by pH and the hydrophobicity of surrounding matrix.[22] In contrast, the NO release for *S*-nitrosothiol systems is not dependent on pH or water uptake, but rather a function of heat, light, and/or the presence of copper ions.[11] In the case of the *N*-diazeniumdiolated scaffolds, both size of the AHAP3/TEOS particles (50 and 100 nm) had similar NO-release properties and exhibited larger payloads over a slightly longer release durations than the AEAP3/TMOS particles. In contrast, the *S*-nitrosothiol-modified MPTMS/TEOS particles delivered the greatest NO payload (3.2 μmol mg^{-1}) and had the longest release durations (>48 h) among all particle systems.

Analogous to the particle stability studies above, the NO release from the electrospun fiber mats was determined in PBS (pH 7.4) at 37 ^{o}C to mimic physiological conditions. Compared to previously reported PROLI/NO-doped electrospun fibers (NO-release duration of 8 min to 1.3 h), the silica particle-doped electrospun fibers exhibited substantially prolonged NO release with durations ranging from 7 h to 14 d (Table 3.4).

Of note, the electrospinning process had no affect on the particles' NO payload. For example, the total NO released from 5 wt% AHAP/TEOS particle-doped 12% (w/v) Tecoflex fiber mats was 98.3% of the theoretically calculated total NO (determined based on particle concentration in starting polymer cocktail).

Table 3.4. Nitric oxide release characteristics of 5 wt% NO-releasing silica particle-doped 12% (w/v) electrospun fiber mats.

NO donor type	*NO-releasing silica particle*	*Type of polyurethane*[b]	*$[NO]_{max}$*[c] *(pmol mg^{-1} s^{-1})*	*t_{max}*[d] *(min)*	*Total NO released*[e] *(nmol mg^{-1})*	*t_d*[f] *(h)*
N-diazeniumdiolate	AHAP3/TEOS[a] (50 nm)	Tecophilic	28.0 ± 9.2	8.4 ± 5.5	62.5 ± 36.1	7.2 ± 3.6
		Tecoflex	13.1 ± 10.1	24.0 ± 16.2	69.4 ± 18.3	13.3 ± 4.1
		Tecoplast	3.2 ± 2.6	28.5 ± 1.1	60.9 ± 15.2	29.9 ± 12.8
	AHAP3/TEOS[a] (100 nm)	Tecophilic	17.6 ± 3.8	1.2 ± 0.1	57.0 ± 6.4	14.5 ± 0.2
		Tecoflex	22.3 ± 2.9	2.6± 1.9	37.3 ± 10.9	14.9 ± 0.8
		Tecoplast	19.7 ± 1.7	1.9 ± 1.5	42.2 ± 19.8	14.1 ± 0.2
	AEAP3/TMOS	Tecophilic	2.2 ± 1.0	1.7 ± 0.5	15.0 ± 5.0	15.3 ± 1.0
		Tecoflex	1.5 ± 0.9	0.8 ± 0.5	10.8 ± 1.0	19.6 ± 2.7
		Tecoplast	1.3 ± 0.3	3.1 ± 2.7	7.5 ± 2.0	14.3 ± 1.6
S-nitrosothiol	MPTMS/TEOS	Tecophilic	15.2 ± 6.1	6.9 ± 0.4	124.7 ± 6.8	366.8 ± 78.2
		Tecoflex	10.1 ± 0.8	0.9 ± 0.4	123.2 ± 16.1	296.6 ± 6.5
		Tecoplast	11.7 ± 9.8	1.8 ± 1.0	86.8 ± 9.0	299.9 ± 2.8

[a] AHAP3/TEOS particles have two distinct sizes but similar NO release properties
[b] Hydrophobicity increases from top to bottom of one particle system
[c] Maximum instantaneous concentration of NO released as measured with NOA
[d] Time required to reach $[NO]_{max}$
[e] Total number of moles of NO released per mg of particle-doped electrospun fiber mat as measured by the Griess assay
[f] Duration of NO release (time to release 99% of total NO).

Although the NO release from fibers doped with *N*-diazeniumdiolated silica particles was limited to <1 d, the NO fluxes from these materials may still prove useful as thromboresistant coatings for blood-contacting biomedical devices (e.g., stents and catheters) since the *N*-diazeniumdiolated NO donor systems release NO at fluxes required to promote hemocompatibilty (i.e., 0.4−5.0 pmol cm^{-2} s^{-1}).[63-66] As expected, longer NO-release durations were achieved with the *S*-nitrosothiol-functionalized particles regardless of the type of polymer system employed (~2 weeks). Of note, the MPTMS/TEOS particle-doped electrospun fiber mats exhibited NO-release durations at or above that reported sufficient to mitigate the foreign body response for subcutaneous implants (i.e., NO release >72 h).[8,62]

The effect of polymer composition on NO-release kinetics was most apparent with the 50 nm *N*-diazeniumdiolated AHAP3/TEOS-doped electrospun fibers (Table 3.4 and Figure 3.7). For example, 5 wt% *N*-diazeniumdiolate particle-doped hydrophobic Tecoplast fibers were characterized by the lowest maximum NO flux (3.2 ± 2.6 pmol mg^{-1} s^{-1}) and longest NO-release duration (29.9 ± 12.8 h) due to lower water uptake. The more hydrophilic Tecophilic-based counterparts had an increased flux and shorter release duration (28.0 ± 9.2 pmol mg^{-1} s^{-1} and 7.2 ± 3.6 h, respectively). The total NO release was constant regardless of polyurethane type as expected.

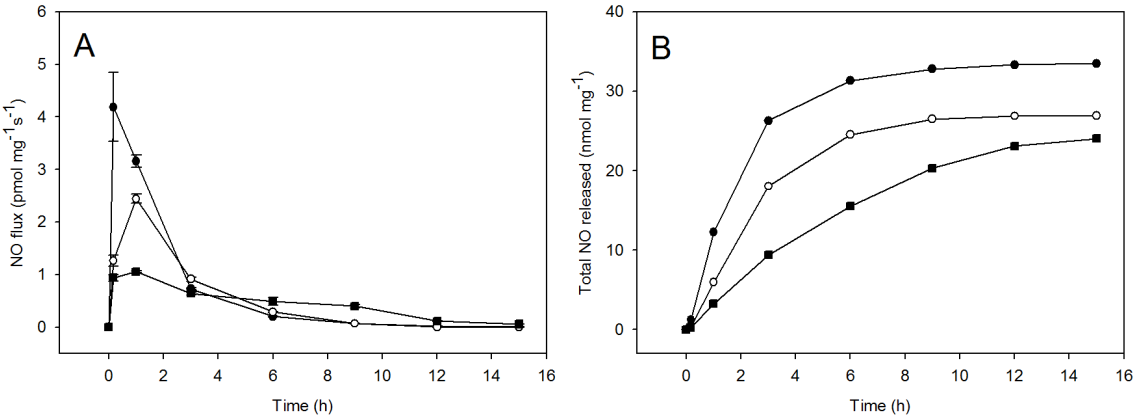

Figure 3.7. (A) Nitric oxide flux and (B) NO totals from 5 wt% AHAP3/TEOS (~50 nm) particle-doped electrospun polyurethane fiber mats with 12% (w/v) of (●) Tecophilic, (○) Tecoflex, and (■) Tecoplast polyurethane.

The NO-release kinetics proved less tunable for the larger particles systems (e.g., AHAP3/TEOS and AEAP/TMOS at 100 nm and 150 nm, respectively) due to the limited fiber diameter and decreased thickness of the water restricting layer around the particles, ultimately eliminating any water uptake-mediated effect on *N*-diazeniumdiolate NO donor decomposition (Figure 3.8).[45] In this respect, increasing the distance water must diffuse through the polymer to reach the particle scaffolds may prove to be an importance method for fine-tuning NO-release kinetics. A future objective is to adopt a co-axial electrospinning strategy[67] where fibers are composed of an inner layer containing the particle dopants and an outer shell comprised of undoped polymer of varied hydrophobicity and/or thickness.

The total NO payload and initial bolus of NO release from the fiber mats were further altered by changing the silica particle concentrations (Figure 3.9). As expected, increasing the concentration of silica particle dopant elevated both the maximum NO flux and total NO released from the electrospun fiber mats (Figure 3.10). For example, electrospun fibers doped with 1, 5, and 10 wt% AEAP3/TMOS particle concentrations resulted in maximum NO fluxes of 0.6 ± 0.7, 2.2 ± 1.0, and 5.4 ± 3.5 pmol mg^{-1} s^{-1}, respectively. Additionally, the total NO released from those electrospun fibers was 3.6 ± 3.3, 15.0 ± 5.0, and 22.3 ± 0.6 nmol mg^{-1} for 1, 5, and 10 wt% silica dopant concentrations, respectively. Similar trends were observed for all other particle compositions. Of importance, the greatest total NO release achieved from the particle-doped electrospun fiber mats was lower than previously reported proven to be cytotoxic or cause apoptosis.[68,69]

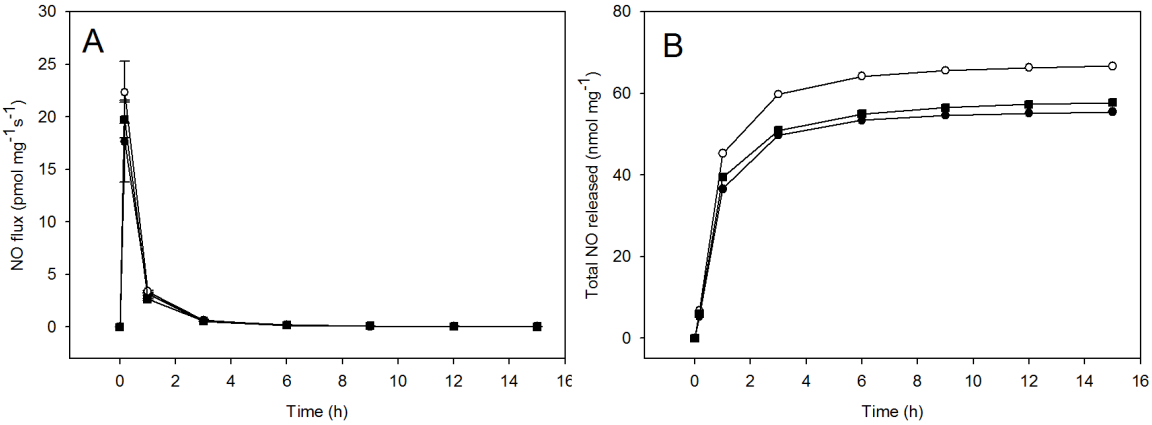

Figure 3.8. (A) Nitric oxide flux and (B) NO totals from 5 wt% AHAP3/TEOS (~100 nm) particle-doped electrospun polyurethane fiber mats with 12% (w/v) (●) Tecophilic, (○) Tecoflex, and (■) Tecoplast polyurethane.

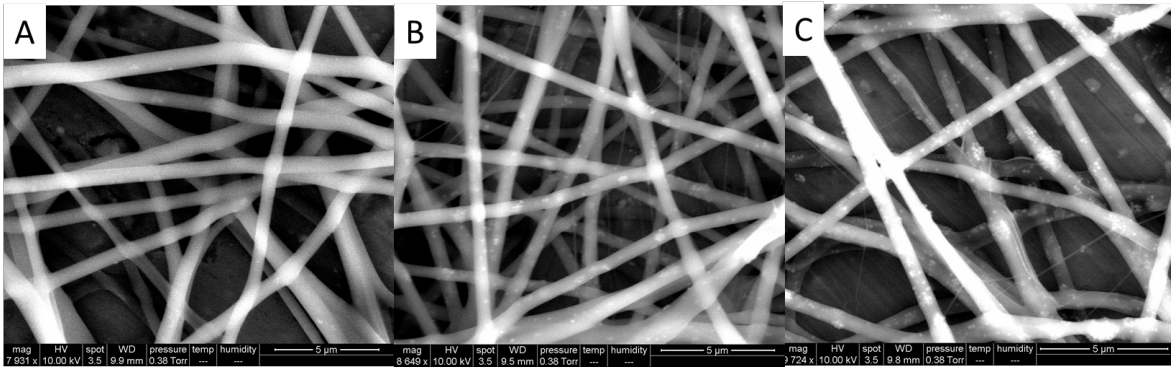

Figure 3.9. Environmental scanning electron microscopy images of AEAP3/TMOS particle-doped 12% (w/v) Tecophilic electrospun fiber mats as a function of dopant concentration, (A) 1, (B) 5, and (C) 10 wt%. Scale bar indicates 5 µm.

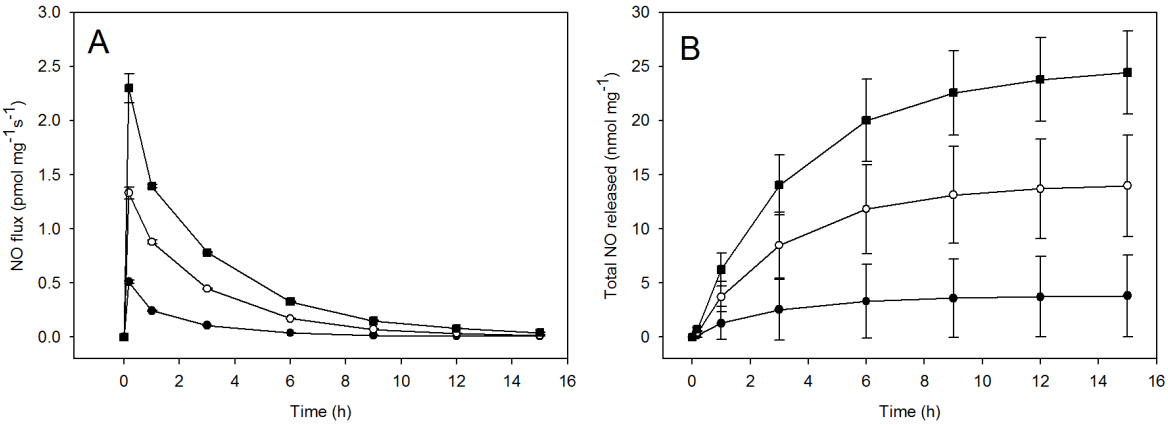

Figure 3.10. (A) Nitric oxide flux and (B) NO release totals from NO donor-modified AEAP3/TMOS particle-doped 12% (w/v) Tecophilic electrospun polyurethane fiber mats as a function of dopant concentration: 1 (●), 5 (○), and 10 (■) wt%.

Not surprisingly, neither the NO-release half-life or duration of *N*-diazeniumdiolated particle-doped electrospun fiber mats was greatly affected by the amount of particle dopant (1 to 10 wt%).

3.4 Conclusion

The electrospun polyurethane fibers doped with NO donor-modified silica particles presented here have allowed us to overcome limitations of previously reported NO-release materials (e.g., short NO release duration and low porosity). The use of electrospun fibers provides a material with high porosity while maintaining mechanical strength compared to bulk polymers doped with NO-releasing silica particles. Moreover, the incorporation of NO-releasing silica particles into electrospun fibers enables greater NO release durations compared to electrospun fibers doped with a low molecular weight NO donor (1 h vs. 2 weeks). Changing the type of NO-releasing particle system, polyurethane water uptake, and dopant concentration resulted in a wide range of NO release characteristics (i.e., total NO payloads of 7.5–124.7 nmol mg^{-1} and durations from 7 h to 2 weeks). Of the systems studied herein, *S*-nitrosothiol-modified silica particles promoted the longest NO release and most stable particle-fiber composites. Other macromolecular scaffolds, such as NO-releasing dendrimers,[13-16] may also prove advantageous as fiber dopants as a result of larger NO payloads that can be incorporated with improved polymer partitioning attributes. As a result of both flexible and open architectures, porous NO-releasing fibers represent ideal candidates for biomedical implant coatings.

3.5 References

(1) Williams, D. L. H. "A chemist's view of the nitric oxide story" *Organic and Biomolecular Chemistry* **2003**, *1*, 441-449.

(2) Ignarro, L. J. *Nitric oxide : biology and pathobiology*; Academic Press: San Diego, Calif.; London, 2000.

(3) Carpenter, A. W.; Schoenfisch, M. H. "Nitric oxide release: Part II. Therapeutic applications" *Chemical Society Reviews* **2012**, *41*, 3742-3752.

(4) Riccio, D. A.; Schoenfisch, M. H. "Nitric oxide release: Part I. Macromolecular scaffolds" *Chemical Society Reviews* **2012**, *41*, 3731-3741.

(5) Jen, M. C.; Serrano, M. C.; van Lith, R.; Ameer, G. A. "Polymer-based nitric oxide therapies: Recent insights for biomedical applications" *Advanced Functional Materials* **2012**, *22*, 239-260.

(6) Marxer, S. M.; Rothrock, A. R.; Nablo, B. J.; Robbins, M. E.; Schoenfisch, M. H. "Preparation of nitric oxide (NO)-releasing sol-gels for biomaterial applications" *Chemistry of Materials* **2003**, *15*, 4193-4199.

(7) Nablo, B. J.; Prichard, H. L.; Butler, R. D.; Klitzman, B.; Schoenfisch, M. H. "Inhibition of implant-associated infections via nitric oxide" *Biomaterials* **2005**, *26*, 6984-6990.

(8) Hetrick, E. M.; Prichard, H. L.; Klitzman, B.; Schoenfisch, M. H. "Reduced foreign body response at nitric oxide-releasing subcutaneous implants" *Biomaterials* **2007**, *28*, 4571-4580.

(9) Riccio, D. A.; Dobmeier, K. P.; Hetrick, E. M.; Privett, B. J.; Paul, H. S.; Schoenfisch, M. H. "Nitric oxide-releasing *S*-nitrosothiol-modified xerogels" *Biomaterials* **2009**, *30*, 4494-4502.

(10) Shin, J. H.; Metzger, S. K.; Schoenfisch, M. H. "Synthesis of nitric oxide-releasing silica nanoparticles" *Journal of the American Chemical Society* **2007**, *129*, 4612-4619.

(11) Riccio, D. A.; Nugent, J. L.; Schoenfisch, M. H. "Stöber synthesis of nitric oxide-releasing *S*-nitrosothiol-modified silica particles" *Chemistry of Materials* **2011**, *23*, 1727-1735.

(12) Shin, J. H.; Schoenfisch, M. H. "Inorganic/organic hybrid silica nanoparticles as a nitric oxide delivery scaffold" *Chemistry of Materials* **2008**, *20*, 239-249.

(13) Lu, Y.; Sun, B.; Li, C.; Schoenfisch, M. H. "Structurally diverse nitric oxide-releasing poly(propylene imine) dendrimers" *Chemistry of Materials* **2011**, *23*, 4227-4233.

(14) Stasko, N. A.; Fischer, T. H.; Schoenfisch, M. H. "*S*-nitrosothiol-modified dendrimers as nitric oxide delivery vehicles" *Biomacromolecules* **2008**, *9*, 834-841.

(15) Stasko, N. A.; Schoenfisch, M. H. "Dendrimers as a scaffold for nitric oxide release" *Journal of the American Chemical Society* **2006**, *128*, 8265-8271.

(16) Sun, B.; Slomberg, D. L.; Chudasama, S. L.; Lu, Y.; Schoenfisch, M. H. "Nitric oxide-releasing dendrimers as antibacterial agents" *Biomacromolecules* **2012**, *13*, 3343-3354.

(17) Coneski, P. N.; Rao, K. S.; Schoenfisch, M. H. "Degradable nitric oxide-releasing biomaterials via post-polymerization functionalization of cross-linked polyesters" *Biomacromolecules* **2010**, *11*, 3208-3215.

(18) Damodaran, V. B.; Joslin, J. M.; Wold, K. A.; Lantvit, S. M.; Reynolds, M. M. "S-Nitrosated biodegradable polymers for biomedical applications: synthesis, characterization and impact of thiol structure on the physicochemical properties" *Journal of Materials Chemistry* **2012**, *22*, 5990-6001.

(19) Damodaran, V. B.; Reynolds, M. M. "Biodegradable S-nitrosothiol tethered multiblock polymer for nitric oxide delivery" *Journal of Materials Chemistry* **2011**, *21*, 5870-5872.

(20) Frost, M. C.; Reynolds, M. M.; Meyerhoff, M. E. "Polymers incorporating nitric oxide releasing/generating substances for improved biocompatibility of blood-contacting medical devices" *Biomaterials* **2005**, *26*, 1685-1693.

(21) Frost, M. C.; Meyerhoff, M. E. "Synthesis, characterization, and controlled nitric oxide release from *S*-nitrosothiol-derivertized fumed silica polymer filler particles" *Journal of Biomedical Materials Research Part A* **2005**, *72A*, 409-419.

(22) Koh, A.; Riccio, D. A.; Sun, B.; Carpenter, A. W.; Nichols, S. P.; Schoenfisch, M. H. "Fabrication of nitric oxide-releasing polyurethane glucose sensor membranes" *Biosensors and Bioelectronics* **2011**, *28*, 17-24.

(23) Heck, D. E.; Laskin, D. L.; Gardner, C. R.; Laskin, J. D. "Epidermal growth factor suppresses nitric oxide and hydrogen peroxide production by keratinocytes. Potential role for nitric oxide in the regulation of wound healing" *Journal of Biological Chemistry* **1992**, *267*, 21277-21280.

(24) Schäffer, M. R.; Tantry, U.; Gross, S. S.; Wasserkrug, H. L.; Barbul, A. "Nitric oxide regulates wound healing" *Journal of Surgical Research* **1996**, *63*, 237-240.

(25) Bogdan, C. "Nitric oxide and the immune response" *Nature Immunology* **2001**, *2*, 907-916.

(26) Mocellin, S.; Bronte, V.; Nitti, D. "Nitric oxide, a double edged sword in cancer biology: Searching for therapeutic opportunities" *Medicinal Research Reviews* **2007**, *27*, 317-352.

(27) Jones, M.; Ganopolsky, J.; Labbé, A.; Wahl, C.; Prakash, S. "Antimicrobial properties of nitric oxide and its application in antimicrobial formulations and medical devices" *Applied Microbiology and Biotechnology* **2010**, *88*, 401-407.

(28) Shin, J. H.; Schoenfisch, M. H. "Improving the biocompatibility of in vivo sensors via nitric oxide release" *Analyst* **2006**, *131*, 609-615.

(29) Yan, Q.; Major, T. C.; Bartlett, R. H.; Meyerhoff, M. E. "Intravascular glucose/lactate sensors prepared with nitric oxide releasing poly(lactide-co-glycolide)-based coatings for enhanced biocompatibility" *Biosensors and Bioelectronics* **2011**, *26*, 4276-4282.

(30) Frost, M. C.; Rudich, S. M.; Zhang, H. P.; Maraschio, M. A.; Meyerhoff, M. E. "In vivo biocompatibility and analytical performance of intravascular amperometric oxygen sensors prepared with improved nitric oxide-releasing silicone rubber coating" *Analytical Chemistry* **2002**, *74*, 5942-5947.

(31) Teo, W. E.; Ramakrishna, S. "A review on electrospinning design and nanofibre assemblies" *Nanotechnology* **2006**, *17*, R89-R106.

(32) Huang, Z.-M.; Zhang, Y.-Z.; Koraki, M.; Ramakrishna, S. "A review on polymer nanofibers by electrospinning and their applications in nanocomposites" *Composites Science and Technology* **2003**, *63*, 2223-2253.

(33) Agarwal, S.; Wendorff, J. H.; Greiner, A. "Use of electrospinning technique for biomedical applications" *Polymer* **2008**, *49*, 5603-5621.

(34) Lu, X.; Wang, C.; Wei, Y. "One-demensional composite nanomaterials: Synthesis by electrospinning and their applications" *Small* **2009**, *5*, 2349-2370.

(35) Li, W.-J.; Laurencin, C. T.; Caterson, E. J.; Tuan, R. S.; Ko, F. K. "Electrospun nanofibrous structure: A novel scaffold for tissue engineering" *Journal of Biomedical Materials Research* **2002**, *60*, 613-621.

(36) Leung, V.; Ko, F. "Biomedical applications of nanofibers" *Polymers for Advanced Technologies* **2011**, *22*, 350-365.

(37) Wang, N.; Burugapalli, K.; Song, W.; Halls, J.; Moussy, F.; Ray, A.; Zheng, Y. "Electrospun fibro-porous polyurethane coatings for implantable glucose biosensors" *Biomaterials* **2013**, *34*, 888-901.

(38) Wilson, G. S.; Gifford, R. "Biosensors for real-time *in vivo* measurements" *Biosensors and Bioelectronics* **2005**, *20*, 2388-2403.

(39) Saino, E.; Focarete, M. L.; Gualandi, C.; Emanuele, E.; Cornaglia, A. I.; Imbriani, M.; Visai, L. "Effect of electrospun fiber diameter and alignment on macrophage activation and secretion of proinflammatory cytokines and chemokines" *Biomacromolecules* **2011**, *12*, 1900-1911.

(40) Cao, H.; McHugh, K.; Chew, S. Y.; Anderson, J. M. "The topographical effect of electrospun nanofibrous scaffolds on the in vivo and in vitro foreign body reaction" *Journal of Biomedical Materials Research Part A* **2010**, *93A*, 1151-1159.

(41) Son, W. K.; Youk, J. H.; Lee, T. S.; Park, W. H. "Preparation of antimicrobial ultrafine cellulose acetate fibers with silver nanoparticles" *Macromolecular Rapid Communications* **2004**, *25*, 1632-1637.

(42) Hong, K. H. "Preparation and properties of electrospun poly(vinyl alcohol)/silver fiber web as wound dressings" *Polymer Engineering and Science* **2007**, *47*, 43-49.

(43) Xu, X.; Yang, Q.; Wang, Y.; Yu, H.; Chen, X.; Jing, X. "Biodegradable electrospun poly(l-lactide) fibers containing antibacterial silver nanoparticles" *European Polymer Journal* **2006**, *42*, 2081-2087.

(44) Vacanti, N. M.; Cheng, H.; Hill, P. S.; Guerreiro, J. D. T.; Dang, T. T.; Ma, M.; Watson, S.; Hwang, N. S.; Langer, R.; Anderson, D. G. "Localized delivery of dexamethasone from electrospun fibers reduces the foreign body response" *Biomacromolecules* **2012**, *13*, 3031-3038.

(45) Coneski, P. N.; Nash, J. A.; Schoenfisch, M. H. "Nitric oxide-releasing electrospun polymer microfibers" *ACS Applied Materials & Interfaces* **2011**, *3*, 426-432.

(46) Carpenter, A. W.; Slomberg, D. L.; Rao, K. S.; Schoenfisch, M. H. "Influence of scaffold size on bactericidal activity of nitric oxide-releasing silica nanoparticles" *Acs Nano* **2011**, *5*, 7235-7244.

(47) Koschwanez, H. E.; Yap, F. Y.; Klitzman, B.; Reichert, W. M. "In vitro and in vivo characterization of porous poly-L-lactic acid coatings for subcutaneously implanted glucose sensors" *Journal of Biomedical Materials Research Part A* **2008**, *87A*, 792-807.

(48) Zhu, X.; Cui, W.; Li, X.; Jin, Y. "Electrospun Fibrous Mats with High Porosity as Potential Scaffolds for Skin Tissue Engineering" *Biomacromolecules* **2008**, *9*, 1795-1801.

(49) Telemeco, T. A.; Ayres, C.; Bowlin, G. L.; Wnek, G. E.; Boland, E. D.; Cohen, N.; Baumgarten, C. M.; Mathews, J.; Simpson, D. G. "Regulation of cellular infiltration into tissue engineering scaffolds composed of submicron diameter fibrils produced by electrospinning" *Acta Biomaterialia* **2005**, *1*, 377-385.

(50) Huang, Z.-M.; Zhang, Y. Z.; Ramakrishna, S.; Lim, C. T. "Electrospinning and mechanical characterization of gelatin nanofibers" *Polymer* **2004**, *45*, 5361-5368.

(51) Coneski, P. N.; Schoenfisch, M. H. "Nitric oxide release: Part III. Measurement and reporting" *Chemical Society Reviews* **2012**, *41*, 3753-3758.

(52) Nichols, S. P.; Koh, A.; Storm, W. L.; Shin, J. H.; Schoenfisch, M. H. "Biocompatible materials for continuous glucose monitoring devices" *Chemical Reviews* **2013**, *113*, 2528-2549.

(53) Tan, S. H.; Inai, R.; Kotaki, M.; Ramakrishna, S. "Systematic parameter study for ultra-fine fiber fabrication via electrospinning process" *Polymer* **2005**, *46*, 6128-6134.

(54) Shawon, J.; Sung, C. "Electrospinning of polycarbonate nanofibers with solvent mixtures THF and DMF" *Journal of Materials Science* **2004**, *39*, 4605-4613.

(55) Helton, K. L.; Ratner, B. D.; Wisniewski, N. A. "Biomechanics of the sensor–tissue interface—Effects of motion, pressure, and design on sensor performance and the foreign body response—Part I: Theoretical framework" *Journal of Diabetes Science and Technology* **2011**, *5*, 632-646.

(56) Wise, D. L. *Human biomaterials applications*; Humana Press, 1996.

(57) Black, J.; Hastings, G. W. *Handbook of biomaterial properties*; Chapman & Hall, 1998.

(58) Landon, G.; Lewis, G.; Boden, G. F. "The influence of particle size on the tensile strength of particulate-filled polymers" *Journal of Materials Science* **1977**, *12*, 1605-1613.

(59) Kunzmann, A.; Andersson, B.; Thurnherr, T.; Krug, H.; Scheynius, A.; Fadeel, B. "Toxicology of engineered nanomaterials: Focus on biocompatibility, biodistribution and biodegradation" *Biochimica et Biophysica Acta (BBA) - General Subjects* **2011**, *1810*, 361-373.

(60) Hudson, S. P.; Padera, R. F.; Langer, R.; Kohane, D. S. "The biocompatibility of mesoporous silicates" *Biomaterials* **2008**, *29*, 4045-4055.

(61) Barbé, C.; Bartlett, J.; Kong, L.; Finnie, K.; Lin, H. Q.; Larkin, M.; Calleja, S.; Bush, A.; Calleja, G. "Silica particles: A novel drug-delivery system" *Advanced Materials* **2004**, *16*, 1959-1966.

(62) Nichols, S. P.; Koh, A.; Brown, N. L.; Rose, M. B.; Sun, B.; Slomberg, D. L.; Riccio, D. A.; Klitzman, B.; Schoenfisch, M. H. "The effect of nitric oxide surface flux on the foreign body response to subcutaneous implants" *Biomaterials* **2012**, *33*, 6305-6312.

(63) Reynolds, M. M.; Frost, M. C.; Meyerhoff, M. E. "Nitric oxide-releasing hydrophobic polymers: Preparation, characterization, and potential biomedical applications" *Free Radical Biology and Medicine* **2004**, *37*, 926-936.

(64) Robbins, M. E.; Hopper, E. D.; Schoenfisch, M. H. "Synthesis and characterization of nitric oxide-releasing sol-gel microarrays" *Langmuir* **2004**, *20*, 10296-10302.

(65) Skrzypchak, A. M.; Lafayette, N. G.; Bartlett, R. H.; Zhengrong Zhou; Frost, M. C.; Meyerhoff, M. E.; Reynolds, M. M.; Annich, G. M. "Effect of varying nitric oxide release to prevent platelet consumption and preserve platelet function in an in vivo model of extracorporeal circulation" *Perfusion* **2007**, *22*, 193-200.

(66) Zhang, H.; Annich, G. M.; Miskulin, J.; Osterholzer, K.; Merz, S. I.; Bartlett, R. H.; Meyerhoff, M. E. "Nitric oxide releasing silicone rubbers with improved blood compatibility: preparation, characterization, and in vivo evaluation" *Biomaterials* **2002**, *23*, 1485-1494.

(67) Moghe, A. K.; Gupta, B. S. "Co-axial electrospinning for nanofiber structures: Preparation and applications" *Polymer Reviews* **2008**, *48*, 353-377.

(68) Brüne, B. "Nitric oxide: NO apoptosis or turning it ON?" *Cell Death and Differentiation* **2003**, *10*, 864-869.

(69) Bonfoco, E.; Krainc, D.; Ankarcrona, M.; Nicotera, P.; Lipton, S. A. "Apoptosis and necrosis: two distinct events induced, respectively, by mild and intense insults with N-methyl-D-aspartate or nitric oxide/superoxide in cortical cell cultures" *Proceedings of the National Academy of Sciences* **1995**, *92*, 7162-7166.

CHAPTER 4: FABRICATION OF NITRIC OXIDE-RELEASING POROUS POLYURETHANE MEMBRANES COATED NEEDLE-TYPE IMPLANTABLE GLUCOSE BIOSENSORS

Original article was co-authored with Yuan Lu and Mark H. Schoenfisch. Text, figures, and tables are adopted and reprinted with permission of ACS publications: Ahyeon Koh, Yuan Lu and Mark H. Schoenfisch, "Fabrication of nitric oxide-releasing porous polyurethane membranes-coated needle-type implantable glucose biosensors", *Analytical Chemistry*, Volume 85, Issue 21, September 2013, Pages 10488-10494, DOI:10.1021/ac402312b.

4.1 Introduction

Percutaneously implanted electrochemical biosensors for continuous glucose monitoring (CGM) hold great potential for reducing complications of diabetes due to their ability to warn of hyperglycemia or hypoglycemia events.[1,2] Limitations such as short sensor life (≤1 week), the need for frequent calibration (2–4 times/day), and unreliable accuracy in the data provided have prevented wide spread use of such devices to date.[1,3,4] Most shortcomings of CGM systems are due to the foreign body response (FBR).[5] Inflammatory cell response and collagen capsule formation, and the risk of infection due to percutaneous implantation result in poor analytical performance in vivo.[2] Recent work has focused on the development of outer membranes to mitigate the FBR and improve tissue integration and in vivo sensor performance.[2,6]

Nitric oxide (NO)—an endogenously produced diatomic free radical—plays a number of physiological roles (e.g., angiogenesis, wound healing, and vasodilation) depending on release location and concentration.[7,8] To utilize NO as a pharmaceutical

agent, we and others have developed macromolecular NO-release scaffolds using *N*-diazeniumdiolate or *S*-nitrosothiol NO donors that enable controlled NO release.[8,9] As biomaterials, NO-releasing interfaces have been shown to decrease the adhesion of inflammatory cell, reduce collagen capsule thickness, and increase blood vessel formation near the biomaterial.[10,11] Additionally, the NO-releasing surfaces have proven to be highly effective at reducing bacteria adhesion, eradicating biofilms, and decreasing implant-associated infections.[12-15]

Release of NO from glucose sensor membranes has been studied as an active strategy to mitigate the FBR and thus improve sensor performance in vivo by addressing the greatest shortcoming of such devices.[16] Nitric oxide release has been imparted to glucose sensors membranes by patterning NO-releasing xerogel array on top of a membrane[17] or physically entrapping NO donors (e.g., NO-releasing silica particles[18,19] or low molecular weight molecules[20]) within polyurethane (PU) sensor membranes. Such NO-releasing membranes exhibited adequate analyte diffusion without compromising sensor performance.[18,19] Gifford et al. reported that NO fluxes >0.83 pmol cm^{-2} s^{-1} for 18 h from a needle-type glucose biosensors were sufficient to reduce inflammation and enhance the sensor accuracy at 24 h post implantation compared to control sensors in a rodent model.[20]

Surface modifications based on porous architectures have also been developed and represent a passive strategy for improving tissue integration and decreasing collagen capsule formation.[21-24] Electrospun fibers appear promising as glucose sensor membranes because of their high surface to volume ratio and superior mechanical properties.[25]

Additionally, electrospun fibers are able to be directly coated onto electrodes without impeding glucose oxidase activity since the polymer fibers solidify as the solvent evaporates during the electrospinning process.[26] Random oriented fibers with submicron diameter (~0.6 μm) have been reported to be effective at reducing secretion of proinflammatory molecules, decreasing the adhesion of foreign body giant cells, and promoting cell migration and proliferation—all resulting in reduced capsule formation.[25,27-29] Wang et al. recently reported coating PU electrospun fibers on implantable glucose sensors using a dynamic collector, highlighting the ability to modify microsensors with porous membranes.[26] While electrospun fibers allow for the encapsulation and release of therapeutics in a controlled manner,[27,30,31] the use of drug-releasing electrospun fibers for implantable glucose sensors has not yet been reported.

In this chapter, the design of NO-releasing dendrimer-doped electrospun PU fibers as porous outermost glucose sensor membranes is described. The characterizations of needle-type glucose biosensors fabricated using such interfaces were demonstrated the ability to combine both active (i.e., NO-release) and passive (i.e., porous) strategies within a single outer sensor membrane coating.

4.2 Experimental

4.2.1 Materials.

Glucose oxidase (type VII from *Aspergillus niger*), D-glucose anhydrous, acetaminophen (AP), L-ascorbic acid (AA), and uric acid (UA) were purchased from Sigma (St. Louis, MO). All salts and organic solvents were laboratory grade and purchased from Fisher Scientific (St. Louis, MO). Methyltrimethoxysilane (MTMOS)

and phenol were purchased from Fluka (Buchs, Switzerland). Tecophilic (HP-93A-100) and Tecoflex (SG-85A) polyurethanes were gifts from Thermedics (Woburn, MA). Hydrothane (AL 25-80A) polyurethane was a gift from AdvanSource Biomaterials Corporation (Willmington, MA). Tecoplast (TP-470) polyurethane was provided by Lubrizol (Cleveland, OH). Stainless steel wire (316L, 381μm diameter) was purchased from McMaster-Carr (Atlanta, GA). Polyterafluoroethylene (PTFE) coated-Pt/Ir (90% Pt) wire (177.8 μm and 246.4 μm bare and coated diameter, respectively) and silver wire (Ag 99.99%, 127 μm diameter) were purchased from Sigmund Cohn Corp. (Mount Vernon, NY). Nitrogen, argon, and nitric oxide calibration gases were purchased from Airgas National Welders Supply (Durham, NC). Fetal bovine serum (FBS), Dulbecco's modified Eagle's medium (DMEM), phenazine methosulfate (PMS), 3-(4,5-dimethylthiazol-2-yl)-5-(3-carboxymethoxyphenyl)-2-(4-sulfophenyl)-2H-tetrazolium inner salt (MTS), trypsin, and penicillin streptomycin (PS) were purchased from the Aldrich Chemical Company (Milwaukee, WI). L929 mouse fibroblasts (ATCC #CCL-1) were purchased from the UNC Tissue Culture Facility (Chapel Hill, NC). Anticoagulated whole blood with 5 U/mL heparin was obtained from healthy pigs at the Francis Owen Blood Research Laboratory (Chapel Hill, NC). Serum was obtained from this sample by centrifuging the blood for 15 min under 2000 $\times g$ at 4 ^{o}C. Water was purified (18.2 MΩ·cm; total organic content <6 ppb) using a Millipore Milli-Q Gradient A-10 purification system (Bedford, MA).

4.2.2 Fabrication of needle-type glucose sensors.

Needle-type glucose sensors were fabricated by adapting a procedure described previously published literatures.[20,32-34] A silver/silver chloride (Ag/AgCl) wire electrode was fabricated by winding silver (Ag) wire on stainless steel wire (2.5 cm length). The wire was converted to AgCl via galvanometry by soaking in saturated ferric chloride ($FeCl_3$) solution for >2 h. After sonicating in water and ethanol for 15 min each, the Ag/AgCl wire was removed from the stainless steel and wrapped around a polytetrafluoroethylene (PTFE)-coated Pt/Ir wire (3.5 cm length). A section of the PTFE coating (~5 mm) was then stripped from the end of wire to expose the sensing cavity. The end of the sensor was sealed with epoxy, resulting in a ~2 mm sensing cavity (surface area ~0.017 cm^2). The sensing cavity consisted of four functional layers: (1) an inner-selective membrane, that excludes electroactive interferents such as ascorbic acid (AA), uric acid (UA), and acetaminophen (AP); (2) a glucose oxidase layer, where glucose is converted to gluconolactone and oxygen to hydrogen peroxide; (3) a diffusion limiting layer that controls the diffusion and partitioning of glucose and oxygen to overcome the oxygen deficit in vivo; and, (4) a porous NO-releasing electrospun fibrous membrane designed to mitigate the FBR. The inner-selective polyphenol layer was applied under control of self-limiting electropolymerization (film thickness of ~10–100 nm) to prevent interfering species from reaching or fouling the electrode surface, affording a great improvement in biosensor selectivity over acetaminophen in particular (Figure 4.1). The electrochemical polymerization of the permselective polyphenol films was carried out potentiostatically at +0.9 V vs. Ag/AgCl for 15 min in 40 mM phenol solution in

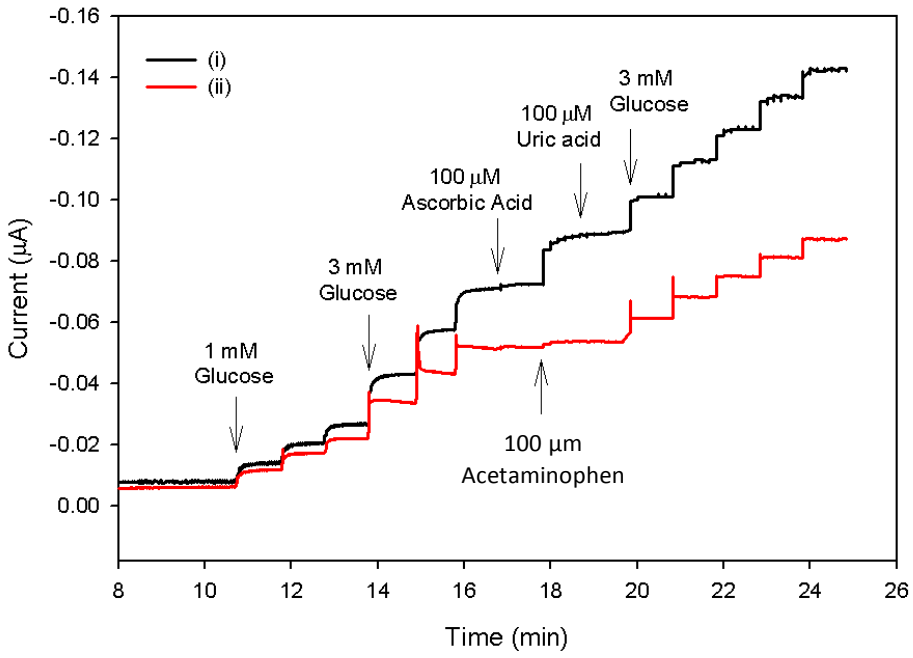

Figure 4.1. Amperometric response of 5 wt% NO-releasing dendrimer-doped 16% (w/v) Tecoplast electrospun fiber-modified needle-type glucose sensors without (i) or with (ii) an inner-selective layer. Glucose and interferences (i.e., ascorbic acid, acetaminophen, and uric acid) were sequentially injected into these solutions at physiologically relevant concentrations.

phosphate buffered saline (PBS, pH 7.4) after degassing with nitrogen for 20 min. The charge passed during electropolymerization was -0.53 ± 0.27 μC. A glucose oxidase (GOx) layer was then applied on top of the inner-selective membrane by immobilizing GOx within a sol-gel matrix. The enzyme-containing sol was prepared as described previously in Chapter 2.[18,19] The needle-type electrodes were dip-coated 15 times (with a single cycle consisting of a 5 s dip with 10 s drying under ambient conditions). The enzyme layer contained an excess of glucose oxidase so that the rate of glucose conversion was only dependent on glucose concentration. The diffusion-limiting layer was added by dip-coating the electrodes twice in a polyurethane (PU) polymer solution consisting of 80 mg mL^{-1} 50% (w/w) Tecoflex and Hydrothane dissolved in 50% (v/v) THF/EtOH solution. Each layer was dried under ambient conditions for 30 min before casting the subsequent layer. The thickness of the diffusion-limiting PU layer was 28.2 ± 13.0 μm, allowing for a dynamic glucose response range over the entire physiological range of blood glucose concentrations (1–30 mM).

4.2.3 Nitric oxide-releasing dendrimer-doped polyurethane solution.

1,2-Epoxy-9-decene (ED) functionalized fourth-generation of poly(amidoamine) (PAMAM) dendrimers (PAMAM G4-ED/NO) were synthesized as previously reported.[35] Subsequent *N*-diazeniumdiolation of the 1,2-epoxy-9-decene (ED) functionalized fourth-generation poly(amidoamine) (PAMAM) dendrimers (PAMAM G4-ED) was performed under high pressure of NO (10 atm) for 3 d in the presence of sodium methoxide at room temperature with constant stirring.[35,36] The NO donor-modified dendrimers were then

Table 4.1. Nitric oxide-release properties of *N*-diazeniumdiolated 1,2-epoxy-9-decene functionalized poly(amidoamine) fourth generation dendrimers (PAMAM G4-ED/NO) in PBS (0.01 M, pH 7.4) at 37 ^{o}C.

$[NO]_{max}$ (pmol $mg^{-1}s^{-1}$)	t_{max} (min)	Total NO released (μmol mg^{-1})	$t_{1/2}$ (h)	t_d (h)
511.2	4.23	0.62	0.91	6.03

stored in a methanol solution with sodium methoxide at -20 °C until use. The NO-release properties of the dendrimers were presented in Table 4.1.

Polyurethane solutions containing NO-releasing dendrimers were prepared by first dissolving the PU in 1.6 mL of a 3:1 (v/v) tetrahydrofuran (THF):*N,N*-dimethylformanide (DMF) mixture, followed by the addition of PAMAM G4-ED/NO solution (400 μL dissolved in methanol). The final concentration of polymer in solution was 12–16% (w/v). Dendrimer concentration is reported as wt% of the polymer mass.

4.2.4 Electrospinning of the outermost glucose sensor membrane.

Polyurethane electrospun fiber membranes were fabricated using a custom electrospinning apparatus consisting of a Series 205B High Voltage Power Supply (Bertan Associates, Inc.; Hicksville, NY), a Kent Scientific Genie Plus syringe pump (Torrington, CT), and a rotating collector (Figure 4.2B).[31] Voltage was applied to a standard stainless steel 22-gauge blunt-tip needle (0.508 mm diameter; Jensen Global, Santa Barbara, CA) attached to a NO-releasing dendrimer-doped PU solution-filled syringe positioned atop the syringe pump. A grounded collector connected with the fabricated glucose sensor was mounted perpendicular to the syringe at a distance of 15 cm and rotated at a speed of 250 rpm. Fibers were prepared via electrospinning at an applied voltage of 15 kV using a flow rate of 15 μL min^{-1}. The fabricated layer-by-layer structure of the needle-type glucose sensor is illustrated schematically in Figure 4.2A.

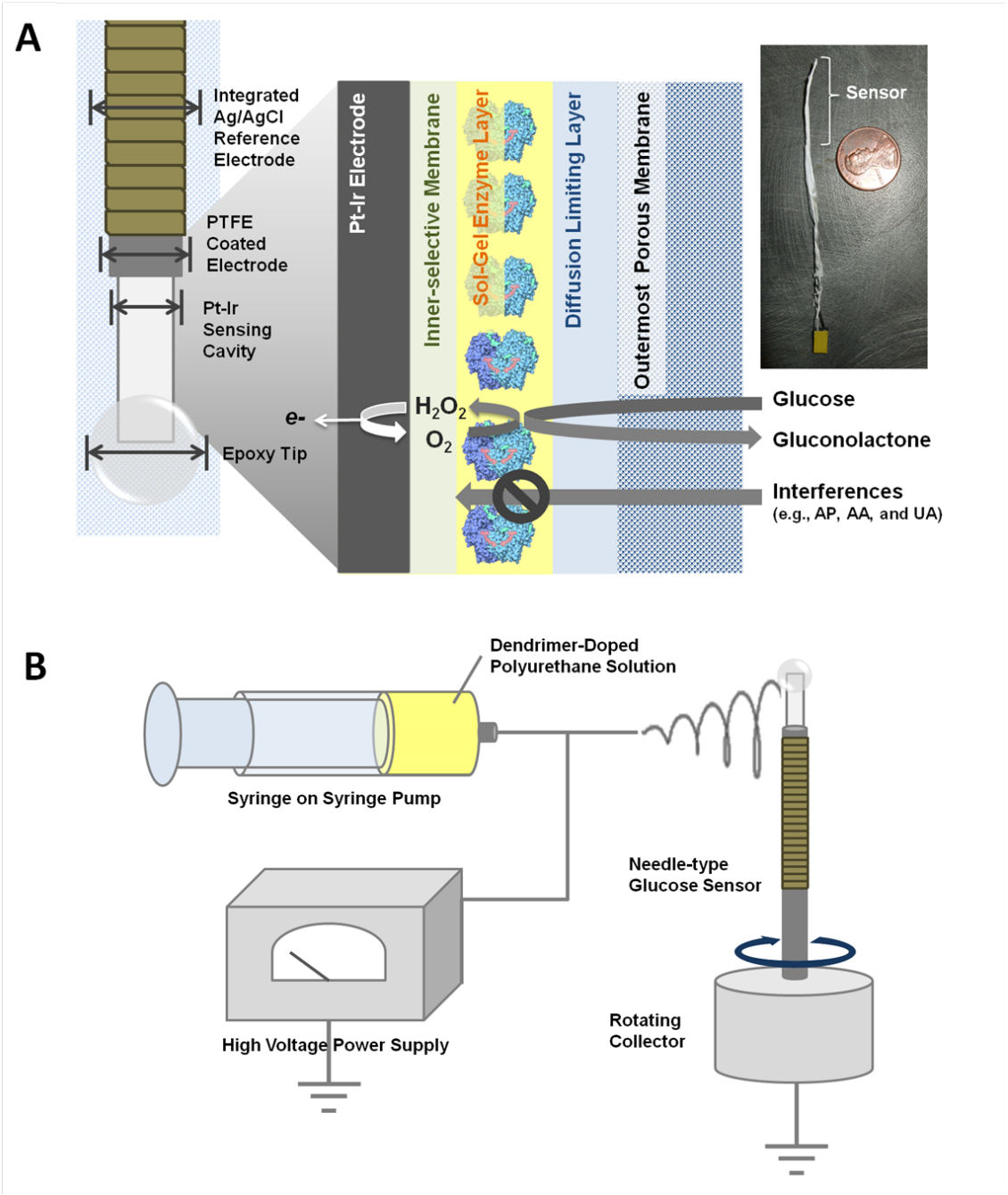

Figure 4.2. Schematics of (A) the layer-by-layer structure of NO-releasing porous electrospun fiber membrane coated needle-type glucose sensors with actual fabricated electrode shown on the right; and (B) electrospinning configuration for coating outermost porous membrane onto needle-type glucose sensors.

4.2.5 Characterization of NO-releasing dendrimer-doped electrospun fiber membrane.

Fiber diameter and percent porosity were determined using an environmental scanning electron microscope (ESEM; Quanta 200 field emission gun; FEI company; Hillsboro, OR) without additional metal coating. Fiber diameters were determined using NIH ImageJ software (Bethesda, MD). The percent porosity of the fibrous membrane was calculated according to the following equation (1), where ρ is the density of the electrospun fiber mats, and ρ_0 is the density of the bulk polymer.[23,37,38]

$$\text{Porosity } (\%) = \left(1 - \frac{\rho}{\rho_0}\right) \times 100\% \quad (1)$$

Nitric oxide release was evaluated as described previously.[31,39] Liberated NO was measured using a Sievers chemiluminescence Nitric Oxide Analyzer (NOA) Model 280i (Boulder, CO). To determine NO flux, electrospun samples were placed in a solution of deoxygenated PBS (0.01 M, pH 7.4) at 37 °C. The NO was carried to the NOA instrument by a stream of N_2 gas at a controlled rate (200 mL min^{-1} instrument collection rate). The NOA was calibrated using a 26.80 ppm NO gas (balance N_2) and air passed through a Sievers NO zero filter. Total amounts of NO released were determined indirectly by measuring the nitrite concentration via the Griess assay using a Labsystem Multiskan RC microplate spectrophotometer (at 540 nm; Helsinki, Finland). Of note, total NO concentrations measured with the Griess assay agreed with those obtained from chemiluminescence analysis indicating that these materials released NO and not nitrite.

The stability and distribution of the dendrimers within the PU fibers was assessed using fluorometry and confocal microscopy.[36] Before modifying the PAMAM

dendrimers with ED functional groups, dendrimers were tagged with rhodamine isothiocyanate (RITC) in a 1:1 molar ratio so that on average only one of the 64 primary amines on the dendrimer surface was modified. After fluorescently labeled dendrimer-doped fiber membranes were incubated in PBS for 7 d at 37 ^{o}C, the fluorescence of the soak solution was measured using Cary Eclipse fluorescence spectrometer (Varian Inc., Palo Alto, CA). The fluorescence intensity represented the degree of dendrimer leaching. In addition to this stability test, confocal fluorescence microscopy was used to image the distribution of fluorescently labeled PAMAM G4-ED/NO dendrimer in the electrospun fibers with an LSM 510 laser scanning confocal microscope (Carl Zeiss, Thornwood, NY).

4.2.6 Cytotoxicity assay.

In vitro cellular toxicity of blank (i.e., fibers without dendrimer), control (i.e., non-NO-releasing dendrimer-doped electrospun fibers), and NO-releasing electrospun fibers were evaluated using L929 mouse fibroblasts. The fibroblasts were cultivated in DMEM supplemented with 10% (v/v) fetal bovine serum and 1% (v/v) penicillin/streptomycin, then incubated in 5% CO_2/balance air under humidified conditions at 37 °C. The cells were trypsinized and seeded onto tissue-culture-treated polystyrene 24-well plates at a density of 3×10^4 cells mL^{-1} after reaching 80% confluency. After 48 h, cells were incubated with blank, control, and NO-releasing electrospun fiber mats for either 24 or 48 h. Subsequently, the fiber mats were removed, cells were washed three times with sterile PBS, and a 1.4 mL mixture of DMEM/MTS/PMS (105/20/1, v/v/v) was added to each well. Once a color change was

observed in the blank wells, the supernatant (100 μL) from each well was transferred to a 96-well plate prior to measuring the absorbance at 490 nm using a microplate reader (Thermoscientific Multiskan EX; Waltham, MA). Untreated cells were used as controls, and results were expressed as percent viability relative to these controls.

4.2.7 Electrochemical sensor performance.

The analytical performance of the fabricated glucose biosensor was evaluated via constant potential amperometry using a CH Instruments 1030A potentiostat (Austin, TX). All electrochemical determinations were conducted in 0.01 M PBS (pH 7.4) or porcine serum at room temperature or 37 ^{o}C using an integrated Ag/AgCl wire as a pseudo counter and reference electrode. After the background current was polarized, the analytical performance (e.g., sensitivity, response time, and selectivity) of the sensors were evaluated by sequentially injecting glucose or interferent aliquots into solution with constant stirring and setting the working electrode to a potential of +0.6 V vs. Ag/AgCl. The sensitivity to glucose was determined based on the slope of the linear regression between the measured oxidation current and glucose concentration. The amperometric selectivity coefficient ($logK_{glu}^{amp}$) was calculated according to equation (2) below where ΔI_{glu} and ΔI_j represent the measured current response to predetermined concentrations of of glucose (c_{glu}) and interference species (c_j; j=AP, AA, and UA), respectively.[18]

$$\log K_{glu}^{amp} = \log \left(\frac{\Delta I_j / c_j}{\Delta I_{glu} / c_{glu}}\right) \quad (2)$$

4.3 Results and Discussion

4.3.1 Characterization of NO-releasing dendrimer-doped electrospun polyurethane fibers

Non-porous PU membranes have been employed to fabricate implantable glucose sensors in order to balance the diffusion ratio of glucose and oxygen, and prevent an oxygen deficit.[20,33,40] Generally, such polymers are also considered tolerable by the body. Nevertheless, the immune response and subsequent collagen encapsulation that forms around the sensor and PU membrane still negatively impacts in vivo glucose sensor performance.[41] To potentially reduce the foreign body response (FBR) and thus improve the analytical performance of CGM sensors,[2,6] NO donor-containing PU fibers were electrospun onto enzyme-based needle-type glucose sensors as an additional outermost membrane on top of the standard diffusion-limiting PU layer to create a porous interface capable of releasing a therapeutic agent known to mitigate the FBR (Figure 4.2).

Prior to bench top sensor testing, the *N*-diazeniumdiolated dendrimer-doped electrospun fibrous PU membranes were characterized with respect to their physical properties (e.g., fiber diameter and porosity), NO release, and stability (i.e., dendrimer leaching). Scanning electron microscopic image of the cross section of the fully fabricated glucose sensor confirmed a three dimensional structure, highlighting the ability to successfully coat porous electrospun fibers onto needle-type microsensor. As shown Figure 4.3, electrospun membranes exhibited a random open pore structure with interconnected fibers and no bead formation over the entire electrode surface (1.4 ± 0.7 mg/sensor) (Figure 4.3A and C).

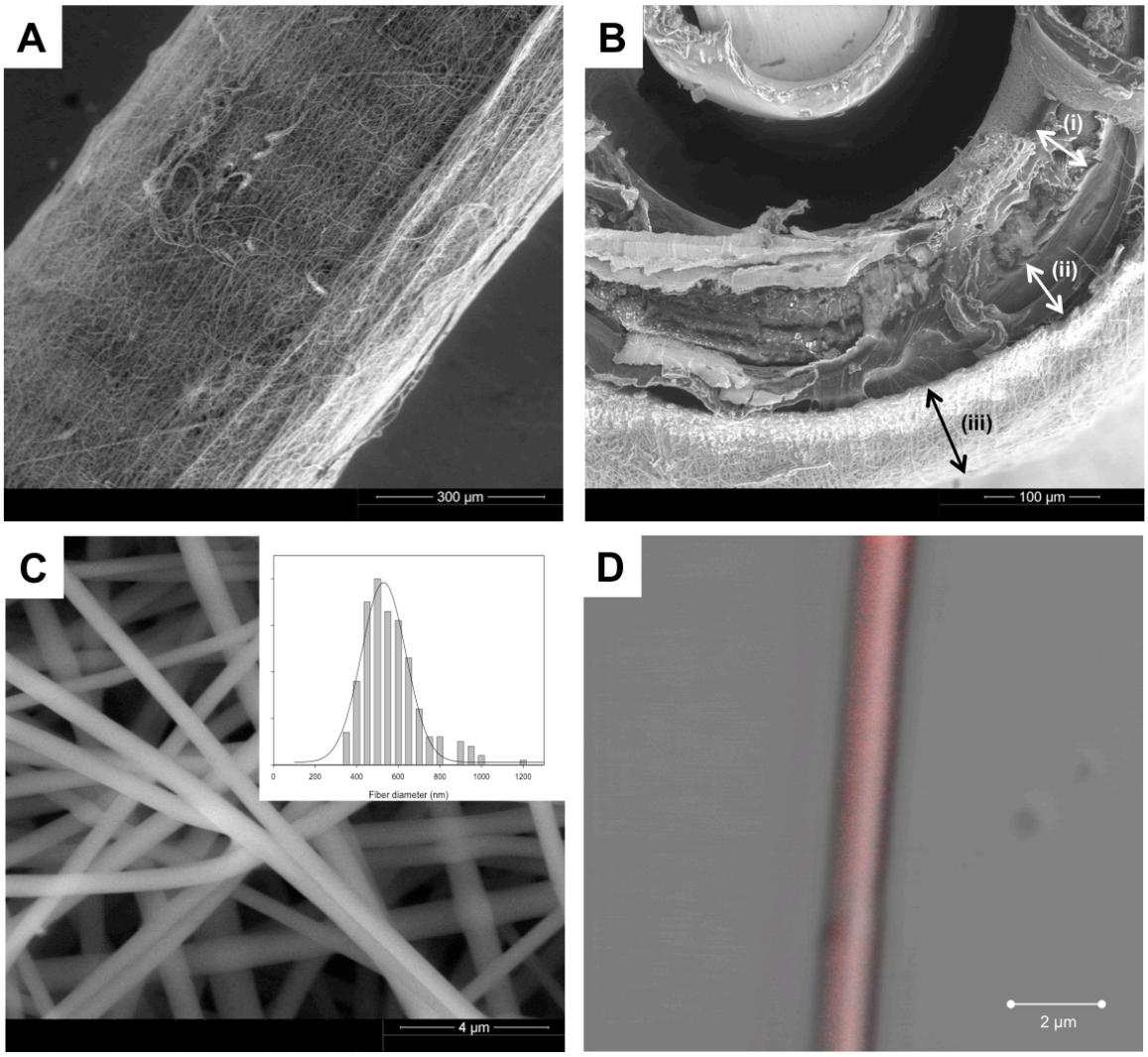

Figure 4.3. Environmental scanning electron microscope (ESEM) images of (A) NO-releasing dendrimer-doped electrospun polyurethane membrane on needle-type glucose sensors and (B) the cross sectional view with (i) a sol-gel/glucose oxidase enzyme layer, (ii) a diffusion-limiting polyurethane layer, and (iii) an electrospun fiber porous membrane; (C) higher magnification view of the electrospun fiber membrane and inset indicating distribution of fiber diameters (540 ± 139 nm); and (D) confocal image of a single fiber embedded with RITC-labeled dendrimer

Table 4.2. Characterization of NO release and glucose sensor performance for the porous NO-releasing electrospun fiber-modified needle-type glucose sensors as a function of the fiber. All porous membranes were doped with 5 wt% *N*-diazeniumdiolated dendrimers (PAMAM G4-ED/NO).

Type of polyurethane[a]		*Tecophilic* *(HP-93A-100)*	*Tecoflex* *(SG-80A)*	*Tecoplast* *(TP-470)*
PU solution concentration[b] (% (w/v))		12	12	16
Physical properties of outermost membrane	Water uptake (mg, H_2O/mg, Fiber mat)	4.7 ± 1.0	1.6 ± 0.2	0.8 ± 0.5
	Percent porosity (%)	67.3 ± 4.4	57.6 ± 2.5	94.1 ± 3.7
	Fiber diameter (nm)	567 ± 288	404 ± 190	540 ± 139
Sensor performance	Glucose Sensitivity (nA mM^{-1})	4.1 ± 3.8	3.0 ± 2.0	2.4 ± 1.6
NO release properties	Response time ($t_{95\%}$; s)	32.1 ± 7.2	43.3 ± 12.7	76.4 ± 21.7
	$[NO]_{max}$ (pmol $mg^{-1}s^{-1}$)	52.0 ± 26.1	24.4 ± 8.2	19.8 ± 6.4
	Total NO released[c] (μmol mg^{-1})	0.15 ± 0.02	0.14 ± 0.03	0.10 ± 0.01
	t_d (h)	7.3 ± 3.6	8.9 ± 1.6	6.7 ± 1.0

[a] The water uptake of polyurethanes was described previously.[18]

[b] Concentration of polymer solution was optimized to achieve 400–600 nm fiber.[28]

[c] Total NO released as determined using the Griess assay.

Water uptake by the fabricated fibers, important for both glucose response and NO release, varied based on the type of PU (4.7 ± 1.0, 1.6 ± 0.2, and 0.8 ± 0.5 mg of water/mg of PU fiber for Tecophilic, Tecoflex and Tecoplast, respectively). Fiber diameters ranging from 400-600 nm were achieved by varying the concentration of PU solution (12–16% (w/v)). Of note, such diameters were previously shown to reduce both the adhesion and activation of macrophage cells, suggesting a lessened initial FBR.[28] The presence of the NO donor-modified dendrimer did not significantly affect fiber diameter. The percent porosity of the fibrous membranes for fiber diameters ranging from 400-600 nm was 67.3 ± 4.4, 57.6 ± 2.5, and 94.1 ± 3.7 % for the Tecophilic, Tecoflex, and Tecoplast fibers, respectively. Such porosity is in line with prior reports describing the use of highly porous interfaces (>90% porosity) to increase cell infiltration and reduce collagen capsule formation (i.e., thickness).[23, 29] Based on the above data and the prior tissue biocompatibility literature, the Tecoplast fiber mat would likely be most effective at reducing the FBR.

Nitric oxide release from PAMAM G4-ED/NO dendrimer-doped electrospun fiber membranes was measured in PBS (pH 7.4) at 37 ^{o}C to mimic physiological conditions (Figure 4.4). The Tecoplast electrospun fiber membrane doped with 5 wt% PAMAM G4-ED/NO dendrimer exhibited a maximum NO flux of 19.8 ± 6.4 pmol mg^{-1} s^{-1} with 0.10 ± 0.08 μmol mg^{-1} total NO released over ~7 h. The time to reach maximum NO flux was 2.2 ± 0.3 min.

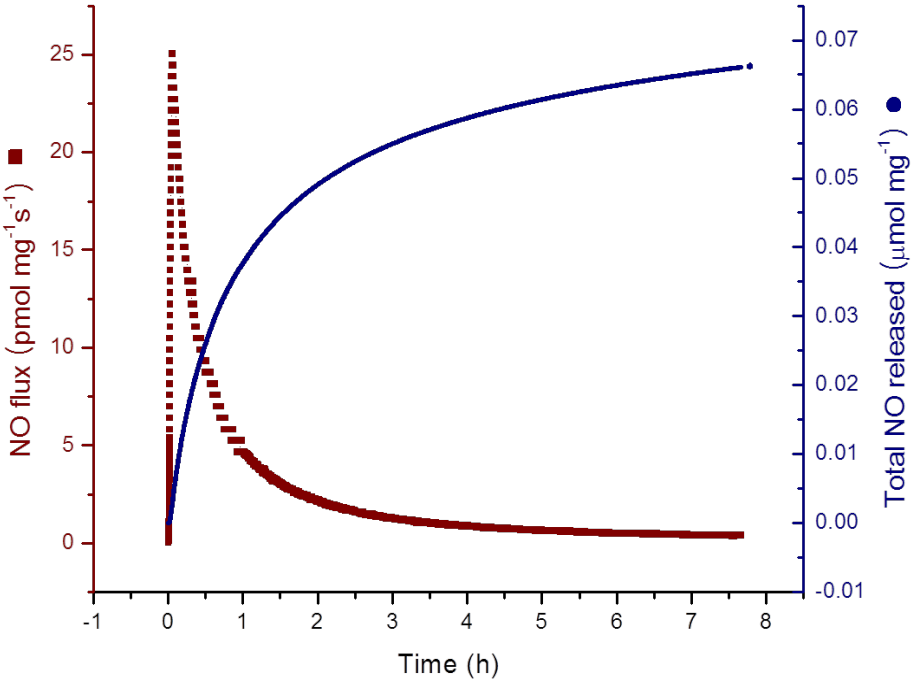

Figure 4.4. Nitric oxide flux and total NO release from 5 wt% PAMAM G4-ED/NO dendrimer-doped 16% (w/v) Tecoplast electrospun polyurethane fiber membranes.

As expected, the total NO released was proportional to the amount of dendrimer embedded within the fibers. For example, the total amount of NO released from the Tecoplast PU fibers was increased from 0.10 ± 0.08 to 0.27 ± 0.12 μmol mg^{-1} upon altering the NO donor (PAMAM G4-ED/NO) concentration from 5 to 10 wt%. Surprisingly, the NO-release kinetics were not altered based on water uptake by the PU. Although the use of more hydrophobic PU (i.e., Tecoplast) resulted in a slightly suppressed maximum NO flux, the duration of NO release was similar to the NO-releasing dendrimer alone (Table 4.2). Such behavior is attributed to the porous structure of the electrospun fiber mat and/or the distribution of dendrimers within the fibers (Figure 4.3D).[31] Based on the most ideal characteristics (i.e., fiber diameter, porosity, and NO release), the Tecoplast fiber mat was chosen for further study.

Rhodamine isothiocyante (RITC) fluorophore-tagged dendrimers were used to evaluate the distribution and stability of NO donor. As indicated in the confocal microscopy images of Figure 4.3D, fluorescent NO-releasing PAMAM G4-ED dendrimers were homogeneously dispersed both within individual fibers and throughout the entire fiber mat. Stability of the NO-releasing dendrimer within the fibers was determined using a leaching assay. Fibers doped with fluorescently tagged dendrimers were immersed in PBS (pH 7.4 at 37 ^{o}C) for 7 d. Fluorescence emission (at 570 nm) of the soak solution was then measured using fluorometer. These soak solution did not fluorescence, indicating negligible leaching (<0.5%) of the dendrimer NO-releasing vehicles from the fibers.

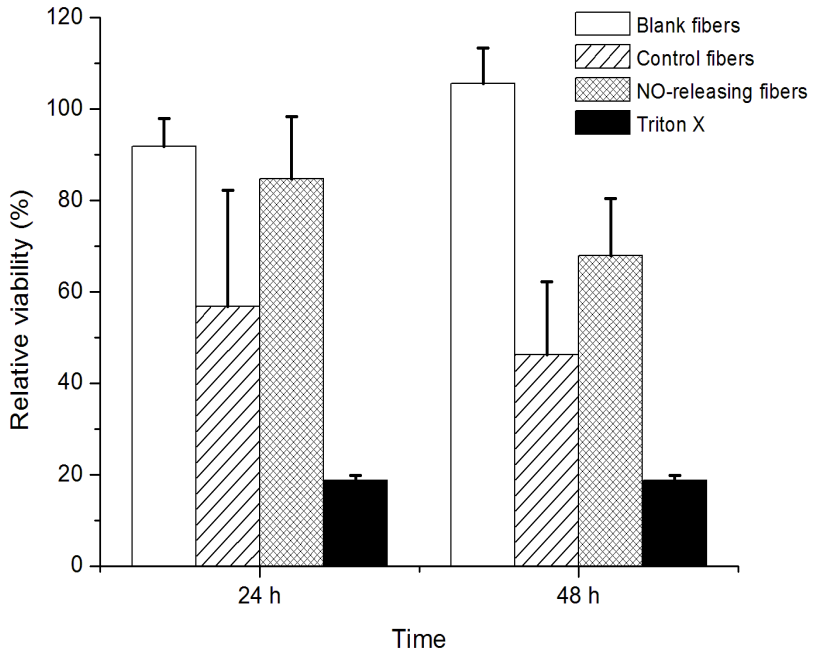

Figure 4.5. Relative viability of L929 mouse fibroblasts to polyurethane electrospun fibers without (blank) and with dopant: non-NO-releasing dendrimer (control) and NO-releasing dendrimer (i.e., PAMAM G4-ED/NO) for 24 and 48 h.

While minimal leaching limits the dendrimer-related toxicity concerns, cytotoxicity of the electrospun fibers was evaluated for future applications. A cytotoxicity assays (i.e., MTS assay) was performed using L929 mouse fibroblasts over 48 h to evaluate the toxicity of the electrospun fiber mats. The normalized cell viabilities, as a function of fiber mat type, after 24 and 48 h are given in Figure 4.5. The Tecoplast polyurethane fibers without dendrimer dopants (i.e., blank) were demonstrated no loss in cell viability, whereas the addition of non-NO-releasing dendrimers (i.e., control) decreased average cell viability to 50–60% despite the absence of dendrimer leaching from the fibers. This decrease in cell viability may be attributed to the distribution of dendrimer throughout the entire fiber, allowing some functional group to become in contact with the cells. However, NO-release from fibers improved fibroblast viability, with a ~20% improvement was observed upon the incorporation of NO release (85 ± 14 and 68 ± 13% viability at 24 and 48 h, respectively). Such a decrease in cytotoxicity for the NO-releasing fibers at 48 h was unexpected given the short duration of NO release (6.7 ± 1.0 h), but suggests that extended release durations may further improve the biocompatibility of such fibers in vitro.

To assess the structured stability of the three-dimensional porous membranes, the electrospun fiber-coated glucose sensors were soaked in porcine serum for 7 d at 37 ^{o}C. As shown in the ESEM images in Figure 4.6B, the topography of the Tecoplast electrospun fiber mat-modified sensor was constant even after 1 week incubation in porcine serum.

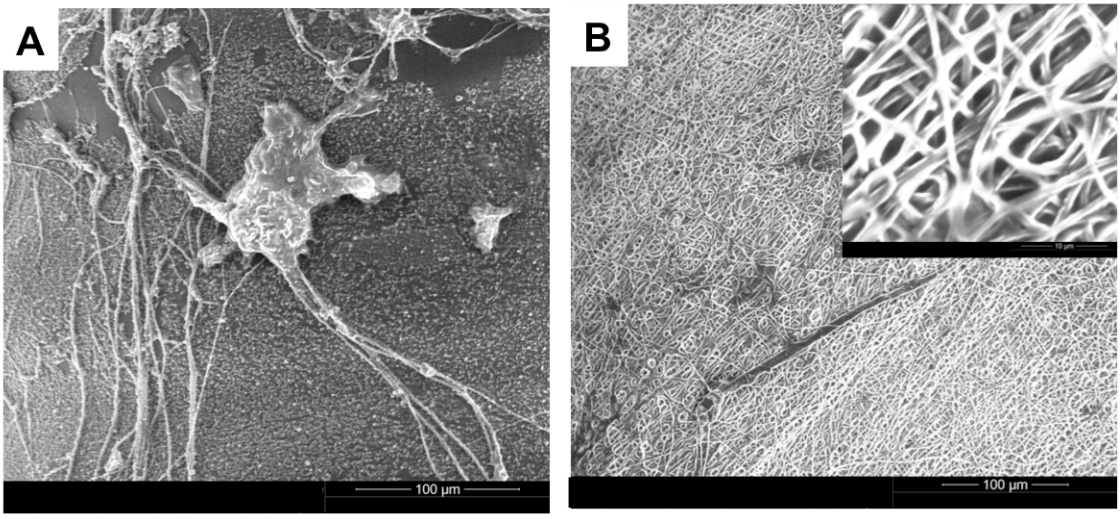

Figure 4.6. Environmental scanning electron microscope (ESEM) images of the sensor surface without porous membrane (A) and with NO-releasing dendrimer-doped outermost electrospun fiber membrane (B) incubated in porcine serum for 7 d.

While protein adhesion, a primary cause of erratic sensor response in vivo,[42] was observed on the non-porous sensor surface (Figure 4.6A), no significant protein adsorption was observed on or beneath the electrospun fiber membranes. Of note, the structural stability and reduced protein adsorption on the porous membranes suggests a potential to improve tissue integration and sensitivity in vivo.[43]

4.3.2 Electrochemical performance of electrospun membrane coated glucose biosensor.

The analytical response of the fabricated NO-releasing electrospun fiber-modified needle-type glucose sensors was characterized in vitro as a function of PU composition to assess the impact of the fiber mat. Neither the electrospinning process nor NO release affected the sensor performance (Figure 4.8).[18,26]

Sensor response was studied as a function of the electrospun membrane thickness using the most hydrophobic PU (i.e., Tecoplast). Fiber mat thickness was varied by adjusting the feed volume of the polymer solution during the electrospinning process. Greater feed volumes resulted in thicker fiber mats (44.5 ± 12.2, 71.5 ± 19.1, and 241.5 ± 84.3 μm for 1, 2, and 3 mL, respectively) that were no longer useful as sensor membranes (Figure 4.7). While the addition of electrospun fiber membranes ≤50 μm thick responded rapidly (~1 min response time ($t_{95\%}$)) to changes in glucose concentrations, thicker (>50 μm) fiber mat membranes exhibited response times similar to non-porous hydrophobic PU sensor membranes ($t_{95\%}$= ~125–250 s). Subsequent sensor performance testing was thus carried out using biosensors fabricated with thin (~45 μm) electrospun fiber mat membranes.

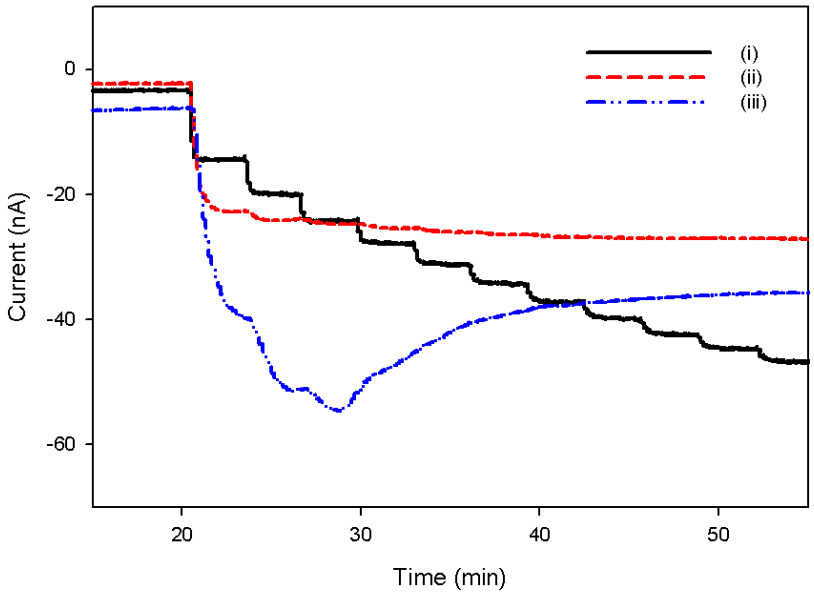

Figure 4.7. Amperometric response of needle-type glucose sensors coated with NO-releasing dendrimer (PAMAM G4-ED/NO)-doped membranes at a fiber mat thickness of (i) 45 to (ii) 72 and (iii) 242 μm. The glucose concentration was changed at 3 mM increments.

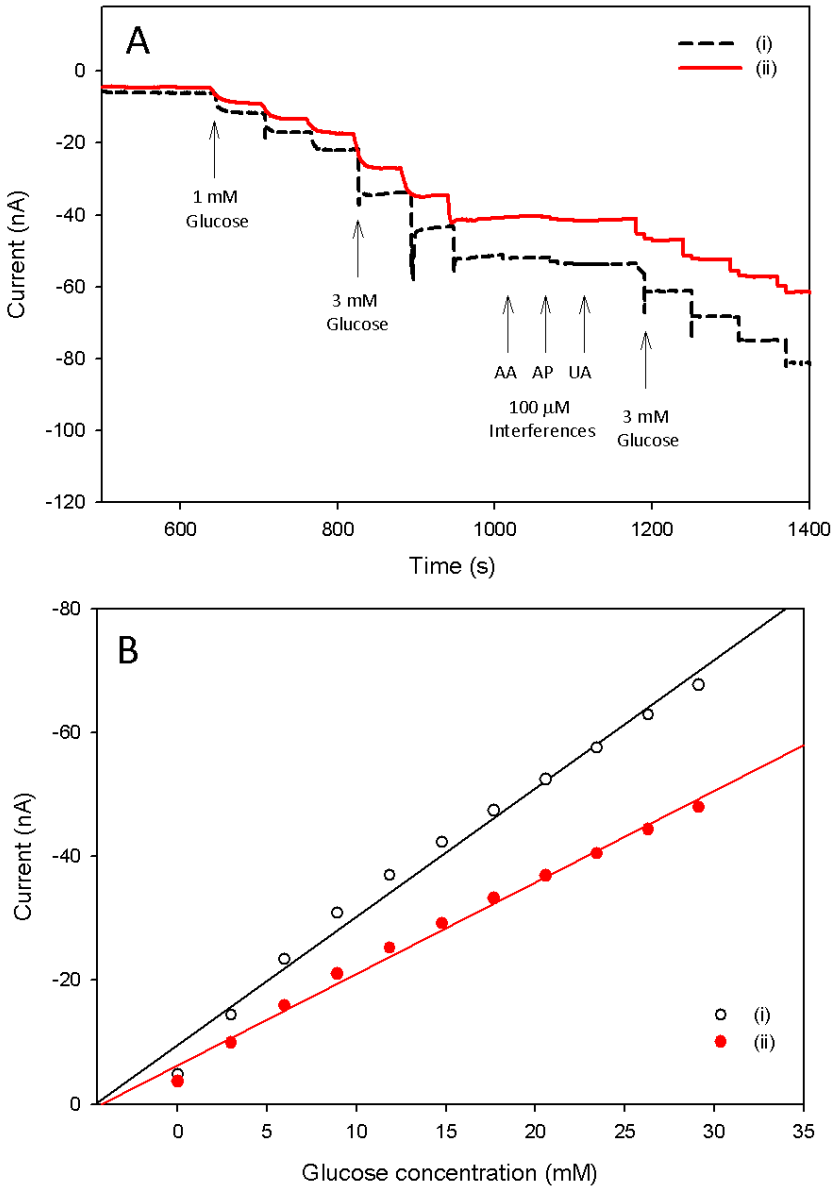

Figure 4.8. (A) Amperometric response of a needle-type glucose sensor for (i) control (i.e., without) and (ii) 5 wt% NO-releasing dendrimer-doped 16% (w/v) Tecoplast electrospun fiber-modified outermost membrane. Glucose, ascorbic acid (AA), acetaminophen (AP), and uric acid (UA) were sequentially injected at relevant in vivo concentrations. (B) Calibration curves of (i) control and (ii) porous electrospun fiber membrane-modified glucose sensors in pH 7.4 PBS. The applied electrode potential was +0.6 V vs. Ag/AgCl.

Glucose sensor performance was also evaluated as a function of PU fiber composition and water uptake. Regardless of PU fiber composition, the dynamic response range of all sensors was 1–30 mM glucose due to the diffusion-limiting full PU membrane layer beneath the porous fiber mat. The use of lower water uptake PU (i.e., Tecoplast) resulted in decreased sensor response to changing glucose concentrations and longer response time (Table 4.2). While Tecophilic PU had a negligible effect on sensitivity and response time, the more hydrophobic PU (i.e., Tecoplast) reduced sensor response to glucose by ~30% while increasing response time ($t_{95\%}$) from 15.9 ± 9.0 to 76.4 ± 21.7 s. The addition of the more hydrophobic porous membrane neither compromised the selectivity nor dynamic range (Figure 4.8). Despite the diminished sensor performance, the sensitivity of the resulting glucose biosensor coated with the dendrimer-doped Tecoplast (16% (w/v) electrospun fiber with 5 wt% PAMAM G4-ED/NO dendrimer) was 2.4 ± 1.6 nA/mM (Figure 4.8), a response comparable to commercially available and previously published implantable glucose biosensors.[40,44] The amperometric selectivity coefficients of the biosensors were -0.73 ± 0.85, 0.96 ± 0.10, and 0.28 ± 0.14 for ascorbic acid, acetaminophen, and uric acid, respectively, indicating that the fiber mat-modified biosensors were adequately selective for glucose over interferences at physiologically relevant concentrations. Finally, the sensor response in a porcine serum solution was characterized to mimic a more physiologically relevant solution. The sensitivity of the NO-releasing sensors in porcine serum at 37 ^{o}C was 2.15 ± 0.60 nA/mM (data not shown). In addition, the biosensors remained functional for at least a week in serum. While bench top evaluation of sensor performance suggests a

viable device, in vivo experiments are obviously necessary to understand and benefit of porosity and NO release on analytical performance.

4.4 Conclusion

Porous fiber mats capable of NO release may reduce the undesirable FBR associated with sensor implantation in subcutaneous tissue. Herein, a facile electrospinning method was developed to modify needle-type electrochemical biosensors with thin, NO-releasing PU fiber mat membranes. Importantly, sensor performance was not diminished with the additional NO-releasing membrane, suggesting similar fibrous coatings could be applied to other tissue-contacting devices with minimal impact to device utility.

4.5 References

(1) Vaddiraju, S.; Burgess, D. J.; Tomazos, I.; Jain, F. C.; Papadimitrakopoulos, F. "Technologies for continuous glucose monitoring: Current problems and future promises" *Journal of Diabetes Science and Technology* **2010**, *4*, 1540-1562.

(2) Nichols, S. P.; Koh, A.; Storm, W. L.; Shin, J. H.; Schoenfisch, M. H. "Biocompatible materials for continuous glucose monitoring devices" *Chemical Reviews* **2013**, *113*, 2528-2549.

(3) Wilson, G. S.; Gifford, R. "Biosensors for real-time *in vivo* measurements" *Biosensors and Bioelectronics* **2005**, *20*, 2388-2403.

(4) Wilson, G. S.; Johnson, M. A. "In-vivo electrochemistry: What can we learn about living systems?" *Chemical Reviews* **2008**, *108*, 2462-2481.

(5) Ratner, B. D. "Reducing capsular thickness and enhancing angiogenesis around implant drug release systems" *Journal of Controlled Release* **2002**, *78*, 211-218.

(6) Koh, A.; Nichols, S. P.; Schoenfisch, M. H. "Glucose sensor membranes for mitigating the foreign body response" *Journal of Diabetes Science and Technology* **2011**, *5*, 1052-1059.

(7) Williams, D. L. H. "A chemist's view of the nitric oxide story" *Organic and Biomolecular Chemistry* **2003**, *1*, 441-449.

(8) Carpenter, A. W.; Schoenfisch, M. H. "Nitric oxide release: Part II. Therapeutic applications" *Chemical Society Reviews* **2012**, *41*, 3742-3752.

(9) Riccio, D. A.; Schoenfisch, M. H. "Nitric oxide release: Part I. Macromolecular scaffolds" *Chemical Society Reviews* **2012**, *41*, 3731-3741.

(10) Hetrick, E. M.; Prichard, H. L.; Klitzman, B.; Schoenfisch, M. H. "Reduced foreign body response at nitric oxide-releasing subcutaneous implants" *Biomaterials* **2007**, *28*, 4571-4580.

(11) Nichols, S. P.; Koh, A.; Brown, N. L.; Rose, M. B.; Sun, B.; Slomberg, D. L.; Riccio, D. A.; Klitzman, B.; Schoenfisch, M. H. "The effect of nitric oxide

surface flux on the foreign body response to subcutaneous implants" *Biomaterials* **2012**, *33*, 6305-6312.

(12) Nablo, B. J.; Prichard, H. L.; Butler, R. D.; Klitzman, B.; Schoenfisch, M. H. "Inhibition of implant-associated infections via nitric oxide" *Biomaterials* **2005**, *26*, 6984-6990.

(13) Nablo, B. J.; Chen, T. Y.; Schoenfisch, M. H. "Sol-gel derived nitric-oxide releasing materials that reduce bacterial adhesion" *Journal of the American Chemical Society* **2001**, *123*, 9712-9713.

(14) Nablo, B. J.; Rothrock, A. R.; Schoenfisch, M. H. "Nitric oxide-releasing sol-gels as antibacterial coatings for orthopedic implants" *Biomaterials* **2005**, *26*, 917-924.

(15) Nablo, B. J.; Schoenfisch, M. H. "Antibacterial properties of nitric oxide-releasing sol-gels" *Journal of Biomedical Materials Research Part A* **2003**, *67A*, 1276-1283.

(16) Shin, J. H.; Schoenfisch, M. H. "Improving the biocompatibility of in vivo sensors via nitric oxide release" *Analyst* **2006**, *131*, 609-615.

(17) Oh, B. K.; Robbins, M. E.; Nablo, B. J.; Schoenfisch, M. H. "Miniaturized glucose biosensor modified with a nitric oxide-releasing xerogel microarray" *Biosensors and Bioelectronics* **2005**, *21*, 749-757.

(18) Koh, A.; Riccio, D. A.; Sun, B.; Carpenter, A. W.; Nichols, S. P.; Schoenfisch, M. H. "Fabrication of nitric oxide-releasing polyurethane glucose sensor membranes" *Biosensors and Bioelectronics* **2011**, *28*, 17-24.

(19) Shin, J. H.; Marxer, S. M.; Schoenfisch, M. H. "Nitric oxide-releasing sol-gel particle/polyurethane glucose biosensors" *Analytical Chemistry* **2004**, *76*, 4543-4549.

(20) Gifford, R.; Batchelor, M. M.; Lee, Y.; Gokulrangan, G.; Meyerhoff, M. E.; Wilson, G. S. "Mediation of in vivo glucose sensor inflammatory response via nitric oxide release" *Journal of Biomedical Materials Research Part A* **2005**, *75A*, 755-766.

(21) Bota, P. C. S.; Collie, A. M. B.; Puolakkainen, P.; Vernon, R. B.; Sage, E. H.; Ratner, B. D.; Stayton, P. S. "Biomaterial topography alters healing in vivo and monocyte/macrophage activation in vitro" *Journal of Biomedical Materials Research Part A* **2010**, *95*, 649-657.

(22) Ju, Y. M.; Yu, B.; West, L.; Moussy, Y.; Moussy, F. "A novel porous collagen scaffold around an implantable biosensor for improving biocompatibility. II. Long-term in vitro/in vivo sensitivity characteristics of sensors with NDGA- or GA-crosslinked collagen scaffolds" *Journal of Biomedical Materials Research Part A* **2010**, *92*, 650-658.

(23) Koschwanez, H. E.; Yap, F. Y.; Klitzman, B.; Reichert, W. M. "In vitro and in vivo characterization of porous poly-L-lactic acid coatings for subcutaneously implanted glucose sensors" *Journal of Biomedical Materials Research Part A* **2008**, *87A*, 792-807.

(24) Sanders, J. E.; Lamont, S. E.; Karchin, A.; Golledge, S. L.; Ratner, B. D. "Fibro-porous meshes made from polyurethane micro-fibers: effects of surface charge on tissue response" *Biomaterials* **2005**, *26*, 813-818.

(25) Teo, W. E.; Ramakrishna, S. "A review on electrospinning design and nanofibre assemblies" *Nanotechnology* **2006**, *17*, R89-R106.

(26) Wang, N.; Burugapalli, K.; Song, W.; Halls, J.; Moussy, F.; Ray, A.; Zheng, Y. "Electrospun fibro-porous polyurethane coatings for implantable glucose biosensors" *Biomaterials* **2013**, *34*, 888-901.

(27) Huang, Z.-M.; Zhang, Y.-Z.; Koraki, M.; Ramakrishna, S. "A review on polymer nanofibers by electrospinning and their applications in nanocomposites" *Composites Science and Technology* **2003**, *63*, 2223-2253.

(28) Saino, E.; Focarete, M. L.; Gualandi, C.; Emanuele, E.; Cornaglia, A. I.; Imbriani, M.; Visai, L. "Effect of electrospun fiber diameter and alignment on macrophage activation and secretion of proinflammatory cytokines and chemokines" *Biomacromolecules* **2011**, *12*, 1900-1911.

(29) Cao, H.; McHugh, K.; Chew, S. Y.; Anderson, J. M. "The topographical effect of electrospun nanofibrous scaffolds on the in vivo and in vitro foreign body

reaction" *Journal of Biomedical Materials Research Part A* **2010**, *93A*, 1151-1159.

(30) Vacanti, N. M.; Cheng, H.; Hill, P. S.; Guerreiro, J. D. T.; Dang, T. T.; Ma, M.; Watson, S.; Hwang, N. S.; Langer, R.; Anderson, D. G. "Localized delivery of dexamethasone from electrospun fibers reduces the foreign body response" *Biomacromolecules* **2012**, *13*, 3031-3038.

(31) Coneski, P. N.; Nash, J. A.; Schoenfisch, M. H. "Nitric oxide-releasing electrospun polymer microfibers" *ACS Applied Materials & Interfaces* **2011**, *3*, 426-432.

(32) Bindra, D. S.; Zhang, Y.; Wilson, G. S.; Sternberg, R.; Thevenot, D. R.; Moatti, D.; Reach, G. "Design and in vitro studies of a needle-type glucose sensor for subcutaneous monitoring" *Analytical Chemistry* **1991**, *63*, 1692-1696.

(33) Chen, X.; Matsumoto, N.; Hu, Y.; Wilson, G. S. "Electrochemically mediated electrodeposition/electropolymerization to yield a glucose microbiosensor with improved characteristics" *Analytical Chemistry* **2002**, *74*, 368-372.

(34) Vaddiraju, S.; Wang, Y.; Qiang, L.; Burgess, D. J.; Papadimitrakopoulos, F. "Microsphere erosion in outer hydrogel membranes creating macroscopic porosity to counter biofouling-induced sensor degradation" *Analytical Chemistry* **2012**, *84*, 8837-8845.

(35) Lu, Y.; Sun, B.; Li, C.; Schoenfisch, M. H. "Structurally diverse nitric oxide-releasing poly(propylene imine) dendrimers" *Chemistry of Materials* **2011**, *23*, 4227-4233.

(36) Sun, B.; Slomberg, D. L.; Chudasama, S. L.; Lu, Y.; Schoenfisch, M. H. "Nitric oxide-releasing dendrimers as antibacterial agents" *Biomacromolecules* **2012**, *13*, 3343-3354.

(37) Zhu, X.; Cui, W.; Li, X.; Jin, Y. "Electrospun Fibrous Mats with High Porosity as Potential Scaffolds for Skin Tissue Engineering" *Biomacromolecules* **2008**, *9*, 1795-1801.

(38) He, W.; Ma, Z.; Yong, T.; Teo, W. E.; Ramakrishna, S. "Fabrication of collagen-coated biodegradable polymer nanofiber mesh and its potential for endothelial cells growth" *Biomaterials* **2005**, *26*, 7606-7615.

(39) Hetrick, E. M.; Schoenfisch, M. H. "Analytical chemistry of nitric oxide" *Annual Review of Analytical Chemistry* **2009**, *2*, 409-433.

(40) Ward, W. K.; Jansen, L. B.; Anderson, E.; Reach, G.; Klein, J. C.; Wilson, G. S. "A new amperometric glucose microsensor: in vitro and short-term in vivo evaluation" *Biosensors and Bioelectronics* **2002**, *17*, 181-189.

(41) Ward, W. K.; Slobodzian, E. P.; Tiekotter, K. L.; Wood, M. D. "The effect of microgeometry, implant thickness and polyurethane chemistry on the foreign body response to subcutaneous implants" *Biomaterials* **2002**, *23*, 4185-4192.

(42) Gifford, R.; Kehoe, J. J.; Barnes, S. L.; Kornilayev, B. A.; Alterman, M. A.; Wilson, G. S. "Protein interactions with subcutaneously implanted biosensors" *Biomaterials* **2006**, *27*, 2587-2598.

(43) Nisbet, D. R.; Forsythe, J. S.; Shen, W.; Finkelstein, D. I.; Horne, M. K. "Review Paper: A Review of the Cellular Response on Electrospun Nanofibers for Tissue Engineering" *Journal of Biomaterials Applications* **2009**, *24*, 7-29.

(44) Klonoff, D. C. "A review of continuous glucose monitoring" *Diabetes Technology and Therapeutics* **2005**, *7*, 770-775.

CHAPTER 5: IN VIVO PERFORMANCE OF PERCUTANEOUSLY IMPLANTED NITRIC OXIDE-RELEASING GLUCOSE SENSORS IN A FREELY MOVING PORCINE MODEL

5.1 Introduction

Continuous glucose monitoring (CGM) devices based on electrochemical real-time measurement represents a pivotal technology for enabling tight control of blood glucose levels and preventing complications associated with diabetes.[1,2] Indeed, the integration of an implantable glucose sensor with an insulin pump holds significant promise in the development of an artificial pancreas.[2] Although the concept of an implantable electrochemical glucose sensor was introduced in the early 1990s, most GCM systems to date have been met with limited success.[2] Shortcomings of current CGM technology including limited sensor lifetime, unpredictable sensor performance, and inaccurate measurement are mainly caused by the foreign body response (FBR).[3,4] Therefore, significant research efforts have focused on the development of more biocompatible sensor membranes that mitigate the FBR.

Membranes that release pharmaceutical agents have been explored as a method to promote angiogenesis and suppress inflammation at the sensor surface.[5,6] To this end, nitric oxide (NO) become a focus due to its wide range of biological roles (e.g., wound healing, anti-inflammatory, and angiogenesis).[7,8] To utilize NO therapeutically, macromolecules that store and deliver NO have been developed to overcome NO's highly

reactive nature.[9] Many NO-release vehicles have been synthesized by modifying polymeric scaffolds (e.g., xerogels[10,11] and silica nanoparticles[12-14]) with two common NO donors: *N*-diazeniumdiolates and *S*-nitrosothiols. To assess the effect of NO on the FBR, Hetrick et al. examined the tissue response of subcutaneously implanted *N*-diazeniumdiolated xerogel membranes in a rodent model.[11] The NO-releasing implants (~1.35 μmol NO/cm^2 released over 72 h) reduced the associated collagen capsule thickness by >50% and up to 20–25% after 3 weeks (even when the NO release was expired) versus blank and control implants, respectively. Additionally, blood vessel formation was improved by ~77% compared to controls after 1 week implantation. With this initial study indicated the ability of NO to reduce the FBR, Nichols et al. studied on the effects of NO-release kinetics and totals on the FBR to subcutaneous implants in a porcine model.[15] In this study, NO-releasing silica nanoparticle-doped polyurethane membranes were utilized to further vary the NO-release properties (NO totals and durations of 2.7–9.3 μmol/cm^2 and 6 h to 2 weeks, respectively). Histological analysis revealed that increased NO-release durations and greater NO payloads significantly reduced collagen encapsulation at both 3 and 6 weeks, suggesting prolonged NO release may be key for mitigating the FBR.

To facilitate the ability of NO release to impact inflammation and wound healing, we designed NO-releasing membrane-coated implantable glucose sensors. Shin et al. described the development of NO-releasing xerogel sensor membranes to enhance biocompatibility while maintaining clinically relevant sensor performance.[16] Unfortunately, the *N*-diazeniumdiolate xerogel membranes exhibited poor analyte

permeability due to the process required to form the NO donor (i.e., exposure to high pressures of NO). To avoid this problem, these membranes were grounded and embedded into the polyurethane sensor membranes.[16] Glucose sensors coated with these hybrid membranes exhibited adequate sensor performance, demonstrating for the first time the ability to combine NO chemistry with an electrochemical glucose biosensor.[16] Additionally, NO-releasing poly(vinylpyrrolidone)-doped xerogel membranes[17] and micropatterned xerogel membranes[18] were designed to improve the permeability of both hydrogen peroxide and glucose using more conventional film-based technology. Glucose sensors coated with these membranes both allowed for glucose detection and reduced bacterial adhesion.[17,18] However, this work stopped short of in vivo testing of any analytical performance enhancements.

Gifford et al. published the first in vivo evaluation of an NO-releasing glucose sensor in a rodent model.[19] A polyurethane membrane doped with a low molecular weight *N*-diazeniumdiolated molecule (i.e., (Z)-1-[*N*-methyl-*N*-[6-(N-butylammoniohexyl)amino]]-diazen-1-ium-1,2-diolate (DBHD/NO)) was coated onto needle-type glucose sensors. The sensors released ~5 pmol cm^{-2} s^{-1} of NO for at least 12 h and met established analytical criteria for implantable glucose sensors (e.g., sensitivity of ~4 nA/mM for both NO-releasing and control sensors).[19,20] Along with a histological evaluation demonstrating a significant reduction in the initial inflammatory response, the NO-releasing glucose sensors yielded 99.7% of the glucose determinations within zones A and B of the Clarke Error Grid (clinically accurate and acceptable zones, respectively) on the first day of implantation. Although the short-term (i.e., <3 d) benefit of the NO-

releasing sensor was reported, an extended implantation period with prolonged NO release from membrane-coated sensors would be necessary to elucidate any FBR improvement in analytical performance of the NO-releasing sensor membranes. Additionally, a porcine model may be a more relevant animal model due to the physiological and anatomical similarities between pigs and humans.[21] Indeed, the development of glucose sensor membrane with prolonged (>24 h) NO release in a porcine model is necessary to fully demonstrate any sensor performance improvement related to NO.

In this chapter, the in vivo performance of needle-type glucose biosensors coated with *S*-nitrosothiol-modified silica nanoparticle-doped polyurethane is described to assess the effect of NO on sensor performance. This membrane released ~1.3 μmol NO/cm^2 for 24 h with the NO flux detectable via chemiluminescence NO analyzer, a similar level to that previously shown to reduce collagen capsule.[11,15] The analytical performance of the NO-releasing sensors was evaluated according to an in vivo numerical accuracy test and compared to controls.

5.2 Methods and materials

5.2.1 Materials

All materials and solvents were analytical grade and used as received. 3-Mercaptopropyltrimethoxysilane (MPTMS) and tetraethoxysilane (TEOS) were purchased from Gelast (Tullytown, PA). Ethanol (EtOH) and tetrahydrofuran (THF) were purchased from Fisher Scientific (Fair Lawn, NJ). The Tecoflex (SG-85A) polyurethane was a gift from Thermedics (Woburn, MA). The Hydrothane (AL 25-80A) polyurethane

was a gift from AdvanSource Biomaterials Corporation (Willmington, MA). CIDEX PLUS® 28 Day Solution was purchased from Johnson and Johnson (Irvine, CA). Phosphate buffered saline (PBS; 0.01 M, pH 7.4) was autoclaved and stored at room temperature in a sterilized hood. Biological fluids were collected from anticoagulated whole blood (5 U/mL heparin) obtained from healthy pigs at the Francis Owen Blood Research Laboratory (Chapel Hill, NC).[22] Platelet rich plasma (PRP) was collected as the supernatant by centrifuging anticoagulated whole blood at 250 ×*g* for 15 min. Serum was obtained by further centrifugation of the PRP fraction at 2,000 ×*g* for 15 min. Serum containing <10 kDa proteins was prepared by filtering serum using Amicon® Ultra-4 centrifugal filter (Millipore; Belerica, MA) at 4,000 ×*g* for 20 min. All centrifugation was conducted under temperature control at 4 ^{o}C. Customized needle-type glucose sensors (i.e., glucose biosensors without outer-diffusion limiting membrane) were purchased from Pinnacle Technologies (Lawrence, KS). Epoxy (5 minute) was purchased from ITW Devcon (Danvers, MA) and superflex silicon adhesive sealant was purchased from Henkel Loctite Corp. (Rocky Hill, CT).

5.2.2 Fabrication of NO-releasing needle-type glucose microsensors

Nitric oxide-releasing needle-type glucose sensors using *S*-nitrosothiol-modified silica particle (MPTMS/TEOS)-doped polyurethane (PU) membranes were prepared as shown in Figure 5.1.

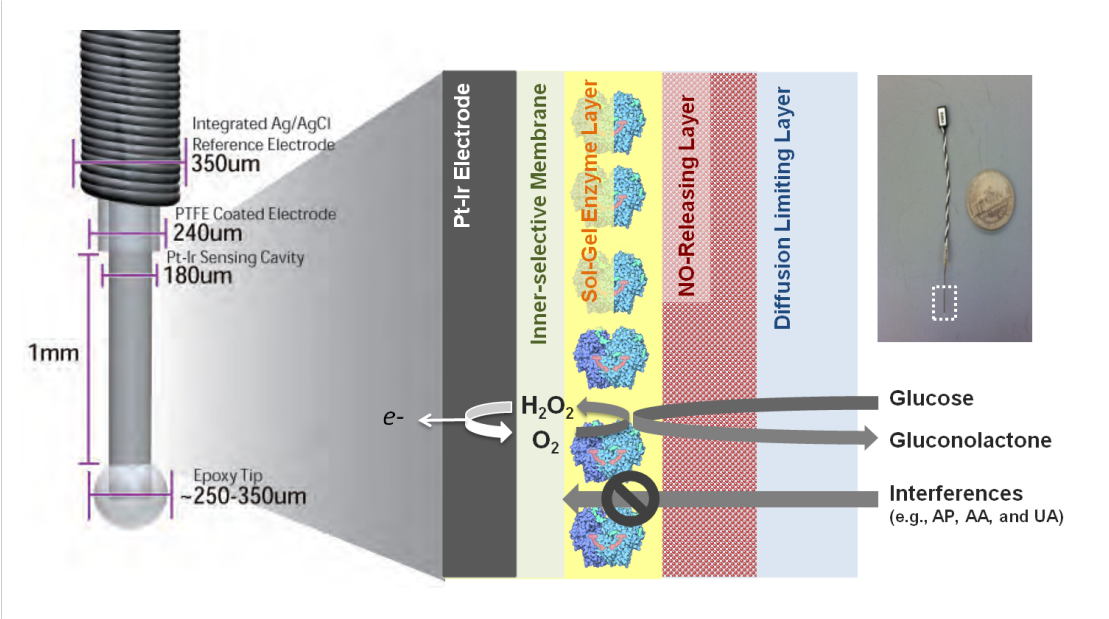

Figure 5.1. Schematic diagram of the layered structure of *S*-nitrosothiol-modified NO-releasing silica particle (MPTMS/TEOS)-doped polyurethane coated needle-type glucose sensors. The resulting electrode is shown to the far right.

The fabricated sensors consisted of four distinct layers including an inner-selective layer, an enzyme layer, an NO-releasing layer, and an outer-diffusion limiting polyurethane membrane. Customized needle-type glucose biosensors purchased from Pinnacle sensors were for these studies and came pre-prepared with inner-selective and enzyme layers following procedures reported elsewhere.[19,23] Exposed electronic parts (e.g., electrical wire) were sealed with epoxy and silicon sealants to prevent short circuits prior to applying additional layers. Electronic parts were sterilized with CIDEX PLUS® solution (3.4% glutaraldehyde) following the manufacturer guidelines. Two exterior membranes were coated onto the customized glucose sensors by dip coating. The NO-releasing layer required one dip-coat into 72 mg/mL MPTMS/TEOS silica nanoparticle containing polymer solution consisting of 80 mg/mL 50% (w/w) TPU/HPU solution dissolved in 50% (v/v) THF/EtOH. An additional dip-coat in the same PU solution without particles was performed to produce an outermost diffusion-limiting membrane. Each layer was dried at ambient conditions for 30 min before coating the subsequent layer. Nitric oxide-releasing silica nanoparticles in the NO-releasing layer were synthesized based on a sol-gel process via the co-condensation of MPTMS with a backbone silane (75 mol% TEOS), as described previously.[14] In order to keep topography/roughness constant, control sensors were prepared using the same procedure with decomposed MPTMS/TEOS particles. All procedures were conducted in a sterilize laminar flow hood. The fabricated sensors were placed into individual sterilized centrifuge tubes and kept in a vacuum-sealed sterilized bag in the dark at -20 ^{o}C until use.

5.2.3 Characterization of NO-releasing glucose sensors

While the sterilized NO-releasing and control glucose sensors could not be tested prior to implantation due to NO donor decomposition, in vitro sensor performance was still characterized with one of electrodes from same batch. The analytical performance of the glucose sensors was evaluated via amperometry with applied electrode potential +0.6 V vs. Ag/AgCl using a CH Instruments 1030A potentiostat (Austin, TX), as well as a two-channel wireless potentiostat (model 8151 BP; Pinnacle Technology, Inc., Lawrence, KS). The electrochemical evaluations were conducted in both 0.01 M PBS (pH 7.4) and biological fluids (i.e., PRP and serum) at 37 ^{o}C using an integrated Ag/AgCl wire as a pseudo counter and reference electrode. Sensor performance criteria (e.g., sensitivity, response time, and selectivity) were evaluated as described in Chapter 2 and 4.[24] Morphology of sensor surface was determined via an environmental scanning electron microscope (ESEM; FEI company; Hillsboro, OR). Nitric oxide-release properties were evaluated using both chemiluminescence and the Griess assay following the methods described in previous chapters.[24-26]

5.2.4 Implantation and in vivo evaluation of sensor performance

The animal protocol used in this study was reviewed and IACUC-approved at Duke University. The NO-releasing and control glucose sensors were implanted in mixed breed Yorkshire-type piglets weighing approximately 7–12 kg. Pigs were initially anesthetized with ketamine:xylazine (20 and 2 mg/kg, respectively) and maintained on 2–4% isoflurane (v/v in O_2) during implantation. After shaving the dorsal fur, the skin was prepared by further hair clipping and triplicate scrubbing with chlorhexidine and alcohol.

Two incisions (~1 cm) were created 4 cm lateral to the dorsal midline and approximately 8 cm caudal to the scapulae using a scalpel. One NO-releasing sensors and one control sensor were implanted in each subcutaneous incision pocket created by blunt surgical scissors (total 4 sensors/pig), and the incisions sutured shut in order to minimize micromotion of percutaneously implanted sensors. Implanted sensors were connected with a wireless potentiostat (Pinnacle Technologies; Lawrence, KS) having its own telemetry channel to allow for real-time measurement in the freely moving pigs. All systems were tagged down with a film dressing (i.e., 3M tagaderm) and gauze. Additionally, each pig wore a life jacket (O'rageous®; Katy, TX) to further secure the electronics. Immediately following sensor insertion, continuous sensor recording (sample rate of 1 sample/s) was initiated to determine run-in time. On days 1, 4, and 7, blood glucose data was collected from the pigs for a period of 6–8 h while continuously monitoring subcutaneous glucose concentration via implanted sensors with +0.6 V vs. Ag/AgCl applied potential. After recovering from anesthesia, blood glucose measurements were taken from pig ear veins every 10 min using a 30-gauge lancet and an One Touch Ultra glucometer (LifeScan Inc.; Milpitas, CA). Typically, the first 3 h were used to measure blood glucose fluctuations at steady state. After this time, a glucose bolus consisting of a known volume of syrup (100 calories and 18 g sugar per 60 mL) was administered orally. Measurements were taken as before for a period of approximately 3 h or until blood glucose was stable once more. After a period of 2 weeks or after all implanted sensors ceased functioning, the pig was sacrificed and the tissue surrounding the implants explanted and flashed frozen with liquid nitrogen, and saved for

further analysis. Two swine with three of NO-releasing and control sensors for each were used in this study.

5.2.5 Data analysis for sensor accuracy in vivo

To determine the accuracy of the implanted glucose sensors throughout dynamic blood glucose fluctuation, the point Clarke Error Grid analysis, mean (or median) absolute and relative absolute differences (MAD and MARD), and International Standard Organization (ISO) criteria were used.[27] Such sensor evaluation methods require comparison to true blood glucose concentrations as determined using an external finger-prick glucose sensor. After the electrochemical sensor responses were smoothed with a 1-minute moving average, implanted sensors were calibrated via a one-point calibration using the first point of blood glucose measurement after full recovery from anesthesia.[28,29] In a one-point calibration, sensitivity (S) is simply determined as the ratio of the current reading ($I(t)$) and glucose concentration ($G(t)$) based on the assumption that the current response without glucose (background current; I_0) is negligible. Thus, the glucose concentration is then estimated from the response current according to the following equation:

$$G(t)=\frac{I(t)}{S} \tag{1}$$

A physiological lag time exists due to the diffusion of glucose from the capillary endothelium to interstitial fluid. This lag time is influenced by the rate of glucose diffusion, the rate of glucose uptake by subcutaneous cells, the metabolic rate of the adjacent cells, the glucose supply, blood flow, and permeability of the capillary.[30] Thus,

an average experimentally determined physiological lag time (i.e., 5 min) was taken into account during data analysis.[30-32] The Clarke Error Grid analysis was constructed using MATLAB (Mathworks Inc.; Natick, MA).[27,33,34] While MAD indicated the propensity of the difference between the continuous glucose measurement and reference readings (i.e., external blood glucose monitor), the MARD was calculated as the relative deviation of implanted sensor from the reference. The MedAD and MedARD were presented as median values rather than mean values. Using MAD and MARD values, run-in time was defined where the initial point showing acceptable accuracy. Both MAD and MARD were calculated using the following equations, where interstitial fluid (IF) glucose concentration determined by current response from continuous glucose monitoring (CGM) system and blood glucose concentration (BG) evaluated by finger prick in vitro glucose sensors.[30]

$$\text{MAD} = \text{Mean}\left(\left|\text{CGM-BG}\right|\right) \tag{2}$$

$$\text{MARD} = \text{Mean}\left(\frac{\left|\text{CGM-BG}\right|}{\text{BG}} \times 100\right) \tag{3}$$

The International Standard Organization (ISO) criteria for an accuracy assessment was based on (1) the percentage of CGM readings which show less than 15 mg/dL difference from the BG when BG ranges ≤75 mg/dL; and, (2) the percentage of CGM readings within 20% difference referencing to BG when BG ranges >75 mg/dL.[30]

5.3 Results and discussion

5.3.1 In vitro electrochemical glucose sensor performance and nitric oxide release properties

The NO-releasing and control glucose biosensors were fabricated by doping NO-releasing silica particles and decomposed particles, respectively, into polyurethane membranes coated on customized Pinnacle glucose sensors. An additional PU membrane served as the diffusion-controlling layer. Without this layer, the linear dynamic range of the sensor was limited with sensitivity significantly affected by oxygen concentration due to an oxygen deficit.[35] Limiting glucose diffusion is especially critical for in vivo glucose measurements due to oxygen consumption by inflammatory cells. Thus, a wide dynamic range over physiological glucose concentrations (i.e., >12 mM) with sufficient sensor sensitivity (i.e. 1.5–3.5 nA/mM) is required for minimizing potential oxygen influence in vivo.[35] As shown in Figure 5.2, applying the NO-releasing and diffusion-limiting polyurethane layers extended the linear dynamic range from 3 to 27 mM, but decreased sensor sensitivity from 25.1 to 3.3 ± 2.0 nA/mM. The response time also increase slightly from 3.5 to 4.8 s. Despite the sensitivity loss caused by the additional polyurethane membranes, the resulting sensitivity was sufficient for in vivo determination.[4] As fabricated, the glucose sensors were stable for ~21 d with a constant applied potential of +0.6 V vs. Ag/AgCl in PBS at room temperature. The selectivity coefficients of the resulting sensors—the logarithmic form of the amperometirc sensitivity ($\Delta I/C$) for the interferent over glucose—were 0.42, 0.62, and -0.03 for ascorbic acid, uric acid, and urea, respectively, showing sufficient selectivity of glucose over electroactive molecules at the

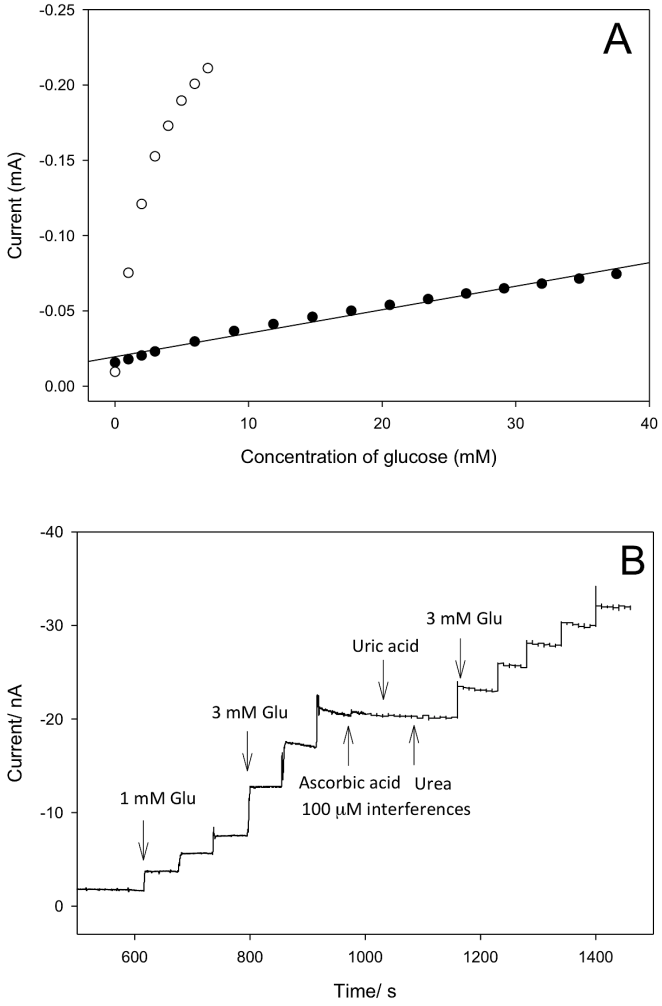

Figure 5.2. (A) Calibration curves for the needle-type customized Pinnacle sensor (●) and fabricated NO-releasing sensor (○) in pH 7.4 PBS at room temperature with applied potential +0.6 V vs. Ag/AgCl. (B) Amperometric response of NO-releasing sensors upon sequential addition of 1 and 3 mM glucose (Glu) and 100 μM ascorbic acid, uric acid, and urea.

Table 5.1. Glucose sensitivity changes in various biological fluids.[a]

Biological Fluid	*Sensitivity (nA/mM)*	*Normalized sensitivity*	*Sensitivity decrease (%)*
PBS	1.55	1.00	-
Serum <10 kDa	0.95	0.61	38.7
Serum	1.06	0.68	31.6
Platelet Rich Plasma	1.04	0.67	32.9
Whole Blood	0.81	0.52	48.0
PBS (after washing)[b]	1.48	0.95	4.8

[a] One sensor was used for all experiment to show relative sensitivity change

[b] The sensor was washed after operation in all biological fluids.

endogenously presented concentration and no synergetic/inhibitory reaction in the presence of these compounds.[36] Of note, no significant difference in sensor performance between control and NO-releasing sensors was observed on the bench top experiments. As such, the fabricated NO-releasing glucose sensors met criteria for further in vivo testing.

Although in vitro sensor characterization does not necessarily predict in vivo performance, the variation in sensor sensitivity between various biological fluids was determined to simulate more challenging environments. Significantly decreased sensitivity was observed in serum containing only <10 kDa proteins, but was restored after washing with PBS (Table 5.1). The sensitivity loss in vivo is known to be reversible, but occurs immediately following implantation due to protein absorption (<15 kDa) by serum albumin and other protein fragments.[37] Thus, a ~50% decrease in sensor sensitivity was expected upon contact with subcutaneous tissue in vivo. Nevertheless, the sensitivities of the fabricated NO-releasing sensors proved adequate in the biological fluids investigated, again setting the stage for the in vivo.

The *S*-nitrosothiol (RSNO)-modified silica nanoparticles were synthesized as an NO donor and characterized with respect to NO-release. As expected, these particles exhibited greater NO storage (2.95 ± 0.25 μmol/mg) with prolonged NO release durations (half-life 213 ± 20 min and duration >48 h in PBS at 37 ^{o}C).[14] Particle leaching from the polyurethane membranes was not observed, likely due to the large particle size of MPTMS/TEOS (~700 nm), eliminating toxicity concerns.[15]

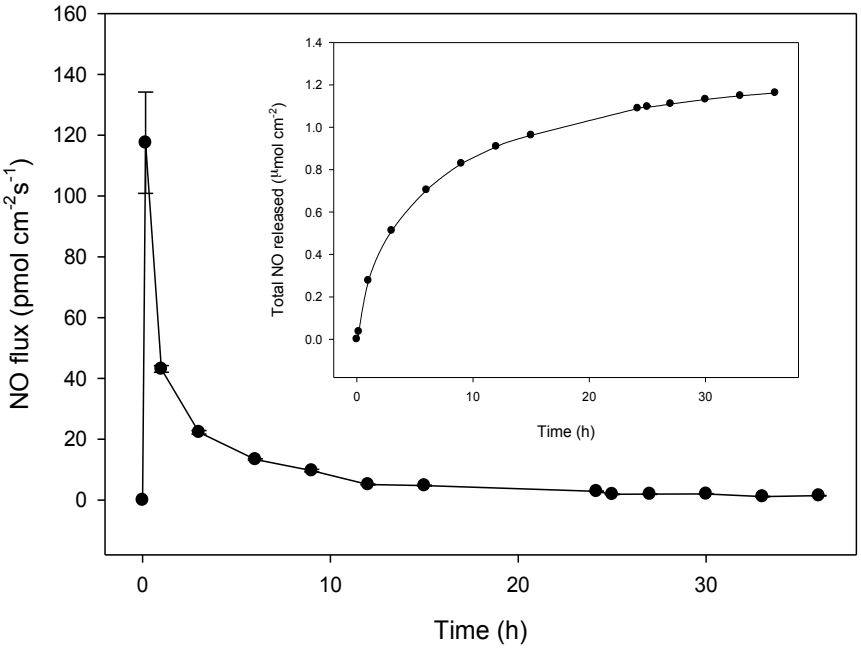

Figure 5.3. Nitric oxide-release profile from 72 mg/mL MPTMS/TEOS particle-doped 50% (w/w) TPU/HPU polyurethane membrane coated needle-type glucose biosensors. Inset represents integrated total NO release.

The NO release from MPTMS/TEOS particle-doped polyurethane membranes was evaluated in PBS (pH 7.4) at 37 ^{o}C to mimic physiological conditions. The membranes exhibited a maximum NO flux of 196.7 ± 2.9 pmol cm^{-2} s^{-1} and total NO release of 1.3 ± 0.8 μmol cm^{-2} (Figure 5.3). The NO-release properties of the particles agreed with that of previously reported NO-releasing xerogels that displayed ~50% less collagen capsule formation and chronic inflammation versus in rodent model.[11] Additionally, the MPTMS/TEOS particle-doped PU membranes showed significantly reduced collagen encapsulation in the porcine subcutaneous tissue due to longer NO-release duration (i.e., 14 d) since the RSNO-modified silica particles allowed the release of NO at low fluxes over extended periods through a thermal release mechanism.[15] Although the fabricated glucose sensor membrane exhibited >24 h NO-release duration due to the limited thickness of the coating employed for the functional glucose sensors, the low levels of NO still being released but analytically undetectable (by NOA) may still mitigate the FBR.

5.3.2 In vivo glucose sensor performance

In vivo sensor performance was evaluated in a freely moving porcine model. Both NO-releasing and control sensors were implanted percutaneously and amperometric current response was immediately monitored under an applied electrode potential of +0.6 V vs. Ag/AgCl. Standard polarization curves from both NO-releasing and control glucose sensors were observed and stabilized ~30 min after implantation. After the pig recovered from anesthesia (i.e., approximately 1.5 h after implantation), the first blood glucose measurement was carried out using a conventional glucometer via ear pricking. The

experimentally determined run-in time was 3.4 h with MAD (MARD) of 14.6 (13.5) and 7.5 (6.9) for control and NO-releasing glucose sensors, respectively. The NO-releasing sensors demonstrated ~50% greater accuracy at the initial time point compared to control sensors. Gifford et al. showed practically same results that the NO-releasing sensors exhibited a short time (~30 min) for reaching to stable basal response versus control sensors (4–10 h) in a rodent model.[19] In other words, the NO-releasing sensor showed greater accuracy at a certain initial time point compared to controls due to fast stabilization after implantation.

The numerical accuracies of both control and NO-releasing glucose sensors were further evaluated as a function of implantation period. In terms of analytical accuracy, a greater percentage of points in zones A and B of the Clarke Error Grid and International Standard Organization (ISO) criteria represent superior performance in vivo. Lower values of MAD (MARD) and MedAD (MedARD) represent better accuracy.

As shown in Table 5.2, the NO-releasing sensors achieved ~6.5% greater accuracy on the Clarke Error Grid analysis on day 4 and 7 compared to controls, while ~2.7% less accurate on the day after implantation. In contrast, the overall value of MAD (MARD) and MedAD (MedARD) values suggested the control sensors were slightly more accurate than the NO-releasing glucose sensors on day 1 and 4. However, the NO-releasing sensors exhibited slightly better accuracy on day 7 compare to the controls based on MedAD and MedARD analysis.

Table 5.2. In vivo numerical and clinical accuracy of control and NO-releasing sensors as a function of implantation period.[a]

Implant period (d)	*1*		*4*		*7*	
Glucose sensor	*Control*	*NO*	*Control*	*NO*	*Control*	*NO*
Percent of points in Zone A and B of Clarke Error Grid	94.6	91.9	82.5	88.5	93.3	100
Number of data points	140	136	47	85	70	37
MedAD[b]	17.1	20.1	15.9	17.6	22.9	11.0
MedARD[c]	13.9	17.0	17.4	18.6	48.0	35.5
MAD[d]	27.4	36.6	60.5	61.2	30.1	30.9
MARD[e]	22.2	34.7	28.7	29.5	49.1	38.9
ISO (≤75 mg/dL; %)[f]	43.5	34.8	82.4	84.6	47.9	91.7
ISO (>75 mg/dL; %)[f]	61.6	59.2	47.5	41.4	3.7	0.0

[a] Two swine with three of NO-releasing and control sensors for each were used.
[b] Median absolute differences (MedAD)
[c] Median relative absolute differences (MedARD)
[d] Mean absolute differences (MAD)
[e] Mean relative absolute differences (MARD)
[f] International standard organization (ISO) criteria: (1) percent reading less that 15 mg/mL difference from in vitro blood glucose (BG) measurement when BG ranges ≤75 mg/dL), and (2) percent reading of implanted glucose sensors within 20% difference referencing to BG when BG ranges >75 mg/dL.

Although the longest sensor lifetime in vivo was 2 weeks, ~50% of both control and NO-releasing sensors were failed before a week time point. Interestingly, 75% of sensors with a first trial pig (7 kg) were worked for 2 weeks, while all sensors with a second trial pig (12 kg) failed after 4 d. These results suggested that greater mechanical stress due to the animal size may critically affect on the sensor lifetime in vivo.

According the ISO criteria evaluation, the NO-releasing sensors were more accurate than controls in hypoglycemia region after one-week of implantation. However, the total number of data points for NO-releasing sensors was less than for controls due to sensor failure. For example, only 37 data points were analyzed on day 7, half of that collected from the controls. The sensor failure was attributed to electrical connection problems mainly due to mechanical stress on the sensor components.

A comparison of the in vivo sensor performance of NO-releasing sensors relative to control sensors was also carried out using accumulated data points. As shown in Figure 5.4 and Table 5.3, both the NO-releasing and control sensors had 91.8% of points in Zones A and B of the Clarke Error Grid, indicating clinically accurate and acceptable determinations, respectively. While NO-releasing sensors yielded more points in the clinically acceptable zone compared to controls (~8%), the control sensors exhibited more data within the clinically accurate zone (166 vs. 159 for controls and NO-releasing sensors, respectively). The percentage of points for NO-releasing and control sensors in Zone E, leading to hyperglycemia treatment for hypoglycemia or vice versa, were similar (3.9 and 3.6%, respectively).

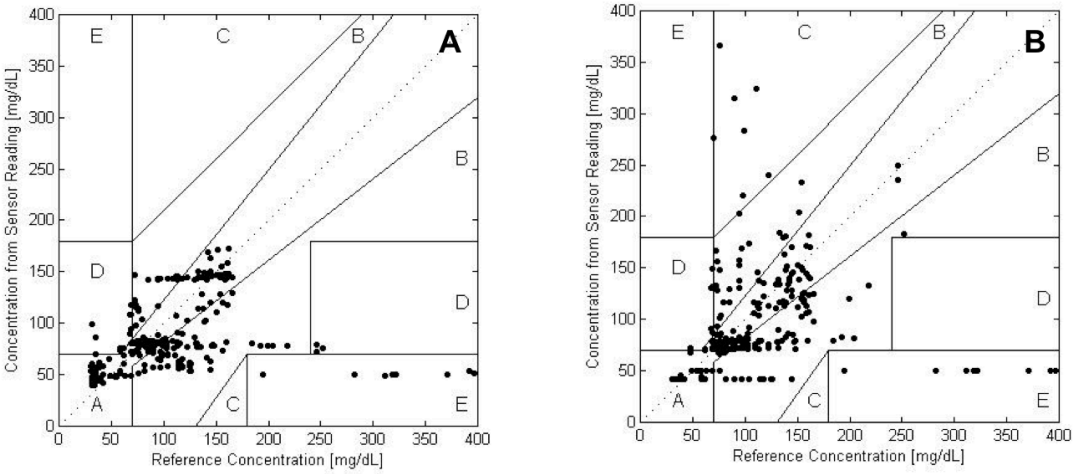

Figure 5.4. Clarke Error Grid analysis for (A) controls and (B) NO-releasing sensors (n=2 pigs and n=3 sensors). Presented data were cumulative results for one-week implantation.

Table 5.3. Total number of data points and percent points in the zone of the Clarke Error Grid analysis.[a]

Clarke Error Grid Zone	*Control*		*NO-releasing*	
	Total	*Percentage (%)*	*Total*	*Percentage (%)*
A	166	59.3	159	56.6
B	91	32.5	99	35.2
C	0	0.0	6	2.1
D	13	4.6	6	2.1
E	10	3.6	11	3.9

[a] Data was collected for one week from two swine with three sensors for each type.

Of note, the NO-releasing sensor exhibited a lower percentage of measurements in Zone D indicating a potentially dangerous failure to detect hypoglycemic or hyperglycemic events. Overall, results using the NO-releasing and the control sensors were not significantly different based on Clarke Error Grid analysis regarding to the clinical use.

According to a power analysis which is statistical determination of sample size required to discover a significant effect,[38] twenty animals are required to detect small differences (i.e., ~2%) at a confidence interval (α) of 0.05 using a two-tailed t-test with a power of 0.8. Thus, inconclusive result presented herein is clearly due to the limited sample size. Additionally, the subject's disease state (healthy vs. diabetes) may contribute to weak correlations. Since pigs with diabetic mellitus are known to have an NO deficiency, compromised immune system, and less wound healing,[39] diabetic pigs may be more suitable for future studies.

Aside from the Clarke Error Grid analysis, other numerical accuracy tests were also conducted and presented in Table 5.4. While MedAD (MedARD) values suggested the NO-releasing sensor exhibited slightly improved accuracy compared to controls, comparisons of the MAD (MARD) values showed opposite results. However, the ISO criteria analysis revealed that the NO-releasing sensors were more accurate in hypoglycemic events compare to the controls. Of note, hypoglycemic events often result in more serious side effects including unconsciousness, brain damage and even death. Thus, the evaluation of the NO-releasing sensors with insulin administration for inducing hypoglycemia may greatly enhance the impact of the study.

Table 5.3. The numerical accuracy test of implanted glucose sensors.[a]

In vivo sensor point accuracy	*Control*	*NO-releasing*
Percent point at Zone A and B of Clarke Error Grid analysis	91.79	91.81
MedAD[b]	18.6	17.6
MedARD[c]	23.2	20.7
MAD[d]	34.8	38.9
MARD[e]	30.7	32.4
ISO (≤75 mg/dL)[f]	54.5	72.6
ISO (>75 mg/dL)[f]	50.5	49.5

[a] Two swine with three of NO-releasing and control sensors for each were used.
[b] Median absolute differences (MedAD)
[c] Median relative absolute differences (MedARD)
[d] Mean absolute differences (MAD)
[e] Mean relative absolute differences (MARD)
[f] International standard organization (ISO) criteria: (1) percent reading less that 15 mg/mL difference from in vitro blood glucose (BG) measurement when BG ranges ≤75 mg/dL), and (2) percent reading of implanted glucose sensors within 20% difference referencing to BG when BG ranges >75 mg/dL.

5.4 Conclusions

Percutaneously implanted both control and NO-releasing sensors in a freely moving porcine model exhibited 91.8% points in clinically accurate and acceptable ranges on the Clarke Error Grid analysis. While subcutaneously implanted polyurethane films doped with *S*-nitrosothiol-modified silica particles showed less collagen encapsulation and reduced inflammatory response,[15] glucose sensors coated with these membranes did not result in significant improvements in sensor accuracy or sensor lifetimes. Limited animal sample size and the disease state, as well as undesirable mechanical stress that may have induced a more pronounced FBR may have caused insignificancy. Specifically, mechanical stress provoking sheer force and thus reducing tissue integration may conceal the effect of NO on the FBR. Therefore, a more biocompatible NO-releasing sensor membrane designed to further enhance tissue integration and thus minimize mechanical stress is required along with NO-release. In turn, the NO-releasing porous electrospun fiber membrane-modified needle-type glucose sensor may enhance in vivo sensor performance especially implanting in a diabetic porcine model.

5.5 References

(1) Vaddiraju, S.; Burgess, D. J.; Tomazos, I.; Jain, F. C.; Papadimitrakopoulos, F. "Technologies for continuous glucose monitoring: Current problems and future promises" *Journal of Diabetes Science and Technology* **2010**, *4*, 1540-1562.

(2) Heller, A.; Feldman, B. "Electrochemical glucose sensors and their applications in diabetes management" *Chemical Reviews* **2008**, *108*, 2482-2505.

(3) Wilson, G. S.; Gifford, R. "Biosensors for real-time *in vivo* measurements" *Biosensors and Bioelectronics* **2005**, *20*, 2388-2403.

(4) Wilson, G. S.; Zhang, Y. "Introduction to the glucose sensing problem" In *In Vivo Glucose Sensing*; Cunningham, D. D., Stenken, J. A., Eds.; Wiley, 2010.

(5) Koh, A.; Nichols, S. P.; Schoenfisch, M. H. "Glucose sensor membranes for mitigating the foreign body response" *Journal of Diabetes Science and Technology* **2011**, *5*, 1052-1059.

(6) Nichols, S. P.; Koh, A.; Storm, W. L.; Shin, J. H.; Schoenfisch, M. H. "Biocompatible materials for continuous glucose monitoring devices" *Chemical Reviews* **2013**, *113*, 2528-2549.

(7) Ignarro, L. J. *Nitric oxide : biology and pathobiology*; Academic Press: San Diego, Calif.; London, 2000.

(8) Ignarro, L. J. "Nitric oxide: A unique endogenous signaling molecule in vascular biology (Nobel lecture)" *Angewandte Chemie International Edition* **1999**, *38*, 1882-1892.

(9) Riccio, D. A.; Schoenfisch, M. H. "Nitric oxide release: Part I. Macromolecular scaffolds" *Chemical Society Reviews* **2012**, *41*, 3731-3741.

(10) Riccio, D. A.; Dobmeier, K. P.; Hetrick, E. M.; Privett, B. J.; Paul, H. S.; Schoenfisch, M. H. "Nitric oxide-releasing *S*-nitrosothiol-modified xerogels" *Biomaterials* **2009**, *30*, 4494-4502.

(11) Hetrick, E. M.; Prichard, H. L.; Klitzman, B.; Schoenfisch, M. H. "Reduced foreign body response at nitric oxide-releasing subcutaneous implants" *Biomaterials* **2007**, *28*, 4571-4580.

(12) Shin, J. H.; Metzger, S. K.; Schoenfisch, M. H. "Synthesis of nitric oxide-releasing silica nanoparticles" *Journal of the American Chemical Society* **2007**, *129*, 4612-4619.

(13) Shin, J. H.; Schoenfisch, M. H. "Inorganic/organic hybrid silica nanoparticles as a nitric oxide delivery scaffold" *Chemistry of Materials* **2008**, *20*, 239-249.

(14) Riccio, D. A.; Nugent, J. L.; Schoenfisch, M. H. "Stöber synthesis of nitric oxide-releasing *S*-nitrosothiol-modified silica particles" *Chemistry of Materials* **2011**, *23*, 1727-1735.

(15) Nichols, S. P.; Koh, A.; Brown, N. L.; Rose, M. B.; Sun, B.; Slomberg, D. L.; Riccio, D. A.; Klitzman, B.; Schoenfisch, M. H. "The effect of nitric oxide surface flux on the foreign body response to subcutaneous implants" *Biomaterials* **2012**, *33*, 6305-6312.

(16) Shin, J. H.; Marxer, S. M.; Schoenfisch, M. H. "Nitric oxide-releasing sol-gel particle/polyurethane glucose biosensors" *Analytical Chemistry* **2004**, *76*, 4543-4549.

(17) Schoenfisch, M. H.; Rothrock, A. R.; Shin, J. H.; Polizzi, M. A.; Brinkley, M. F.; Dobmeier, K. P. "Poly(vinylpyrrolidone)-doped nitric oxide-releasing xerogels as glucose biosensor membranes" *Biosensors and Bioelectronics* **2006**, *22*, 306-312.

(18) Oh, B. K.; Robbins, M. E.; Nablo, B. J.; Schoenfisch, M. H. "Miniaturized glucose biosensor modified with a nitric oxide-releasing xerogel microarray" *Biosensors and Bioelectronics* **2005**, *21*, 749-757.

(19) Gifford, R.; Batchelor, M. M.; Lee, Y.; Gokulrangan, G.; Meyerhoff, M. E.; Wilson, G. S. "Mediation of in vivo glucose sensor inflammatory response via nitric oxide release" *Journal of Biomedical Materials Research Part A* **2005**, *75A*, 755-766.

(20) Frost, M. C.; Batchelor, M. M.; Lee, Y. M.; Zhang, H. P.; Kang, Y. J.; Oh, B. K.; Wilson, G. S.; Gifford, R.; Rudich, S. M.; Meyerhoff, M. E. "Preparation and characterization of implantable sensors with nitric oxide release coatings" *Microchemical Journal* **2003**, *74*, 277-288.

(21) Refai, A. K.; Textor, M.; Brunette, D. M.; Waterfield, J. D. "Effect of titanium surface topography on macrophage activation and secretion of proinflammatory

cytokines and chemokines" *Journal of Biomedical Materials Research Part A* **2004**, *70*, 194-205.

(22) Allen, J.; Khan, S.; Serrano, M. C.; Ameer, G. "Characterization of porcine circulating progenitor cells: Toward a functional endothelium" *Tissue Engineering Part A* **2008**, *14*, 183-194.

(23) Endo, H.; Yonemori, Y.; Hibi, K.; Ren, H.; Hayashi, T.; Tsugawa, W.; Sode, K. "Wireless enzyme sensor system for real-time monitoring of blood glucose levels in fish" *Biosensors and Bioelectronics* **2009**, *24*, 1417-1423.

(24) Koh, A.; Riccio, D. A.; Sun, B.; Carpenter, A. W.; Nichols, S. P.; Schoenfisch, M. H. "Fabrication of nitric oxide-releasing polyurethane glucose sensor membranes" *Biosensors and Bioelectronics* **2011**, *28*, 17-24.

(25) Coneski, P. N.; Schoenfisch, M. H. "Nitric oxide release: Part III. Measurement and reporting" *Chemical Society Reviews* **2012**, *41*, 3753-3758.

(26) Hetrick, E. M.; Schoenfisch, M. H. "Analytical chemistry of nitric oxide" *Annual Review of Analytical Chemistry* **2009**, *2*, 409-433.

(27) Clarke, W. L.; Kovatchev, B. P. "Continuous glucose sensors: Continuing questions about clinical accuracy" *Journal of Diabetes Science and Technology* **2007**, *1*, 669-675.

(28) Choleau, C.; Klein, J. C.; Reach, G.; Aussedat, B.; Demaria-Pesce, V.; Wilson, G. S.; Gifford, R.; Ward, W. K. "Calibration of a subcutaneous amperometric glucose sensor: Part 1. Effect of measurement uncertainties on the determination of sensor sensitivity and background current" *Biosensors and Bioelectronics* **2002**, *17*, 641-646.

(29) Choleau, C.; Klein, J. C.; Reach, G.; Aussedat, B.; Demaria-Pesce, V.; Wilson, G. S.; Gifford, R.; Ward, W. K. "Calibration of a subcutaneous amperometric glucose sensor implanted for 7 days in diabetic patients: Part 2. Superiority of the one-point calibration method" *Biosensors and Bioelectronics* **2002**, *17*, 647-654.

(30) Kulcu, E.; Tamada, J. A.; Reach, G.; Potts, R. O.; Lesho, M. J. "Physiological differences between interstitial glucose and blood glucose measured in human subjects" *Diabetes Care* **2003**, *26*, 2405-2409.

(31) Rebrin, K.; Steil, G. M.; van Antwerp, W. P.; Mastrototaro, J. J. "Subcutaneous glucose predicts plasma glucose independent of insulin: implications for continuous monitoring" *American Journal of Physiology - Endocrinology And Metabolism* **1999**, *277*, E561-E571.

(32) Gough, D. A.; Kumosa, L. S.; Routh, T. L.; Lin, J. T.; Lucisano, J. Y. "Function of an implanted tissue glucose sensor for more than 1 year in animals" *Science Translational Medicine* **2010**, *2*, 42ra53.

(33) Clarke, W. L.; Cox, D.; Gonder-Fedrick, L. A.; Carter, W.; Pohl, S. L. "Evaluating clinical accuracy of systems for self-monitoring of blood glucose" *Diabetes Care* **1987**, *10*, 622-628.

(34) Clarke, W. L. "The original clarke error grid analysis" *Diabetes Technology and Therapeutics* **2005**, *7*, 776-779.

(35) Zhang, Y.; Wilson, G. S. "In vitro and in vivo evaluation of oxygen effects on a glucose oxidase based implantable glucose sensor" *Analytica Chimica Acta* **1993**, *281*, 513-520.

(36) Heller, A. "Implanted electrochemical glucose sensors for the management of diabetes" *Annual Review of Biomedical Engineering* **1999**, *1*, 153-175.

(37) Gifford, R.; Kehoe, J. J.; Barnes, S. L.; Kornilayev, B. A.; Alterman, M. A.; Wilson, G. S. "Protein interactions with subcutaneously implanted biosensors" *Biomaterials* **2006**, *27*, 2587-2598.

(38) Fitzner, K.; Heckinger, E. "Sample size calculation and power analysis: A quick review" *The Diabetes Educator* **2010**, *36*, 701-707.

(39) Le, N. N.; Rose, M. B.; Levinson, H.; Klitzman, B. "Implant healing in experimental animal models of diabetes" *Journal of Diabetes Science and Technology* **2011**, *5*, 605-618.

CHAPTER 6: SUMMARY AND FUTURE DIRECTIONS

6.1 Summary

The dissertation research presented herein focused on nitric oxide (NO)-releasing biocompatible sensor membranes for developing implantable glucose biosensors that function more reliably in vivo. Due to numerous complications (e.g., heart disease, kidney failure, blindness, or even death) caused by diabetes, implantable glucose biosensors capable of monitoring and strict control of blood glucose levels are essential for effective treatment. The utility of implantable glucose sensors is limited due to poor tissue biocompatibility and sensor biofouling associated with the foreign body response (FBR). My research has focused on the development of NO-releasing sensor membranes that may mitigate the FBR, reduce bacterial adhesion, enhance wound healing, and thus improve analytical performance in vivo. Both film and porous NO-releasing polyurethane membranes were developed with controlled release capabilities and coated on needle-type implantable electrochemical sensors for continuous glucose monitoring.

In Chapter 2, the fabrication of NO-releasing silica particle-doped polyurethane glucose sensor membranes was described to control NO-release kinetics and sensor performance. Nitric oxide-releasing silica particles were embedded in polyurethane films and utilized as sensor membranes. The NO-release properties and performance of sensors

modified with such coatings were characterized. Tunable NO release was achieved by altering the type of NO donor (i.e., *N*-diazeniumdiolate and *S*-nitrosothiol), amount of dopant, as well as the water uptake (i.e., hydrophobicity) and concentration of polyurethane. For example, the NO-release duration was extended from 25 h to 4 d by adding a hydrophobic water barrier polyurethane layer (i.e., Tecoplast) and tuning the concentration of polyurethane. Of note, the NO-release vehicle and the NO-release kinetics did not affect glucose sensor performance (e.g., sensitivity). Selectivity for sensing glucose over NO was achieved by using an electrode potential of +0.6 V vs. Ag/AgCl to avoid NO oxidation. Along with the controlled NO release, increased the sensor membrane thickness and hydrophobicity of the polyurethane film decreased glucose sensor sensitivity and increased response time and the dynamic range. These results illustrate the capability of controlled nitric oxide release with enzymatic biosensors regarding to sensor performance.

In Chapter 3, electrospun polyurethane fibers doped with NO-releasing silica particles were studied to take advantages of both active and passive strategies that may mitigate the FBR. The fiber diameter and mechanical strength of the electrospun fibrous mats were varied by altering the concentration and type of the polyurethane solution, as well as the concentration of NO-releasing silica particles. The fabricated NO donor-doped electrospun nanofibers (150–630 nm) exhibited ~83% relative porosity, with flexible plastic or elastomeric behavior depending on polyurethane composition. A wide range of NO-release kinetics and totals (i.e., total NO release of 7.5–120 nmol mg^{-1} with release durations from 4 h to 2 weeks) were achieved by selection of appropriate NO

donor-modified silica particles, varying the NO donor concentration, and/or altering polyurethane composition. While silica particles are generally believed not to be cytotoxic to subcutaneous tissue,[1] the NO-releasing silica particles leached from the electrospun polyurethane fibers causing concern. Leaching from these fibers was minimized by increasing particle size and/or the hydrophobicity of the polyurethane.

In Chapter 4, needle-type implantable glucose sensors were fabricated with NO-releasing polyurethane electrospun fibers as a possible method to improve the biocompatibility of continuous glucose monitoring systems. Although the level of silica particle leaching from the studied membranes in Chapter 3 was lower than the reported cytotoxic level, NO-releasing dendrimers were chosen as dopants for the electrospun fibers. *N*-diazeniumdiolated 1,2-epoxy-9-decene (ED) functionalized fourth-generation poly(amidoamine) (PAMAM) dendrimers are characterized by diverse NO-release kinetics. They also possess exterior chemical moieties that undergo facile modifications. After confirming minimal leaching with this NO donor, NO-releasing porous membranes were applied to needle-type glucose sensors as an outermost membrane via electrospinning. The fabricated electrospun fiber membrane maintained its porous structure in serum. Electrospinning allowed direct coating of the needle-type glucose sensors with variable chemical and physical properties without compromising sensor function.

In Chapter 5, NO-releasing needle-type glucose sensors were percutaneously implanted in a freely moving healthy porcine model to assess in vivo sensor accuracy. Numerical accuracy criteria were used to compare the analytical performance of NO-

releasing vs. control biosensors. Both the NO-releasing and control glucose sensors showed 91.8% points in the clinically accurate and acceptable ranges of the Clarke Error Grid analysis. However, the small sample size precluded any conclusion regarding the benefits of NO release on sensor performance. Furthermore, many of the sensors suffered from undesirable mechanical stress caused by the orientation of percutaneous implants. This in turn may have obscured the effect of NO release on the FBR.

6.2 Future Directions

6.2.1 Topography controlled co-axial electrospun fibers

The high degree of controllable NO release from *N*-diazeniumdiolate- and *S*-nitrosothiol-modified NO donor-doped polyurethane films and fibers were described for use as implantable glucose sensor membranes. Since extended NO release from membranes has been shown to be important for mitigating the FBR,[2] longer NO-release durations were achieved by increasing the hydrophobicity and/or thickness of the water barrier layers described in Chapter 2. As presented in Chapter 3 and 4, the controllability of NO-release kinetics from electrospun fibers using *N*-diazeniumdiolate-modified NO donor was however limited to the high porosity of the fiber mats and the lack of a barrier layer around the NO donors. Additionally, the electrospun fibers were oriented randomly while aligned fibers have been shown to foster greater cell proliferation and indistinctive fibrous capsulation boundary in vivo.[3]

Extending this research, co-axial electrospun fibers—possessing a core-sheath biocomponent nanofiber structure—may enhance the ability to control and tune the NO

release from polyurethane fibers.[4] To fabricate co-axial electrospun fibers, two dissimilar or antithetical materials are independently fed into a co-axial spinneret (e.g., concentric needles of different sizes) generating a core-sheath configuration.[4] Especially for biomedical applications, these types of fibers hold advantages including: (1) isolation of an unstable component to prevent undesired decomposition under a reactive environment; (2) controlled release of therapeutic agents from the core by modifying sheath composition; and, (3) reinforcement of chemical and physical properties by surrounding core with biocompatible sheath materials.[4] The use of various polymeric NO-release scaffolds in the core and hydrophobic polymers as a sheath may enable to control over NO release. For example, the NO-releasing core could consist of *N*-diazeniumdiolated xerogels and chitosan or any other NO donor-doped polymer (e.g., dendrimer-doped hydrogel or hydrophilic polyurethane). The sheath layer could consist of hydrophobic polyurethane, polyvinyl chloride, or silicon rubber to reduce water diffusion and thus further extend NO release duration. The sheath may also prove useful in reducing the cytotoxicity of certain scaffolds (e.g., dendrimer) to surrounding tissue. To fabricate NO-releasing co-axial electrospun fibers, the following parameters should be evaluated during electrospinning process: electrospinnable solution viscosity and conductivity of the sheath polymer; interfacial tension between the sheath and the core solution to allow stable Taylor cone formation; and, solvent vapor pressure.[4] In addition to these parameters, the applied voltage and feed rates should also be considered.[4]

In addition to fabricating NO-releasing co-axial electrospun fibers, the morphology of fiber mats should be studied. Since the FBR is affected by both the NO

release[2] and implant topography,[3] varying the orientation of the NO-releasing fibers may also prove useful. Aligned electrospun fibers can be fabricated by changing the collector geometry to manipulate the electric field (e.g., parallel electrodes) and/or using a dynamic collector (e.g., rotating drum collector).[5] As shown in Figure 6.1, aligned fibers can be achieved by modifying the electric field using a window-type metal collector. In this regard, a rectangular gap (i.e., window) on the disk type collector can be used to collect aligned fibers.[6] Random fibers are also observed on the solid part of the disk collector, highlighting the ability to simultaneously collect both aligned and random fibers. Three-dimensional substrates (e.g., implants or sensors) can be coated with aligned fibers by rotating the substrate in the void of this collector type. These preliminary results indicate the potential for controlling the morphology of fibrous membranes on needle-type glucose sensors.

The porosity of the fibers can also be tuned by changing the polymer solution flow rate, the rotation speed of the drum collector and the collector type (e.g., spherical dish and frame cylinder).[7,8] Although the porosity control of electrospun fibers is challenging, lower feed rate or rotating speed generally results in greater porosity.[8] Alternatively, co-electrospinning with a sacrificial polymer can be utilized to increase the pore size of fiber mat creating pores by dissolving away sacrificial polymer in a solvent that has no effect on the structure of the polymer of interest.[7]

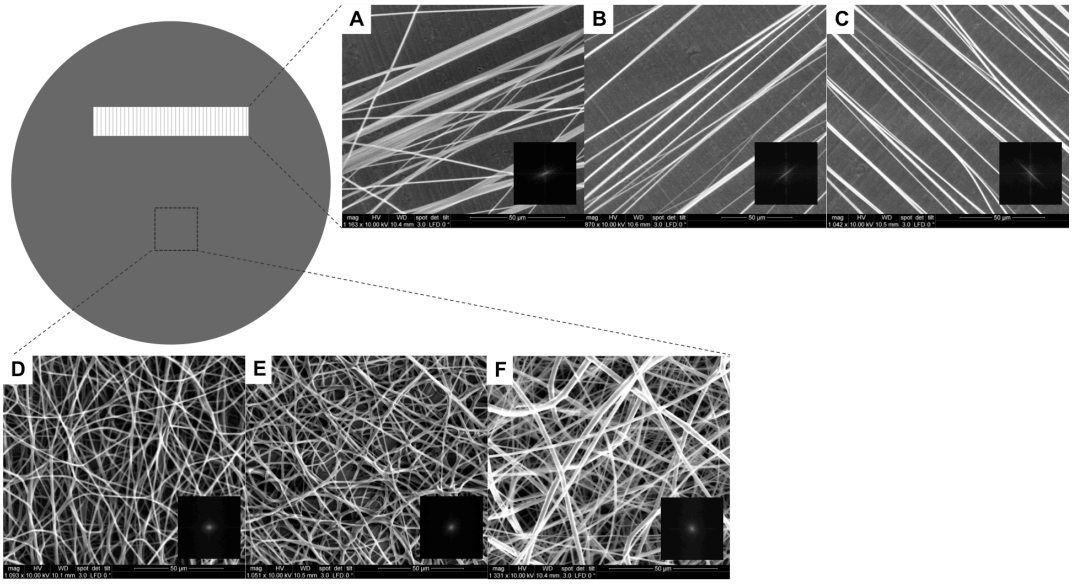

Figure 6.1. Environmental scanning electron microscopy (ESEM) images of (A–C) aligned and (D–E) random fibers collected on the window type of metal collector. Tecophilic (A and D), Tecoflex (B and E), and Tecoplast (C and F) polyurethane were electrospun on this collector. Insert of each ESEM image is the fast Fourier transform images of spatial frequency of fibers.

Fibers having significantly extended NO release duration with various morphologies via co-axial electrospinning may open up the potential for other biomedical applications, advancing these materials not only as implantable sensor membranes but also wound dressings and tissue engineering scaffolds.

6.2.2 The topographical effect of localized NO delivery on the foreign body response

Although advantages of NO-release materials and electrospun fibers mitigating the FBR have been reported independently, the effect on the FBR using combined NO release and porous structure scaffolds has not yet been studied. As an extension of the results described in Chapter 2, Nichols et al. reported the effects of NO-release kinetics on the FBR by varying the NO-release duration from hours to weeks.[2] *S*-nitrosothiol-modified silica particle-doped polyurethane films (NO-release duration of ~2 weeks) most significantly reduced capsule thickness after 3 weeks of implantation. Likewise, Cao et al. published on the topographical effect of both random and aligned electrospun poly(ε-carprolactone) nanofibers on the FBR in a rodent model, showing less collagen capsule formation compared to film implants. Based on the promising results from both studies, the topographical effects (e.g., non-porous vs. porous and/or random vs. aligned) of implants with and without NO-release ability should also be studied as a function of NO-release kinetics, and electrospun fiber mat properties (e.g., porosity and alignment).

Researchers often use rodent (e.g., mouse and rat) and porcine models to assess in vivo biocompatibility, though others (e.g., dog, rabbit, and chimpanzees) have been used as well.[9] While the rodent models is often selected due to cost, the porcine model is more ideal for tissue implant studies as pig skin closely resembles that of humans.[10]

Additionally, the vascular and immune system of the pig and human have a high degree of similarity.[10] It has been reported that diabetic subjects exhibit an NO deficiency associated with the breakdown of NO, causing impaired insulin-mediated vasodilation and glucose metabolism.[11] Thus, a diabetic porcine model should be considered for future work since diabetic patients may have delayed and diminished wound healing, physiological responses affecting sensor performance.[12,13]

Since the FBR is a sequential event, NO release and porous features may distinctly affect the inflammatory response depending on the FBR phases. A time-dependent investigation (e.g., 1 and 3 d; and 1 and 4 week for acute and chronic inflammatory stages, respectively) is thus needed to determine the effects of NO release and porosity on each stage of the FBR, with histological analysis.

6.2.3 Percutaneous implantation of nitric oxide-releasing porous membrane coated sensors for real-time glucose monitoring in healthy and diabetic porcine model.

Optimized NO-releasing electrospun fibers could be applied to functional needle-type glucose sensors as described in Chapter 4. In vivo sensor performance could be evaluated in diabetic and healthy pigs as described in Chapter 5. Optimal NO-releasing porous membranes may concomitantly allow for improvement of in vivo sensor performance and increased sensor lifetime. Implanting these glucose sensors in diabetic pigs may further highlight the prominent effects of NO-releasing porous membranes. Along with histological evaluation, demonstration of quantitative electrochemical analysis based on clinical utility may greatly advance the development of continuous glucose monitoring systems.

Although numerical accuracy analysis compared to blood glucose concentration using a conventional glucose sensor is usually conducted at certain time points, a quantitative analysis of the rate and direction change is often ignored. Such trends via an implantable glucose sensor are important, and have been proposed (with appropriate algorithms) as necessary for developing the artificial pancreas. Both the point- and rate-Clarke Error Grid analysis should be demonstrated using glucose challenges.[14] Administrating glucose through a catheter (i.e., intravenous glucose tolerance test (IVGTT) should enable a significant change in glucose concentration, especially in diabetic pigs. Additionally, insulin injections using commercially available insulin pens can be used to create a hypoglycemic event. Alternatively, a triphasic glycemic pattern following sterptozotocin injection (initial hyperglycemia peak ~60 min duration and secondary hypoglycemia ~4 h duration preceding the establishment of permanent hyperglycemia) could be used as a way to realize more spontaneous changes in blood glucose level over a larger concentration ranges.[15] Such studies may provide reliable quantification of sensor accuracy and enable determination of anticipated dual benefits of NO release and porosity.

Ultimately, more biocompatible and accurate implantable sensors should be integrated with an insulin pump to allow the automatic administration of insulin and thus improved regulation of blood glucose concentrations. Such an artificial pancreas would greatly improve the lives of diabetes patients and decrease the morbidity and mortality associated with diabetes mellitus.

6.3 References

(1) Kunzmann, A.; Andersson, B.; Thurnherr, T.; Krug, H.; Scheynius, A.; Fadeel, B. "Toxicology of engineered nanomaterials: Focus on biocompatibility, biodistribution and biodegradation" *Biochimica et Biophysica Acta (BBA) - General Subjects* **2011**, *1810*, 361-373.

(2) Nichols, S. P.; Koh, A.; Brown, N. L.; Rose, M. B.; Sun, B.; Slomberg, D. L.; Riccio, D. A.; Klitzman, B.; Schoenfisch, M. H. "The effect of nitric oxide surface flux on the foreign body response to subcutaneous implants" *Biomaterials* **2012**, *33*, 6305-6312.

(3) Cao, H.; McHugh, K.; Chew, S. Y.; Anderson, J. M. "The topographical effect of electrospun nanofibrous scaffolds on the in vivo and in vitro foreign body reaction" *Journal of Biomedical Materials Research Part A* **2010**, *93A*, 1151-1159.

(4) Moghe, A. K.; Gupta, B. S. "Co-axial electrospinning for nanofiber structures: Preparation and applications" *Polymer Reviews* **2008**, *48*, 353-377.

(5) Teo, W. E.; Ramakrishna, S. "A review on electrospinning design and nanofibre assemblies" *Nanotechnology* **2006**, *17*, R89-R106.

(6) Li, D.; Wang, Y.; Xia, Y. "Electrospinning Nanofibers as Uniaxially Aligned Arrays and Layer-by-Layer Stacked Films" *Advanced Materials* **2004**, *16*, 361-366.

(7) Rnjak-Kovacina, J.; Weiss, A. S. "Increasing the pore size of electrospun scaffolds" *Tissue Engineering Part B: Reviews* **2011**, *17*, 365-372.

(8) Zhu, X.; Cui, W.; Li, X.; Jin, Y. "Electrospun Fibrous Mats with High Porosity as Potential Scaffolds for Skin Tissue Engineering" *Biomacromolecules* **2008**, *9*, 1795-1801.

(9) Williams, R. "Animal Models in Biomedical Research" In *Principles of Molecular Medicine*; Runge, M., Patterson, C., Eds.; Humana Press, 2006.

(10) Sullivan, T. P.; Eaglstein, W. H.; Davis, S. C.; Mertz, P. "The pig as a model for human wound healing" *Wound Repair and Regeneration* **2001**, *9*, 66-76.

(11) Honing, M. L. H.; Morrison, P. J.; Banga, J. D.; Stroes, E. S. G.; Rabelink, T. J. "Nitric oxide availability in diabetes mellitus" *Diabetes/Metabolism Reviews* **1998**, *14*, 241-249.

(12) Blakytny, R.; Jude, E. "The molecular biology of chronic wounds and delayed healing in diabetes" *Diabetic Medicine* **2006**, *23*, 594-608.

(13) Gerritsen, M.; Lutterman, J. A.; Jansen, J. A. "Wound healing around bone-anchored percutaneous devices in experimental diabetes mellitus" *Journal of Biomedical Materials Research* **2000**, *53*, 702-709.

(14) Clarke, W. L.; Kovatchev, B. P. "Continuous glucose sensors: Continuing questions about clinical accuracy" *Journal of Diabetes Science and Technology* **2007**, *1*, 669-675.

(15) Kvist, P. H.; Bielecki, M.; Gerstenberg, M.; Rossmeisl, C.; Jensen, H. E.; Rolin, B.; Hasselager, E. "Evaluation of Subcutaneously-implanted Glucose Sensors for Continuous Glucose Measurements in Hyperglycemic Pigs" *In Vivo* **2006**, *20*, 195-203.